

EFFICIENT USE OF RECYCLED CONCRETE IN TRANSPORTATION INFRASTRUCTURE

Jacob E. Hiller, Ph.D.
Yogini S. Deshpande, Ph.D.
Yinghong Qin
Cory J. Shorkey

Michigan Technological University
Dept. of Civil and Environmental Engineering
1400 Townsend Drive
Houghton, MI 49931 USA

1. Report No. RC-1544	2. Government Accession No.	3. MDOT Project Manager J.F. Staton	
4. Title and Subtitle Efficient Use of Recycled Concrete in Transportation Infrastructure		5. Report Date January 21, 2011	
		6. Performing Organization Code	
7. Author(s) J.E. Hiller, Y.S. Deshpande, Y. Qin, and C.J. Shorkey		8. Performing Org. Report No.	
9. Performing Organization Name and Address Michigan Technological University 1400 Townsend Drive Houghton, MI 49931		10. Work Unit No. (TRAIS)	
		11. Contract No.	
		11(a). Authorization No.	
12. Sponsoring Agency Name and Address Michigan Department of Transportation Construction and Technology Division P.O. Box 30049 Lansing, MI 48909		13. Type of Report & Period Covered Final	
		14. Sponsoring Agency Code	
15. Supplementary Notes			
16. Abstract Sustainable engineering includes the economic, environmental, and social impacts of design and construction choices and soon will become part of the standard approach to all engineering decision-making. One area for sustainable engineering is the efficient use of recycled and post-industrial products that optimize economic, environmental, and societal benefits derived from the construction of transportation infrastructure. This not only means the incorporation of materials into infrastructure that would otherwise be destined for the landfill, but the optimized use of these materials to add longevity to the structure being built. This study examined current national and international practices regarding the use of recycled concrete aggregates (RCA) as engineered materials by the transportation industry as well as a history of Michigan's experience with RCA. In the laboratory investigation, this study performed aggregate characterization and comparison to high-quality virgin aggregate materials in addition to porosity analyses of RCA. The use of RCA in concrete was evaluated through characterization of standard properties, ASR potential, and volumetric stability. Assessment of leachates occurring in the base material when using RCA was also conducted in comparison to blast furnace slag, limestone, and natural gravel.			
17. Key Words Recycled concrete, crushed concrete, aggregate, shrinkage, leachate		18. Distribution Statement No restrictions. This document is available to the public through the Michigan Department of Transportation.	
19. Security Classification - report	20. Security Classification - page	21. No. of Pages	22. Price

TABLE OF CONTENTS

TABLE OF CONTENTS.....	ii
LIST OF TABLES.....	vi
LIST OF FIGURES.....	vii
CHAPTER 1. RESEARCH OVERVIEW.....	1
1.1. Introduction.....	1
1.2. Background.....	1
1.3. Study Objective.....	2
CHAPTER 2. LITERATURE REVIEW ON RECYCLED CONCRETE AGGREGATES.....	4
2.1. Background.....	4
2.2. Construction Operations.....	4
2.2.1 Preparation of Existing Concrete.....	4
2.2.2 Breaking and Separation of Existing Concrete.....	5
2.2.3 Crushing Operations.....	7
2.2.4 Sizing and Yield of Recycled Concrete Aggregates.....	9
2.2.5 Storage Issues for Recycled Concrete Aggregates.....	10
2.3. Physical Properties of Recycled Concrete Aggregates.....	10
2.3.1 Mortar Content.....	10
2.3.1.1 Cement Type, Fineness, and Unhydrated Cement.....	11
2.3.2 Specific Gravity.....	12
2.3.3 Absorption Capacity.....	13
2.3.4 Freeze-Thaw Resistance.....	14
2.3.5 Soundness.....	14
2.4. Application of Recycled Concrete Aggregates in New Concrete.....	14
2.4.1 Fresh Concrete Properties.....	14
2.4.2 Compressive Strength.....	15
2.4.3 Flexural and Tensile Strength.....	15
2.4.4 Fracture Resistance.....	16
2.4.5 Modulus of Elasticity.....	16
2.4.6 Coefficient of Thermal Expansion.....	17

2.4.7	Drying Shrinkage	17
2.4.8	Creep	19
2.4.9	Material Durability.....	20
2.4.10	Carbonation and Carbon Sequestration	20
2.4.11	Concrete Mixture Design.....	21
2.5.	Application of Recycled Concrete Aggregates as Base Material	22
2.5.1	Unstabilized	23
2.5.2	Stabilized with Concrete.....	23
2.5.3	Stabilized with Asphalt Binder	24
2.6.	Other Applications of Recycled Concrete Aggregates	25
2.7.	Performance of Pavements Utilizing Recycled Concrete Aggregates.....	25
2.7.1	Construction Issues	31
2.7.2	Two-Lift Construction	32
2.8.	Michigan Experiences with Recycled Concrete Aggregates	33
2.8.1	Recycled Concrete Aggregate in New PCC	33
2.8.1.1	MDOT Specifications for Recycled Concrete Aggregate in New PCC	34
2.8.1.2	Load Transfer of RCA Concrete Pavements.....	35
2.8.1.3	Other RCA Concrete Pavement Performance Parameters	39
2.8.2	Recycled Concrete Aggregate as Base Material.....	39
2.8.3	Recycled Concrete Aggregate in Asphalt Concrete.....	40
2.8.4	Issues and Opportunities for Utilization of Recycled Concrete Aggregate in Michigan	40
2.9.	Summary	41
CHAPTER 3. SPECIFIC GRAVITY AND ABSORPTION CAPACITY OF RECYCLED CONCRETE AGGREGATE.....		43
3.1.	Introduction.....	43
3.2.	Experimental Procedures	44
3.2.1	Thin Sections of Aggregates.....	46
3.2.2	Image Analysis.....	47
3.3.	Results and Analysis	49
3.4.	Pore size distribution comparison using image analysis.....	51

3.5. Significance of Pore System for RCA	55
3.6. Summary and Conclusions	56
CHAPTER 4. LABORATORY INVESTIGATION OF RCA IN CONCRETE	58
4.1. Introduction.....	58
4.2. Experimental Methods	58
4.2.1 Material.....	58
4.2.2 Mixing Methodology	61
4.2.3 Testing Procedures.....	62
4.2.3.1 Preparation of Lapped Slabs	62
4.2.3.2 Black and White Contrast Enhancement Procedure	63
4.2.3.3 Image Collection	63
4.2.3.4 Automated ASTM C457	63
4.3. Hardened Properties Testing Plan.....	64
4.4. Fresh Concrete Properties Results	65
4.5. Hardened Concrete Properties	67
4.5.1 Modulus of Rupture	68
4.5.2 Elastic Modulus	69
4.5.3 Rapid Chloride Penetrability.....	70
4.5.4 Hardened Air Content.....	72
4.5.5 Volumetric Stability of RCA Concretes	74
4.5.5.1 Unsealed Prisms in 100% Relative Humidity.....	74
4.5.5.2 Unsealed and Sealed Prisms in 50% Relative Humidity	76
4.5.5.3 Restrained Shrinkage	81
4.6. Summary and Conclusions	82
CHAPTER 5. EXPERIMENTAL TESTING FOR THE LEACHATE	
CHARACTERISTICS OF BASE AGGREGATES.....	84
5.1. Background.....	84
5.2. Field observations	86
5.3. Laboratory leachate investigation.....	87
5.3.1 Leachate chemical analysis.....	88
5.3.1.1 SEM analysis.....	88

5.3.1.2 XRD analysis	91
5.4. Leachability volume and pH analysis	93
5.4.1.1 Total cumulative precipitate.....	93
5.4.1.2 Leachability of RCA	94
5.4.2 Leachate pH analysis	95
5.5. Discussion.....	96
5.6. Summary and Conclusions	97
CHAPTER 6. ASR EXPANSION ASSESSMENT USING ASTM C1260 MORTAR BAR TESTING.....	98
6.1. Background and Experimental Procedures.....	98
6.1.1 Aggregate Preparation	98
6.1.2 Mortar Bar Preparation	99
6.1.3 Mortar Bar Testing Procedure	99
6.2. ASR Expansion Results	100
6.3. ASTM C1260 Discussion	105
6.4. Recommendations.....	105
CHAPTER 7. SUMMARY AND CONCLUSIONS.....	107
CHAPTER 8. References.....	111
APPENDIX A.....	119
APPENDIX B	126
APPENDIX C	130

LIST OF TABLES

Table 2-1. Example of recycled concrete coarse aggregate specific gravity and absorption capacity by sieve size after (ACPA 2009).	13
Table 2-2. General performance of several concrete pavements using RCA for new PCC after (Cuttell et al. 1996).	28
Table 2-3. Comparison of performance of RCA and virgin aggregate sections from 1994 to 2006 surveys that have not had rehabilitation after (Sturtevant 2007).30	
Table 2-4. Cost savings from recycling concrete on US-59 project after (Halverson 1982).	31
Table 2-5. Volumetric surface texture test results after (Buch et al. 2000).	37
Table 2-6. Performance summary as a function of aggregate type, size, and treatment after (Frabizzio et al. 2000).	38
Table 3-1. Specific gravity and absorption by different test methods.	50
Table 4-1. Aggregate types used in laboratory assessment.	59
Table 4-2. Matrix of concrete mixtures prepared in the project.	59
Table 4-3 Mixture proportions of concretes (in lb/yd ³ of concrete).	61
Table 4-4. Fresh properties of concrete mixtures.	66
Table 4-5. Concrete chloride ion penetrability based on charge passed as per ASTM 1202.	71
Table 4-6. Spacing details of hardened air content in concrete (1 inch=25.4mm).	73
Table 4-7. Restrained ring shrinkage strains at 28 days for virgin and RCA MDOT P1 concretes.	82
Table 5-1. Summary of spot analyses from 1-2 week evaporation pan deposits collected from blast furnace slag aggregate.	91
Table 5-2. Mass of leachate deposits (unit: grams).	93

LIST OF FIGURES

Figure 2-1. Examples of (a.) impact breaker and (b.) resonant breaker.	5
Figure 2-2. Typical concrete pavement break pattern before removal (left) and Rhino horn attachment for use in separating concrete for removal (right) after (ACPA 2009).	6
Figure 2-3. Examples of crushing equipment used to produce RCA after (ACPA 2009).	8
Figure 2-4. Primary jaw crusher for reduction of concrete size after (USDOT 2004). ...	9
Figure 2-5. Virgin aggregate (left) and recycled concrete aggregate (right) in a moist condition after (Sturtevant 2007).	11
Figure 2-6. Average load-crack mouth opening displacement curves for virgin aggregate concrete (VAC), RCA concrete (RCAC), and 50-50 VA/RCA blend concrete mixtures after (Bordelon et al. 2009).....	16
Figure 2-7. Drying shrinkage values over time for partial replacement of virgin aggregate with RCA after (Roesler et al. 2009).	19
Figure 2-8. Concrete's carbon footprint reconsidered after (Deretzky 2009).	21
Figure 2-9. RCA stockpile containing small amount of RAP after (FHWA 2004).....	22
Figure 2-10. Weight loss from shearing of laboratory specimens for cement-treated base material after (Jung et al. 2009).	24
Figure 2-11. Wire gabion retaining wall structure.....	25
Figure 2-12. States recycling concrete as aggregate after (FHWA 2008a).	26
Figure 2-13. States recycling concrete as aggregate for base/subbase after (FHWA 2008a).....	27
Figure 2-14. States recycling concrete as aggregate in new PCC after (FHWA 2008a).	27
Figure 2-15. Two-lift concrete paving using two pavers after (Fick 2008).	32
Figure 2-16. Concrete pavement containing RCA as aggregate on I-94 WB, West of Kalamazoo.....	34
Figure 2-17. RCA concrete pavement LTE deterioration in southwest region of Michigan, Site 12 after (Frabizzio et al. 2000).	38

Figure 2-18. Effect of coarse aggregate type on number of cracks per slab for 41 foot (12.5m) joint spacing after (Frabizzio et al. 2000).....	39
Figure 3-1a. EDA (GeoPyc).	44
Figure 3-2. Schematic of EDA adopted from (Vitton et al. 1998).	45
Figure 3-3. Thin section of slag RCA.....	47
Figure 3-4. Thin section of limestone RCA.....	47
Figure 3-5. Section of scanned image.....	48
Figure 3-6. Methodology adopted for image analysis.	48
Figure 3-7. Comparison of porosity by different test techniques.	51
Figure 3-8. Percentage frequency of pore diameter for surface porosity using image analysis for (a) smaller pores and (b) larger pores.....	52
Figure 3-9. Image Analysis for Crushed Gravel Sample for (a.) Original Image, (b.) Image Processed for Blue Resin (Surface Porosity), and (c.) Image Processed for Yellow Resin (Internal Porosity).....	53
Figure 3-10. Image Analysis for Crushed Gravel RCA Sample for (a.) Original Image, (b.) Image Processed for Blue Resin (Surface Porosity), and (c.) Image Processed for Yellow Resin (Internal Porosity).....	53
Figure 3-11. Characterization of pore sizes and type in Portland cement-based materials (1 inch = 25.4 mm = 25,400 μ m).....	54
Figure 3-12. Percentage frequency of pore diameter for internal porosity using image analysis.....	54
Figure 4-1. Gradation of aggregates used in the study.	60
Figure 4-2. Unsealed, sealed, and restrained shrinkage specimens.	65
Figure 4-3. Comparison of initial slump using two different specific gravity measurement techniques.....	67
Figure 4-4. Compressive strength at 28 days.....	68
Figure 4-5. Modulus of rupture at 28 days.	69
Figure 4-6. Elastic modulus at 56 days.....	70
Figure 4-7. Chloride ion penetrability at 56 days.	71
Figure 4-8. Comparison of hardened air-content in concrete and air-content of RCA mortar fraction.....	72

Figure 4-9. Uniaxial shrinkage strains (growth) of prism specimens in 100% RH.	75
Figure 4-10. Weight loss of shrinkage prism specimens in 100% RH.	75
Figure 4-11. Uniaxial shrinkage strains of prism specimens at 50% RH in sealed conditions.	76
Figure 4-12. Weight loss by prism samples stored at 50% RH in sealed conditions.	77
Figure 4-13. Uniaxial shrinkage strains of prism specimens at 50% RH (unsealed).	78
Figure 4-14. Weight loss by prism samples stored at 50% RH in unsealed conditions.	79
Figure 4-15. Optical micrograph showing unhydrated cement (white particle) in attached mortar phase of RCA.	80
Figure 4-16. Uniaxial drying shrinkage strains of prism specimens at 50% RH.	81
Figure 5-1. 0.45 power gradation chart for MDOT open graded aggregate series 4G.	86
Figure 5-2. I-69 east of Flint; (left) partially plugged rodent screen; (right) blast furnace slag sludge behind screen.	86
Figure 5-3. I-75 near Bridgeport; Precipitate from high fines crushed concrete OGDC under shoulder.	87
Figure 5-4. SEM images taken from the leachate precipitated deposit of RCA in 1-2 weeks. Note: simulated acid rain water—first row, deionized water—second row; from left to right, upper, middle, lower gradation specification; magnification, 650x.	89
Figure 5-5. SEM images taken from the leachate precipitated deposit of blast furnace slag in 1-2 weeks. Note: simulated acid rain water—first row, deionized water—second row; from left to right, upper, middle, lower gradation specification; magnification, 650x.	89
Figure 5-6. Characteristic X-ray spectrum from a blast furnace slag leachate precipitate using SEM.	90
Figure 5-7. X-ray diffraction patterns obtained from the different aggregate precipitates.	92
Figure 5-8. Total cumulative precipitate weight vs. number of weeks soaking.	94
Figure 5-9. The leachate characteristics of RCA for acidic and de-ionized water sources.	95

Figure 5-10. pH vs. number of weeks soaking (4G lower (coarse) gradation—deionized water).....	96
Figure 6-1. Results of ASTM C1260 expansion tests for control experiment (no chert addition).	100
Figure 6-2. Expansion plot of 1.0% chert replacement experiment.	101
Figure 6-3. Expansion plot of 2.5% chert replacement experiment.	102
Figure 6-4. Expansion plots for natural gravel blends with error bars at one std deviation.	102
Figure 6-5. Expansion plots for limestone blends with error bars at one standard deviation.	103
Figure 6-6. Expansion plots for RCA blends with error bars at one standard deviation.	103
Figure 6-7. Expansion plots for fresh slag blends with error bars at one standard deviation.	104
Figure 6-8. Expansion plots for weathered slag blends with error bars at one std deviation.	104

CHAPTER 1. RESEARCH OVERVIEW

1.1. Introduction

Sustainable engineering includes the economic, environmental, and social impacts of design and construction choices and soon will become part of the standard approach to all engineering decision-making. One area for sustainable engineering is the efficient use of recycled and post-industrial products that optimize economic, environmental, and societal benefits derived from the construction of transportation infrastructure. This not only means the incorporation of materials into infrastructure that would otherwise be destined for the landfill, but the optimized use of these materials to add longevity to the structure being built.

The construction industry produces concrete as demolition waste. This material can be landfilled, used as rip-rap, or crushed to create aggregate for engineering applications (Wai K. et al. 2006; Wong et al. 2007). Since there are tremendous amounts of this material ready for reuse and a shortage of high-quality natural or virgin aggregates, the appropriate use of this material lowers the demand for natural resources, reduces the embodied energy of the finished structure, and reduces waste going to landfills (Wong et al. 2007).

The most common approach to using waste concrete is crushing the material to create recycled concrete aggregate (RCA). RCA can be incorporated into soil stabilization, subbase and base courses, and as aggregate for use in hot-mix asphalt (HMA) or Portland cement concrete (PCC). In general, the coarse-sized fraction is more easily utilized with the fine-sized fraction being used most often in the subbase and to improve the subgrade stability.

The ultimate goal is to increase the use of RCA in highway construction applications by incorporating best practices for application and standardization into the construction and engineering communities (Attarian 2007). To be a more widely used construction material, RCA must be readily available, economically feasible, environmentally acceptable under applicable regulations, and of sufficient quality to meet performance demands. Increased use of RCA in properly engineered transportation structures will ultimately improve the sustainability of concrete construction.

1.2. Background

Michigan's highway infrastructure is exposed to harsh winter conditions where concrete structures must endure cyclic freeze-thaw conditions under various stages of saturation and

exposure to deicing chemicals. Concrete pavement durability will also depend greatly on the performance of the unbound and bound materials on which the pavement is constructed. To construct sustainable pavements, it is essential to select materials that have a positive impact on the environmental footprint without compromising the structural integrity or durability of the structure.

However, there has been a reluctance to use RCA in highway infrastructure construction due to RCA's varying composition and the impact that variation can have on the durability and performance of the finished product. Today, available opportunities for RCA are typically restricted to access roads, non-structural applications, and precast applications, with the finer-sized particles and fillers going largely unused (Wong et al. 2007). Key factors that must be better understood to more efficiently utilize RCA include the amount of debris material generated annually, usable yield of recycled concrete, amount of residual adhered cement paste in the coarser sized material, chloride content, freeze-thaw susceptibility of a given source, and the source's potential for exacerbating alkali-silica reactivity (ASR).

Environmental considerations are also of high importance as identified in the key factors listed above. RCA is highly alkaline and typically contains uncharacterized levels of chlorides and other substances that can potentially contaminate groundwater during processing operations. When RCA is used, these substances may also result in corrosion of embedded steel, thereby reducing the long-term performance of the end product. When combined with binder in HMA or in PCC, the risk associated with runoff of these substances is believed to be reduced to a great extent (Wong et al. 2007). These concerns must be addressed before RCA is to gain widespread use in transportation infrastructure applications.

1.3. Study Objective

The main objective of this study was to identify and assess uses and risks associated with RCA as an engineered material in the transportation industry and thus to provide a framework for the use of this resource.

This study examined the following:

- Current national and international practices regarding the use of RCA engineered materials by the transportation industry
- A history of Michigan's experience with RCA in several applications

- Aggregate characterization and comparison to high-quality virgin aggregate materials
- In-depth porosity analyses of RCA
- Laboratory analysis of standard properties for concrete using RCA
- Volumetric stability of concrete using RCA
- Assessment of leachates occurring in the base material when using RCA in comparison to blast furnace slag, limestone, and natural gravel
- ASR expansion potential of mortars using RCA and a variety of other aggregate sources

CHAPTER 2. LITERATURE REVIEW ON RECYCLED CONCRETE AGGREGATES

2.1. Background

As high-quality natural aggregate resources become limited, the use of manufactured and recycled materials will become a more prevalent choice for aggregates in Portland cement concrete (PCC) structures. RCA provides an economical alternative while reducing the waste produced from PCC pavement reconstruction. While the performance of the majority of recycled concrete pavements has been satisfactory, some sites have performed poorly enough to cause concern regarding the feasibility of RCA use.

Variability in the quality of recycled aggregates is traceable to factors such as the mortar content, high absorption, quality of the natural aggregate used in the original concrete, microcracks in the aggregate due to breaking, crushing and processing of the existing PCC pavement, bond strength between the RCA and the new cement paste, and angularity and grading of the RCA. If these factors can be accounted for in the concrete mixture design and pavement structural design, recycled concrete pavements can be engineered to provide long-term sustainable solutions.

This chapter reviews the main factors involved in production, material characterization of recycled aggregates, applications of RCA in concrete and base material, as well as their documented performance in PCC pavement structures.

2.2. Construction Operations

The use of crushed concrete as an aggregate involves preparation, demolition, material sorting, crushing, sizing, and temporary storage of the material. This section outlines factors and general procedures for these processes.

2.2.1 Preparation of Existing Concrete

One of the most important factors for producing quality RCA is knowledge of the existing concrete in terms of its original mixture design, constituents, and material performance (ACPA 2009). The concrete mixture design gives some indication of the original water-to-cement ratio and the subsequent amount of mortar potentially adhering to the original aggregates. Knowing the constituents that comprised the original concrete such as the cement type, cement

fineness, aggregate type and air content, as examples, can help initially determine the waste concrete's potential quality as RCA. The original PCC field performance is perhaps one of the most important factors in determining an existing concrete's suitability for use as RCA. If the original concrete suffered distresses such as alkali-silica reaction (ASR) or D-cracking, that information is critical in determining the concrete's potential for use as RCA in a high-end application (e.g., concrete aggregate) as compared to a less risky application (e.g. base material, granular fill).

An existing concrete pavement must be prepared to minimize contamination issues. Surface preparation to prevent contamination of the concrete can include removal of joint sealant, and complete removal of asphalt overlays and patches (NHI 1998). Some agencies in Europe have reported contamination of recycled asphalt up to 20% by weight to have little effect on new concrete containing RCA as the primary coarse aggregate (FHWA 1992). These contamination level thresholds are dependent on eventual application of the RCA, agency experiences in using such material, and level of acceptable risk.

2.2.2 *Breaking and Separation of Existing Concrete*

Several methods exist for breaking existing concrete into sizes appropriate for crushing operations. These methods can be placed in two general categories: impact breakers (Figure 2-1a) and resonant breakers (Figure 2-1b). The impact breaker uses a single dynamic force (drop) to fracture the concrete pavement while the resonant breaker uses a high-frequency, low-amplitude pulse to fracture the concrete.

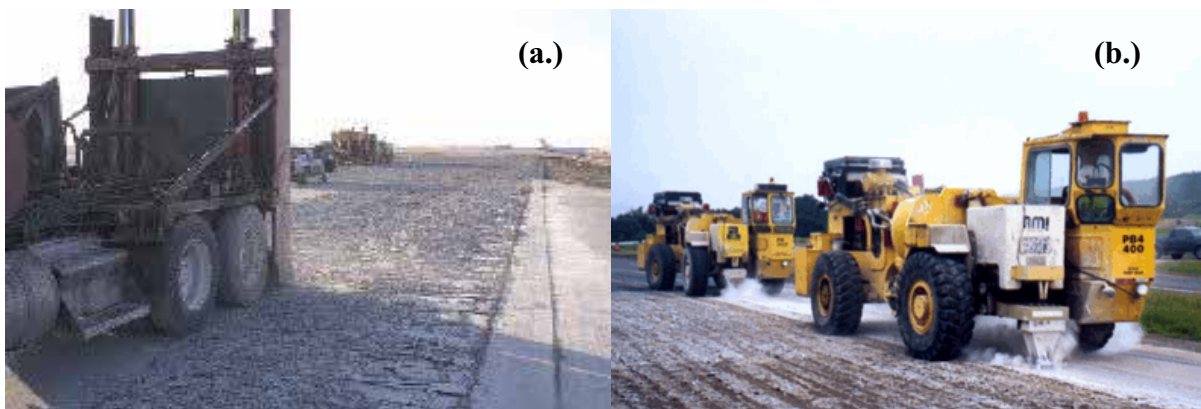


Figure 2-1. Examples of (a.) impact breaker and (b.) resonant breaker.

While both breaker types can be utilized to break up concrete effectively, each method has positive and negative factors that must be considered. Impact breakers have higher surface production rates of 9700 to 12000 ft²/hr (900 to 1,100 m²/hr) than that achieved by resonant breakers, which are typically less than 7200 ft²/hr (670 m²/hr) (Dykins and Epps 1987; NHI 1998). However, resonant breakers typically produce more uniform slabs of concrete as the fracture process is more consistent. Resonant breakers also produce less disturbance to the underlying layers, sewers, and utilities, which may be important in urban concrete recycling operations or for pavements that are placed on softer subgrades.

Removal of large-sized concrete pieces (e.g. less than 24 inches or 60 cm length) is typically accomplished using a backhoe with a rhino horn attachment (Figure 2-2) to separate the larger pieces from the fractured slabs that were created by the breaker. After this initial separation of concrete, front-end loaders can be utilized to lift and remove the fractured concrete slabs. Typically, these slabs are then transported to a crushing operation, which may either be on or off-site depending on the scope of the project.



Figure 2-2. Typical concrete pavement break pattern before removal (left) and Rhino horn attachment for use in separating concrete for removal (right) after (ACPA 2009).

The breaking operation must also ensure debonding of the existing concrete from the reinforcing steel. Since the current Michigan concrete pavement network is primarily jointed reinforced concrete pavements (JRCP), this issue is of the utmost importance for assuring limited contamination of the RCA. Further removal of reinforcing bars, wire mesh, or dowels can be

accomplished using large-scale electromagnetic separators. This action is most common with large projects where the concrete is brought to an off-site facility with this capability. Additional screening using manual labor to remove embedded and loose steel may also be required if the breaking operations were not completely successful. Transportation of fractured slabs and additional screening of material often adds significant cost to RCA material production and should be factored in the construction decision-making process.

2.2.3 Crushing Operations

While the preparation and breaking operation is significant in manufacturing quality RCA, the most important factor is the crushing operation. This step takes the fractured slabs generated from the breaking operations and reduces the size of the concrete to a level that can be utilized as aggregate. As crushers have traditionally been designed for mining operations that tend to crush and grind material to fine particle sizes, some challenges exist in utilizing these machines to get a usable coarse aggregate size, gradation, and yield from crushed concrete. While the crushing and sizing process can debond much of the old mortar from the original aggregate, these operations can also create micro-cracking in the attached mortar and original aggregate. This microcracking leads to potential RCA/new mortar bonding and RCA concrete fracture resistance problems when used in new concrete applications.

Off-site concrete recycling plants typically have multi-phase crushing operations to bring the fractured concrete slabs to more manageable sizes of 3-4 inches (8-10cm) during the primary crushing phase and then to the desired aggregate size in a secondary crushing phase (ACPA 2009). Three types of crushers exist to provide this step of the recycling operation and include jaw, cone, and impact crushers as seen in Figure 2-3. While jaw crushers are typically used for the primary crushing operation (Figure 2-4), cone crushers are used in a secondary step to reduce the size of the concrete to a product with a more uniform size distribution when compared to a jaw crusher. Impact crushers can be used in either primary or secondary crushing applications, depending on their size and capacity. The major advantage of the impact crusher is its ability to remove a larger percentage of old mortar from the original aggregates in comparison to the cone crusher. While mortar removal is important for producing a high quality RCA, it often results in less yield of coarse aggregates and produces more fine material that typically gets landfilled (ACPA 2009). A balance must be achieved for each project based on the desired aggregate

application and economics, which depends on local transportation costs, concrete quantity, and quality of the original concrete.

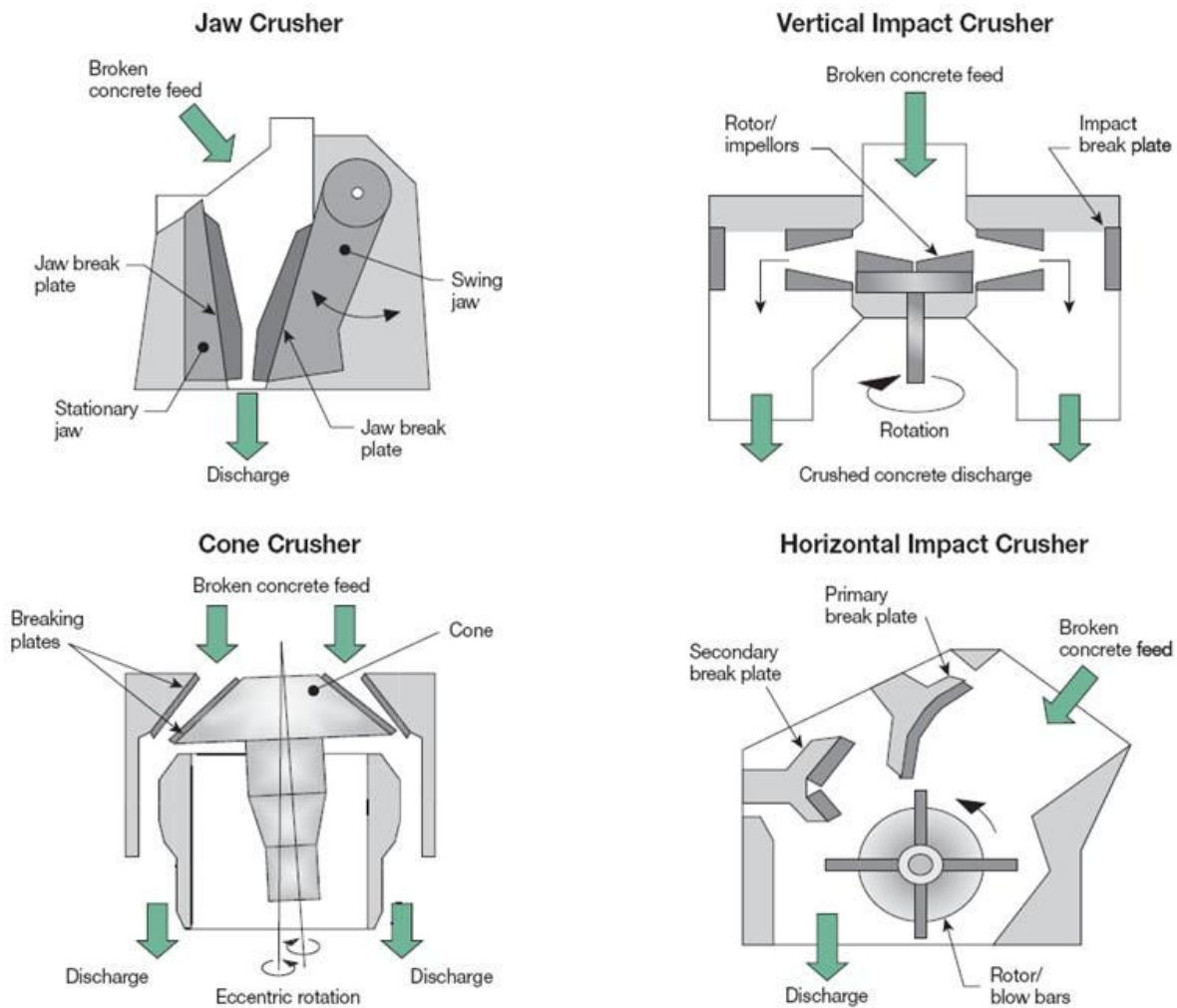


Figure 2-3. Examples of crushing equipment used to produce RCA after (ACPA 2009).

More commonly, relatively small projects utilize portable mini-concrete crushers that can be towed behind a truck for easy movement as well as less space requirements on the job site. These crushers also significantly reduce the hauling costs associated with off-site crushing operations. These smaller portable crushers can be effectively used to crush smaller quantities of concrete from 6-8 inch (150-200mm) sizes to aggregate sizes and tend to increase yield of coarse aggregate from the original concrete by leaving high contents of mortar on the RCA. This high attached mortar content can have a significant negative effect on the RCA performance in both bound and unbound applications and should be considered when the RCA is anticipated to be utilized in new concrete applications. While the cost of using these types of machines may be

less than off-site, two-phase crushing operations, the resulting quality of RCA must also be considered by both the contractor and transportation agency looking to reuse old concrete.



Figure 2-4. Primary jaw crusher for reduction of concrete size after (USDOT 2004).

2.2.4 Sizing and Yield of Recycled Concrete Aggregates

During the crushing operations, the maximum size of the aggregate can be controlled by adjusting the break plate distances. While this helps control the top-size of the aggregate, the overall grading is more difficult to control. Typically, the crushing operation provides a large amount of top-sized aggregate and a large volume of finer material. However, mid-range material sizes of 0.3-0.5 inches (8-13mm) are often less plentiful. This lack of mid-sized material leads to difficulties in achieving gradation specifications for use as base material or aggregate for new concrete. Due to this gap-graded phenomenon, utilization of recycled concrete can require additional sieving operations. This procedure can require greater expense by adding additional production time as well as leading to smaller yields of usable RCA as the mid-range sized material can govern the usage volumes due to gradation specifications.

The yield of aggregates from the crushing operation is typically related to the top-size of the required aggregate size. Larger top-size aggregates near 1.5 inches (38mm) can provide for

yields reaching 80% when comparing the volume of in-place concrete to aggregate produced. Smaller top-sized recycled concrete aggregates of 0.75 inches (19mm) may only result in a 55-60% yield due to the higher amount of fines produced through longer crushing times (NHI 1998). Austrian specifications require a minimum 65% yield to limit fines production and material loss due to demolition processes (Sommer 1994). This specification helps strike a balance between yield and achieving desired gradations from the crushing operations.

2.2.5 Storage Issues for Recycled Concrete Aggregates

Coarse RCA can generally be stockpiled using the same techniques and equipment as traditional coarse aggregates, although some differences exist. The exposure of precipitation to mortar and unhydrated cement in the RCA can lead to runoff from stockpiles that can be highly alkaline (Snyder et al. 1994). This alkalinity tends to level off after a few weeks. Runoff alkalinity is also partially neutralized by rain water, which is slightly acidic (Reiner 2008).

Concrete typically includes a small percentage of unhydrated cement as the full cement hydration process is not typically achieved in the original concrete. This unhydrated cement becomes a significant issue in fine RCA stockpiles as these aggregates can experience cementing through either direct water exposure or high humidity. Fine aggregate stockpiles should therefore be protected from external moisture when possible (ACPA 2009). Protecting fine RCA from external moisture is one of several factors that make the use of fine aggregates produced through RCA crushing operations difficult.

2.3. Physical Properties of Recycled Concrete Aggregates

Recycled concrete aggregates have physical similarities and distinct differences from virgin aggregates. As the original aggregate comprises a majority of the volume of RCA, its physical properties have a clear effect on the subsequent RCA properties. However, unhydrated cement and the attached mortar's porosity make RCA a more complicated material for characterization.

2.3.1 Mortar Content

A Canadian study on RCA reported the mortar content of RCA can be as high as 41% by volume depending on the original concrete mix proportions and crushing operations (Fathifazl 2008). The volume of mortar in the RCA also depends significantly on the original aggregate

type. Rounded, less porous aggregates tend to break at the aggregate-mortar interface more often than aggregates that do not need to rely solely on shear resistance for bond (i.e. porous or crushed aggregates). The mechanical properties of the RCA as either an unbound base material or bound by cement or asphalt sources are highly influenced by this factor. A visual difference is apparent between the RCA and virgin aggregate sources, in most cases, due to this attached mortar (Figure 2-5).



Figure 2-5. Virgin aggregate (left) and recycled concrete aggregate (right) in a moist condition after (Sturtevant 2007).

2.3.1.1 Cement Type, Fineness, and Unhydrated Cement

The Portland cement production process can have an impact on the resulting concrete and eventual characteristics of RCA. After production of clinker in the cement kiln, this material is ground with calcium sulfate (typically gypsum) to be utilized as Portland cement. Over time, the grinding process has become more substantial in its impact on the fresh and hardened properties of concrete (Higginson 1970). As the demand for higher early strength concrete has become more prevalent, the chemical composition of the cement has changed to include additional faster-hydrating tricalcium silicate (C_3S) and less dicalcium silicate (C_2S), which contributes to long-term strength (Gebhardt 1995; Tennis and Bhatta 2006). In addition, the fineness of Portland cement has increased, leading to earlier strength gains required to expedite construction of concrete structures. The increase in fineness and specific surface area of modern cement has also lead to quicker hydration of the cement and less unhydrated cement particles (Price 1974).

For recycled concrete, the unhydrated cement grains from older, coarser cement has an impact on its use in new applications. The crushing process can re-expose the unhydrated cement in RCA to water, which then can lead to changes in physical properties of both the aggregate and new RCA concrete that may be unexpected. These may include positives factors such as increased strength due to an artificially decreased water-to-cementitious material ratio (w/c), but may also lead to unexpected issues such as increases in drying shrinkage that may result in unintended stresses and premature cracking in the new concrete. For more recently produced cements with a high Blaine fineness (ASTM-C204 2008), this may be less of an issue as more, but not all, of the original cement may be hydrated.

Since older Portland cements typically contain a higher percentage of slow-reacting C_2S as compared to modern cement, RCA produced from older concrete may have more unhydrated cement present and available for reaction with water when re-exposed to water in new concrete. Newer Portland cements have less C_2S and a higher percentage of C_3S , which produces a higher volume of porous and weaker crystalline calcium hydroxide (CH) in comparison to a more durable and less porous amorphous calcium silicate hydrate (CSH) (Mindess et al. 2002). This change in Portland cement composition may have negative impacts on the bonding and permeability of the RCA with new concrete. CH also undergoes carbonation, leading to a progressive increase in permeability near the concrete surface over time.

2.3.2 *Specific Gravity*

The specific gravity of RCA is highly dependent in its mortar content. As the aggregate size is reduced, the amount of mortar, as a percentage of the total volume of the RCA, increases and subsequently reduces the specific gravity as voids from the mortar are more prevalent in the RCA. This trend is illustrated in Table 2-1.

The impact of grading on the specific gravity and absorption capacity of RCA is also important. RCA particles at the finer end of a gradation specification may meet the standard, but will result in a concrete with a high water demand from the aggregates. Workability from RCA concrete can be reduced due to this water demand as aggregates pull mix water into the aggregate pore structure. The additional fine RCA material can likely lead to other serious issues such as high drying shrinkage, low modulus of elasticity, and low fracture resistance in new concrete. If used as a base material, these same properties will lead to a reduction in draining

potential and longer lengths of time in saturation conditions, resulting in less support and poorer pavement performance.

Table 2-1. Example of recycled concrete coarse aggregate specific gravity and absorption capacity by sieve size after (ACPA 2009).

Sieve size, inches	% Retained	Bulk specific gravity	Absorption Capacity (%)
1 (25mm)	2	2.52	2.54
0.75 (19mm)	22	2.36	3.98
0.5 (12.5mm)	33	2.34	4.5
0.375 (9.5mm)	18	2.29	5.34
0.19 (4.75mm)	25	2.23	6.5
Weighted average	100	2.31	5.0

2.3.3 Absorption Capacity

Absorption capacities of RCA are consistently higher than virgin aggregate due to the inclusion of the old mortar (Vancura et al. 2010). These values can range from 2% to 10% in some extreme cases, depending on the original aggregate's absorption capacity, original concrete's mix proportions, and crushing operations.

For use in new concrete, the water demand created by the use of RCA can be significant. Ensuring saturation of the RCA during the mixing process can also be a concern. Due to the porous nature of RCA, the water demand using a semi-long term soaking test such as ASTM C127 (2008) may not represent the absorption of the RCA during the mixing process and subsequent cement hydration process. This standard semi-long moisture conditioning period is typically 24 hours (+/- 4 hours) as described in ASTM C127. This can lead to poor workability or a short window of good workability for RCA concretes.

In an attempt to aid the water absorption process during concrete mixing, many researchers have proposed saturating the RCA before mixing (Abrams 1922; Roesler et al. 2009; Tam and Tam 2008; Tam et al. 2008). However, one study (Poon et al. 2004b) showed that when RCA aggregates were conditioned to a saturated surface dry (SSD) state, the high water content inside the RCA resulted in localized bleeding. This led to a higher localized w/c ratio, weaker interfacial transition zone (ITZ), poorer fracture resistance, and strength (Poon et al. 2004a).

2.3.4 Freeze-Thaw Resistance

The freeze-thaw resistance of RCA varies (Blankenagel and Guthrie 2006) and is dependent on factors such as the absorption of the original aggregate source and the pore system of the attached mortar in order to relieve internal pressure that may cause fracturing of the aggregate (Mindess et al. 2002). D-cracked pavements have been successfully recycled into aggregates for use in unstabilized subbases (ACPA 2009). When D-cracking susceptible RCA has been used in new concrete, the RCA top-sized aggregate has typically been reduced to 0.75 inches (19mm) in order to alleviate the distance entrapped water would need to travel to find relief from hydraulic pressures in a properly air-entrained mortar system (ACPA 2009).

2.3.5 Soundness

Soundness testing of an aggregate is an indirect method to assess an aggregate's durability. While RCA typically fails the sulfate soundness test (ASTM-C88 2008) using sodium sulfate, the same aggregates tended to perform well in ASTM C88 using magnesium sulfate in a limited study (Snyder et al. 1994). This result is contrary to how most virgin aggregates perform. Overall, ASTM C88 testing has been inconclusive and may not be applicable to RCA.

2.4. Application of Recycled Concrete Aggregates in New Concrete

As discussed previously, the properties of recycled concrete aggregates differ greatly from those of virgin aggregates primarily due to the existence of mortar attached to the aggregate. While virgin aggregates are typically considered semi-inert filler in concrete, these differences in RCA can cause the aggregates to become active in modifying the performance of new concrete. This excess mortar tends to affect the mechanical and deformation properties of the RCA concrete (Ravindrarajah et al. 1987). The following sections provide an overview of both fresh and hardened concrete properties as affected by RCA use.

2.4.1 Fresh Concrete Properties

Ravindrarajah et al. (1987) found that RCA concrete mixtures tended to exhibit higher workability loss over the first two hours in comparison to virgin aggregate mixtures prepared using the same *w/c*. The initial and final set time measured through penetration resistance of RCA mixtures tended to be shorter when compared to concrete made using virgin aggregates.

This trend was attributed to the higher absorption characteristics of the recycled aggregates compared to virgin aggregates (Ravindrarajah et al. 1987). Other issues such as the inherent angularity and rough surface texture can also explain the workability decrease in comparison with normal concrete mixtures (Wade et al. 1997).

Due to the porous nature of most recycled aggregates, air content is preferably measured using a volumetric meter (ASTM-C173 2008) instead of the more commonly used pressure meter (ASTM-C231 2008).

2.4.2 Compressive Strength

Ravindrarajah et al. (1987) found that RCA mixtures consistently produced compressive strengths that were 10% lower on average than those found in virgin aggregate mixtures, at the same w/c , regardless of curing time. In another study by Tavakoli and Soroushian (1996b), the mean 28-day compressive strengths of RCA concretes were shown to differ from that of virgin aggregate concretes, at a 98% level of confidence, at identical w/c and mixing conditions. This result was correlated with the mortar content and increased Los Angeles (L.A.) abrasion loss of the recycled aggregates. However, it was also found that the original aggregate quality had a large influence as the compressive strength of the original concrete tended to correlate with the compressive strength of the RCA concrete. As a contradiction, compressive strengths were found to equal or surpass those of control specimens in many cases in a study of RCA pavement concretes (Wade et al. 1997). These conflicting results would suggest there is no clear trend of reduced compressive strength associated with using recycled aggregates, but the potential for reduced compressive strengths may exist.

2.4.3 Flexural and Tensile Strength

Research shows that while the flexural and tensile strength of RCA concrete is lower than concrete mixtures using virgin coarse aggregate, the difference is 10% or less for a given w/c ratio (Ravindrarajah et al. 1987). Again, compared to concrete prepared using virgin coarse aggregate, splitting tensile strength was shown to be equal, or in some cases greater, when comparing RCA concrete to conventional concrete mixtures (Tavakoli and Soroushian 1996b). However, conventional relationships based upon the measured compressive strength tended to under predict the splitting tensile and flexural strength of the RCA concrete due to its lower compressive strengths.

2.4.4 Fracture Resistance

Several researchers have shown that concrete using RCA had a reduced fracture energy and critical stress-intensity value of fracture toughness, K_{Ic} , in comparison to concrete prepared with virgin aggregates (Casuccio et al. 2008; Jianzhuang et al. 2010; Nishibata et al. 2006; Park et al. 2008). For RCA concrete, the post-peak behavior during the formation of a structural crack is typically more brittle, which leads to rapid crack propagation and deterioration (Bordelon et al. 2009). Due to the increased size of the RCA concrete's ITZ (aggregate-mortar surface) and inherent micro-fractures within the old mortar, the fracture process zone near the crack tip will have less resistance to further propagation and become more susceptible to the formation of structural cracks in the concrete (Poon et al. 2004a). While the use of 100% RCA tends to decrease the concrete's fracture resistance, blending virgin aggregate with RCA can provide fracture toughness similar to that of virgin aggregate mixtures as seen in Figure 2-6.

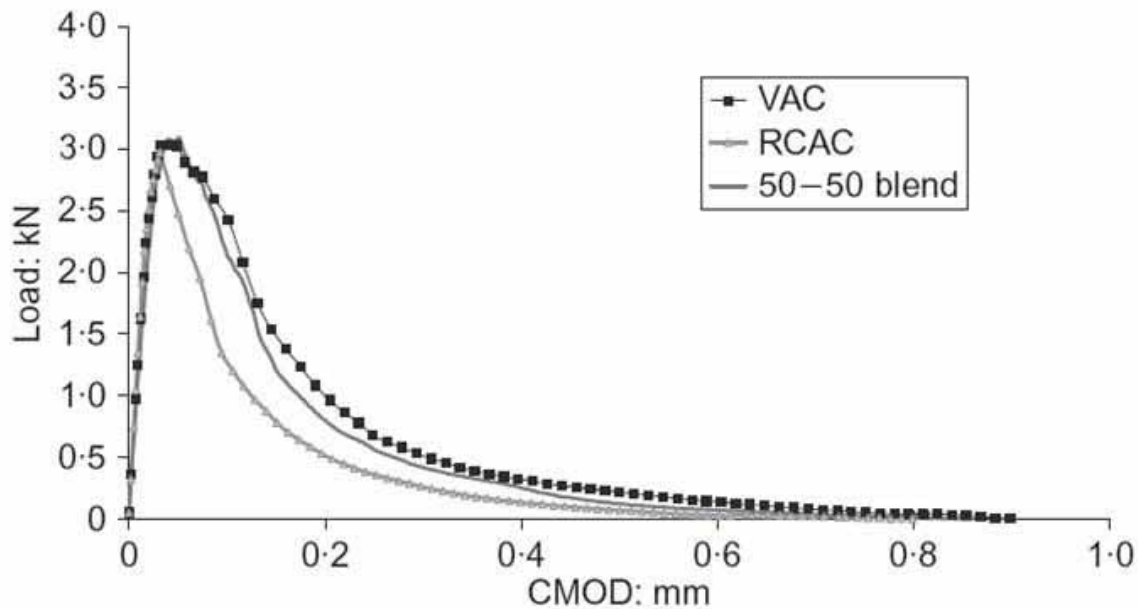


Figure 2-6. Average load-crack mouth opening displacement curves for virgin aggregate concrete (VAC), RCA concrete (RCAC), and 50-50 VA/RCA blend concrete mixtures after (Bordelon et al. 2009).

2.4.5 Modulus of Elasticity

Static modulus values for RCA concretes have been shown to be reduced by 25-35% from that of virgin aggregate concretes, depending on the curing conditions (Tavakoli and Soroushian 1996b). In one study (Ravindrarajah et al. 1987), the dynamic modulus was found to

be lower by approximately 15% after 7 days and approximately 25% after 90 days of curing. Wade et al. (1997) reported that static modulus values of RCA concretes were consistently lower and that dynamic moduli values were up to 18% lower when compared to virgin aggregate control specimen counterparts. The elastic moduli of the old mortar, new mortar, and the aggregates are typically higher than when combined in the resulting RCA concrete. Since the elastic modulus is a function of the composite system of these three factors, the lower elastic modulus of concrete containing RCA is actually a function of the deformations resulting at the ITZ, microcracking in the attached mortar, and the incompatibility of these materials at this interface.

2.4.6 Coefficient of Thermal Expansion

There is some debate whether the use of RCA reduces or increases the coefficient of thermal expansion (CTE) of new concrete in comparison to virgin aggregate concrete. While most studies have shown up to a 30% increase in the coefficient of thermal expansion through the use of RCA (ACPA 2009), others have shown little to no effect (Li 2007). A Canadian study on RCA concrete has actually shown a significant decrease in the CTE as the percentage replacement of virgin aggregate increases up to 50% (Smith and Tighe 2009). This result agrees with FHWA conclusions regarding CTE of RCA concretes (FHWA 2004). With the advent of mechanistic-empirical analysis and design procedures for concrete pavements (ARA 2007), this factor needs clarification as its impact is significant to the predicted performance of rigid pavement structures in terms of fatigue crack development.

2.4.7 Drying Shrinkage

RCA concrete has historically had a higher level of drying shrinkage than that of virgin aggregate concretes due to the combined effects of adhering mortar on the aggregates and lower modulus of elasticity values (Ravindrarajah et al. 1987). Instead of being filler material as normal virgin aggregates have been considered in the past, RCA actively affects concrete in terms of creating higher drying shrinkage and subsequent stresses in restrained concrete structures.

With three days of water curing, the average drying shrinkage level for virgin aggregate concrete was found to be approximately 200 $\mu\epsilon$ after 90 total days of hydration (Ravindrarajah et al. 1987). For the RCA concrete specimens, the drying shrinkage level was about 325 $\mu\epsilon$ under

the same conditions. This 60% increase in shrinkage would have a profound effect on the design of a PCC pavement if taken into consideration due to the differential drying phenomenon that occurs in a pavement structure. These severe differential drying shrinkages manifest themselves as one of the factors leading to permanent built-in curling, in addition to construction curl from temperature gradients at time of set and cyclic moisture warping (Heath et al. 2003; Hiller and Roesler 2008; Rao and Roesler 2005a; Rao and Roesler 2005b). Built-in curling of concrete slabs can lead to ride quality issues in addition to promoting slab corners to be unsupported by underlying layers. This built-in curling can become significant enough to affect the timing and location of fatigue cracks that fail concrete pavements (Hiller and Roesler 2006).

Tavakoli and Soroushian (1996b) reported similar drying shrinkage results comparing concrete with virgin and recycled aggregates in Michigan, for a variety of w/c ratios and maximum aggregate sizes, using ASTM C157 (2008). This same study also noted that higher amounts of adhering mortar, as estimated by the RCA water absorption, lead to higher shrinkage levels of the concrete.

For RCA concrete with only partial replacement of virgin aggregate, drying shrinkage is still consistently higher than that of solely virgin aggregate concrete (Fathifazl 2008). The use of silica fume (SF) or fiber-reinforcement may help reduce the concrete's permeability or increase the slab's bending capacity, respectively, but these solutions will not help lessen the drying shrinkage causing volumetric instability issues as seen in Figure 2-7.

Other researchers have consistently noted that the drying shrinkage of RCA concrete is significantly higher than that of virgin aggregate concrete (Ayano et al. 2009; Ayano and Wittmann 2002; Cusson and Hoogeveen 2008; Domingo-Cabo et al. 2009; Gómez-Soberón 2003; Poon et al. 2009; Roesler et al. 2009; Tavakoli and Soroushian 1996a; Tia et al. 2009a; Tia et al. 2009b). While this may be a problem when using standard concrete pavement sections with RCA concrete, design modifications such as smaller slabs, slightly thicker cross-sections, or two-lift paving with RCA concrete under more volumetrically stable concrete may help alleviate the additional stresses induced in the pavement system. The use of RCA concrete in the bottom lift of two-lift paving controls the driving force of drying shrinkage (relative humidity) in the RCA concrete pores, thereby keeping that concrete more volumetrically stable.

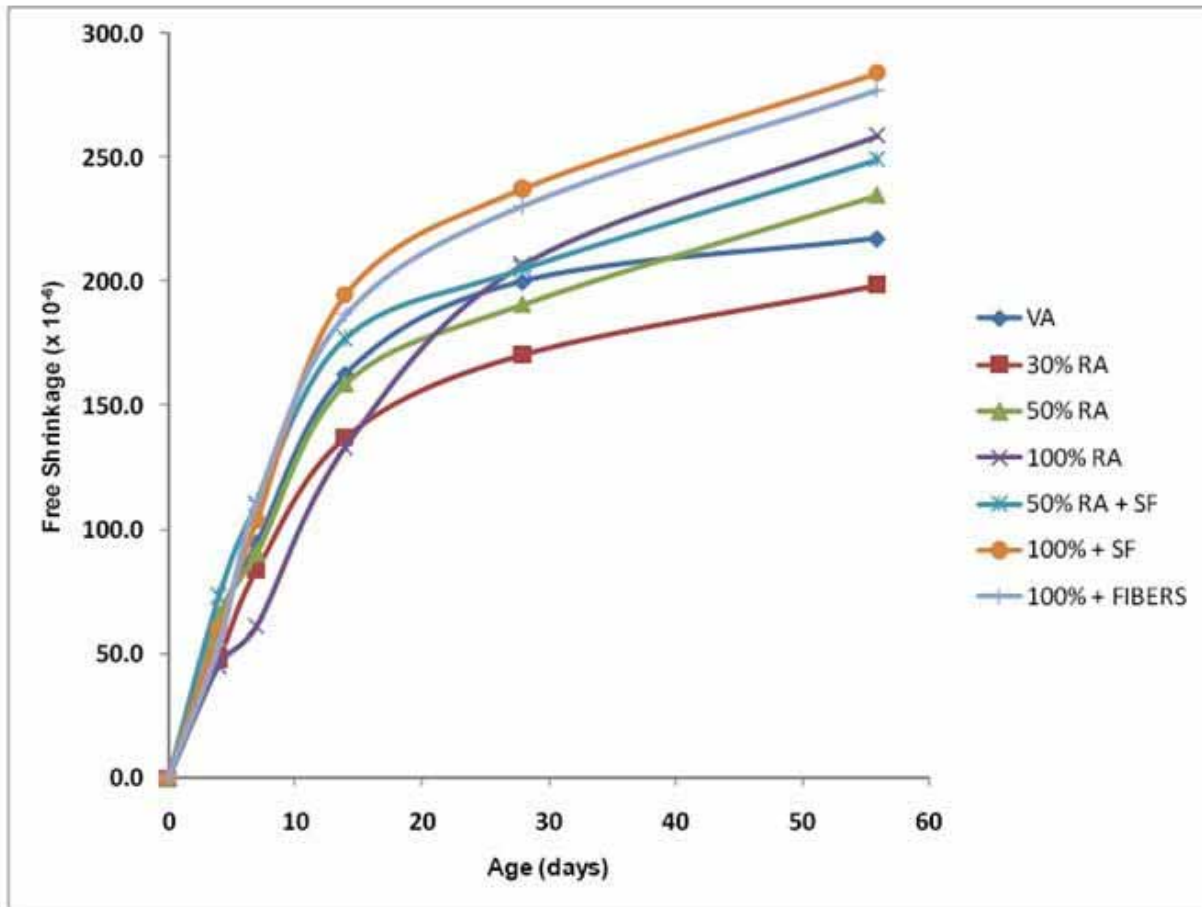


Figure 2-7. Drying shrinkage values over time for partial replacement of virgin aggregate with RCA after (Roesler et al. 2009).

2.4.8 Creep

Due to the higher absorption capacity of RCA, creep in RCA concrete is greater than that observed in concrete made from virgin aggregates (Gómez-Soberón 2003). This difference has been reported to be in the range of 30-100% greater than virgin aggregate concrete, depending upon the concrete mixture proportions, curing conditions, and characteristics of the RCA used in the concrete mixture (ACPA 2009; Ayano et al. 2009; Domingo-Cabo et al. 2009; Tia et al. 2009b).

For use in pavement structures, the creep characteristics of RCA concrete can be somewhat advantageous as the resulting concrete has the ability for relaxation of residual stresses due to dowel and tie bar restraint as well as curling and warping stresses. However, the level to which this advantage can be utilized is design-specific. The increased drying shrinkage

induced in the pavement may negate the advantage of stress relaxation completely depending upon the RCA type, mixture design, and early-age curing practices.

2.4.9 Material Durability

RCA concretes have been found to perform similarly to virgin aggregate concretes in many durability related tests including chloride resistance, freeze-thaw resistance and abrasion (Limbachiya et al. 2000). Salem and Burdette (1998) found that RCA concrete had a reduced level of freeze-thaw resistance due to the high absorption level of the RCA. The freeze-thaw resistance was found to improve significantly by the addition of fly ash to the mixture to decrease permeability, or by the addition of air entrainment to create a more effective pore system.

Coarse aggregates with a previous history of alkali-silica reaction (ASR), or the potential for such a reaction, are quite susceptible to ASR when used in RCA concrete (Gress and Kozikowski 2000). D-cracking susceptible coarse aggregates are generally known to increase the potential for recurrent problems in RCA concretes as well (Wade et al. 1997).

2.4.10 Carbonation and Carbon Sequestration

Carbonation is the process of concrete absorbing carbon dioxide (CO_2) from the atmosphere. The primary contributor to this process is the CO_2 reaction with the calcium hydroxide ($\text{Ca}(\text{OH})_2$) in the hardened cement paste to form calcium carbonate (CaCO_3) (Neville 1996). While carbonation does not cause severe deterioration of the concrete itself, it can have serious effects including destruction of the protective passivity layer on reinforcing steel. In restrained systems, the near surface of the concrete can undergo carbonation shrinkage, inducing some levels of stress. On the positive side, carbonation, or carbon sequestration, can allow for concrete's carbon footprint to be reduced through this absorption process.

The rate and depth of carbonation is dependent on the w/c ratio, hydration processes, permeability of the hardened cement paste, and ambient relative humidity. Recent studies suggest that 5% of the CO_2 production during Portland cement production can be reabsorbed through the normal service life of a concrete structure as demonstrated in Figure 2-8 (Deretzky 2009). Carbonation is important for RCA as the crushing operation re-exposes hydrated cement paste that may not have been exposed to CO_2 , since only concrete near the surface with exposure to CO_2 becomes carbonated. This CO_2 absorption may help reduce concrete's carbon footprint

even more if the concrete crushing and storage plan is made to maximize expose of the RCA to the atmosphere with minimal disturbance to the construction processes.

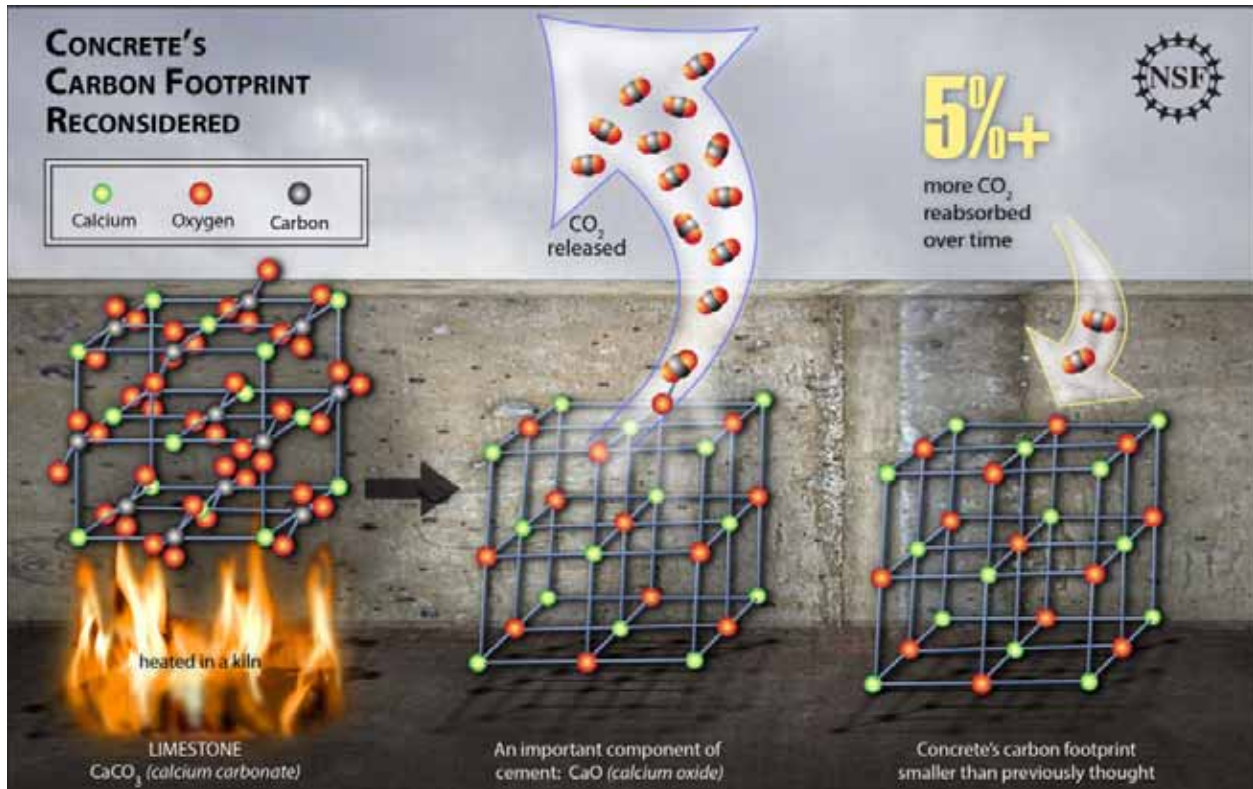


Figure 2-8. Concrete's carbon footprint reconsidered after (Deretzky 2009).

2.4.11 Concrete Mixture Design

Concrete mix design using standard procedures for proportioning and mixing for RCA mixtures can lead to poor concretes with respect to fresh and hardened states in comparison to similar virgin aggregate mixtures. A more appropriate method for addition of mixing water into RCA concrete may lie in a two-stage mixing approach (TSMA) (Tam and Tam 2008). This process allows for addition of water at two distinct times in an attempt to improve the absorption of water into the RCA first, and then provide the water for cement hydration later in the mixing process. This mixing process helps alleviate issues with localized variances of w/c ratios in the paste. This method also provides some partial addition of cement with early water additions to introduce a cement slurry to the mixer and help fill some of the RCA porosity and micro-cracking in its attached mortar phase.

Another approach to concrete mixture design is to count the mortar fraction of the RCA as part of the mortar system in the new concrete. Research in Canada has developed an

equivalent mortar volume (EMV) method to account for this factor (Fathifazl 2008). This method assures that the total amount of virgin aggregate in the new concrete is consistent with a concrete mixture prepared using a virgin aggregate. Initial research using the EMV method has shown promising results in alleviating detrimental effects such as shrinkage, reduced elastic modulus, and poor durability (Fathifazl 2008).

2.5. Application of Recycled Concrete Aggregates as Base Material

Unbound pavement layers used in flexible and rigid pavements have multiple functions regardless of the aggregate type used, including the following:

- Stable construction platform for placing the surface layer
- Insulation to prevent frost in a fine-grained subgrade
- Sub-surface drainage
- Structural capacity, particularly in flexible pavements.

Many transportation agencies have successfully employed RCA as a supporting material for the pavement surface layer. The use of RCA in unbound pavement layers is beneficial to contractors with respect to processing and stockpiling RCA as these types of uses allow for modest amounts of contaminants to be present (e.g. asphalt concrete) in the RCA stockpile (Figure 2-9). The Minnesota Department of Transportation permits up to 3% of recycled asphalt pavement (RAP) in its RCA (FHWA 2005), while Caltrans has no specific limit of the RCA/RAP ratio for inclusion as unstabilized subbase material (FHWA 2004).



Figure 2-9. RCA stockpile containing small amount of RAP after (FHWA 2004).

2.5.1 Unstabilized

Due to its angularity and potential for some level of re-cementing, RCA can serve well in a dense-graded base application (ACPA 2009). A recent report (NCHRP 2008) notes that the properties of RCA affect unstabilized base and subbase pavement layers properties, including shear strength, stiffness, toughness, durability, frost susceptibility, and permeability. However, the primary performance indicator of an unstabilized layer is shear strength and stiffness as determined by the resilient modulus test. With respect to these properties, RCA performed well, although the stiffness was not as high compared to base layers constructed using virgin aggregates or RCA/virgin aggregate blends (NCHRP 2008).

The ability for crushing operations to produce larger-sized angular aggregates tends to allow a structurally sound supporting layer when RCA is used in a drainable base layer. Concerns with using RCA in an open-graded system include dust, leachate, and alkalinity issues. One way of treating these problems is through washing of the RCA stockpiles before placement to reduce fine particles that contribute significantly to high pH and sedimented leachates that can clog the collector pipes in sub-surface drainage systems (Bruinsma 1995). Unstabilized RCA bases can increase the pH level of subsurface moisture that can runoff into drainage systems and groundwater. This effect is reduced over time as pH values stabilize to normal levels.

2.5.2 Stabilized with Concrete

The use of stabilization with Portland cement can help provide a stronger and stiffer base for better support of the pavement surface layer. The potential for leachate in these systems is also reduced as migration of fine-grained RCA, and the dissolution and transport of $\text{Ca}(\text{OH})_2$, is limited by the hardened cement paste system (ACPA 2009). Research in Texas has shown that a 1.5% cement addition should be made for RCA stabilized base layers instead of the customary 3% as some re-cementing will likely occur from previously unhydrated material in the RCA (Guthrie et al. 2002). The remnant unhydrated cement can cause these bases to set quicker than cement-treated bases with virgin aggregates while providing higher densities (roughly 2% higher) and better long-term strength (Lim et al. 2003).

The erosion potential of RCA cement stabilized bases was found to be similar to that of normal cement-treated bases, yet better performing than bases with RAP inclusions mixed with virgin aggregates (Jung et al. 2009). In a shear-inducing test to monitor both shear resistance of

a base material as well as the base material's ability to maintain bond with a concrete surface layer, the RCA stabilized base material had very little erosion at both low and high shear stresses as shown in Figure 2-10.

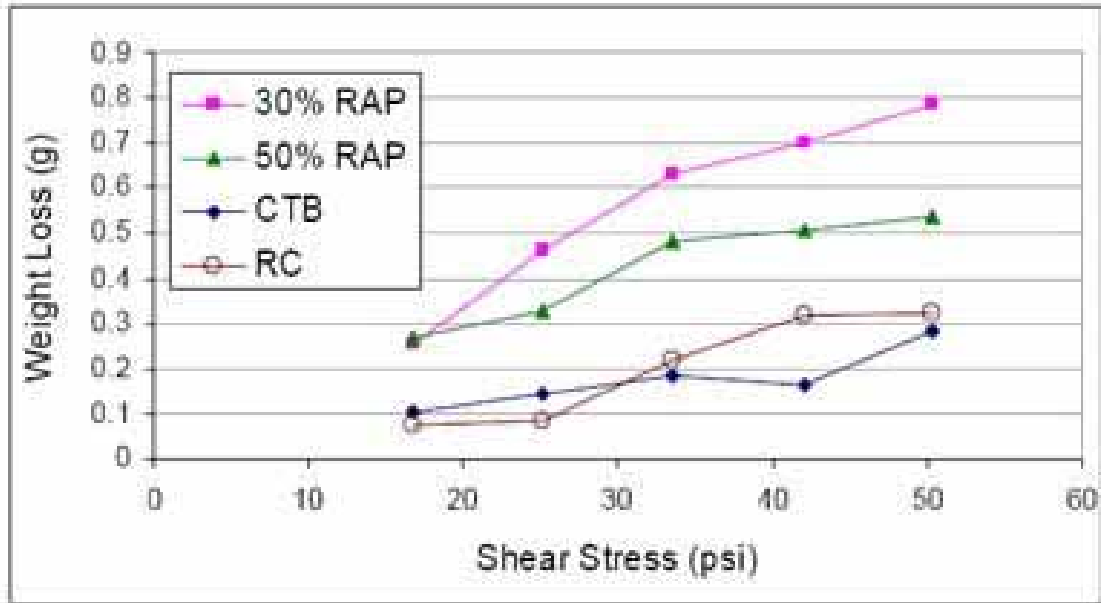


Figure 2-10. Weight loss from shearing of laboratory specimens for cement-treated base material after (Jung et al. 2009).

2.5.3 Stabilized with Asphalt Binder

An Australian study of RCA asphalt-stabilized base material found that the bulk density, voids in mineral aggregates, and voids filled with binder and film thickness were lower when using RCA in comparison with mixtures prepared using virgin aggregates. The resilient modulus was found to be lower, while air voids were generally higher for RCA asphalt concrete material (Paranavithana and Mohajerani 2006). While the quality of the RCA asphalt-stabilized base material was generally less than that obtained using virgin aggregates, the material could still be constructed to meet minimum specifications. With the highly porous surface of RCA, the amount of asphalt absorbed into the aggregate is greater than typically achieved with virgin aggregate. This increased absorption leads to reduced resistance to aging or the need for an increased amount of asphalt binder to provide film thickness (greater than 0.4 mils or 10 μm) for durability and meet air void requirements for stability. The need for clean aggregates may potentially lead to bonding issues with the asphalt binder as RCA typically contains much fines on the surface after crushing and processing.

2.6. Other Applications of Recycled Concrete Aggregates

RCA has other applications in transportation infrastructure that are not related to structures including use as granular fill, erosion control, soil stabilization, landscaping, railroad ballast, agricultural soil treatments, treatment of acidic lake waters, trickling filters and effluent treatment, and to fill wire gabions (Figure 2-11) for use in retaining walls (ACPA 2009). In most cases (erosion control using rip-rap, granular fill, railroad ballast), larger-sized particles can be utilized to limit the required crushing operations, increase yield of usable RCA material, and provide an economical alternative to virgin aggregates for these applications. The use of fine-grained RCA for soil stabilization is potentially a source for low-cost construction platform building during months when the soil moisture content is high.



Figure 2-11. Wire gabion retaining wall structure.

2.7. Performance of Pavements Utilizing Recycled Concrete Aggregates

According to a survey of state DOT's in 1996 (Chini et al. 1996), 10 of the 32 responding agencies that recycle concrete utilized RCA in new PCC pavements. Some of the primary

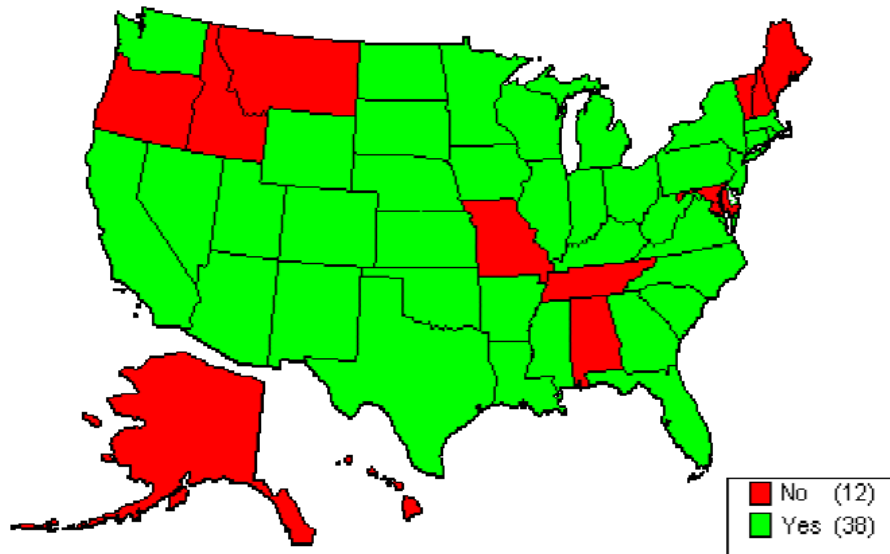


Figure 2-13. States recycling concrete as aggregate for base/subbase after (FHWA 2008a).

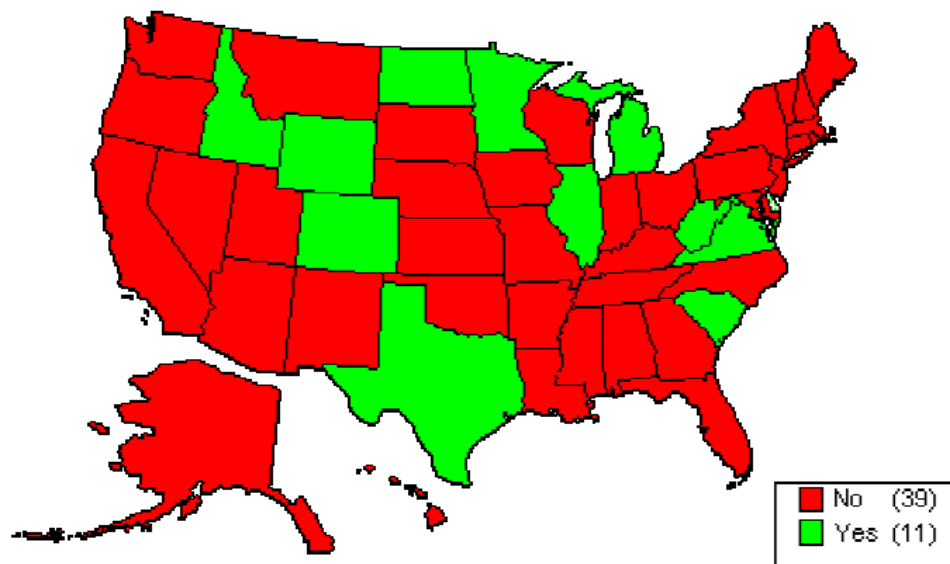


Figure 2-14. States recycling concrete as aggregate in new PCC after (FHWA 2008a).

In a multi-state study of RCA concrete pavements, Cuttell et al. (1996) reviewed some similarities and differences between good-performing pavements and pavements with early distresses. While the study focused only on pavements that were fairly young (7-15 years after construction), the performance of the sections were generally similar to expectations for concrete using virgin aggregates. Some failures could be explained by poor structural design (Table 2-2). However, some pavements in Minnesota, Wisconsin, and Wyoming exhibited distress that could be traced back to materials.

Wade et al (1997) found that the mortar content for most sections did not correlate clearly with the amount of cracking in a RCA concrete pavement study. It should be noted that this comparison was made for RCA concrete pavements across states with different specifications for design, materials, and construction practices. However, for some Minnesota sections with extremely high mortar contents, the percentage of slabs cracked was dramatically different in comparison to the virgin aggregate control section (88% to 22%).

Table 2-2. General performance of several concrete pavements using RCA for new PCC after (Cuttell et al. 1996).

Pavements with "good performance."						
Project Location	Control Section	Pavement Age as of Fall 1994 (yrs)	Pavement Type	Joint Spacing (ft)	Dowel Diameter (in)	Aggregate Top Size (in)
CT1, I-84	yes	14	JRCP	12	1.5 (38mm) (I-beam)	2 / 1.5 (51 / 38mm)
MN1, I-94	yes	6	JRCP	8.2	1.25 (32mm)	0.75 (19mm)
KS1, K-7	yes	9	JPCP	4.7	none	1.5 / 0.75 (38 / 19mm)
Pavements with "structural problems."						
Project Location	Control Section	Pavement Age*	Pavement Type	Joint Spacing, m	Dowel Diameter, mm	Aggregate Top Size, mm
MN4, U.S. 52	yes	10	JRCP	8.2	1 (25mm)	1 / 1.5 (25 / 38mm)
MN2, I-90	no	10	JRCP	8.2	1 (25mm)	0.75 (19mm)
WI1, I-94	no	10	JPCP	3.7-4.0- 5.8-5.5	none / 1.4 (35mm)	1.5 (38mm)
Pavements with "other distresses."						
Project Location	Control Section	Pavement Age*	Pavement Type	Joint Spacing, m	Dowel Diameter, mm	Aggregate Top Size, mm
MN3, U.S. 59	no	14	JPCP	4.0-4.9- 4.3-5.8	none	0.75 (19mm)
WI2, I-90	no	8	CRCP	n/a	n/a	1.5 (38mm)
WY1, I-80	yes	9/10	JPCP	4.3-4.9- 4.0-3.7	none	1 / 1.5 (25 / 38mm)

While not widespread at the time of this assessment, recurrent ASR cracking was identified as a problem with RCA sections in Wyoming 10 years after reconstruction using RCA (Wade et al. 1997). This is in spite of the fact that the ASR potential as moderate using uranyl acetate testing according to ASTM C856 (2008) of the recycled aggregate mortar before construction of this section. In this study, recurrent D-cracking problems have not appeared in the new PCC sections in spite of the fact that the original aggregate was a known D-cracking susceptible aggregate. The success of the recycled D-cracking aggregates was attributed to the use of fly ash to decrease permeability, decreased top-size aggregate in the mixture, as well as the possible exhaustion of D-cracking mechanisms during the original performance period (Wade et al. 1997).

Sturtevant (2007) looked at these same sections 12 years later (in 2006) to assess longer-term performance of the RCA concrete pavements in comparison to control sections. Table 2-3 summarizes these results and shows that RCA concrete pavement sections that did not originally need rehabilitation from the 1994 assessment (Wade et al. 1997) performed similarly to the control sections with virgin aggregates. The difference in performance is suggested by Sturtevant by the additional ASR cracking, differences in top-sized coarse aggregate, and the use of RCA fines (Sturtevant 2007). The use of these fines contributes to a high level of drying shrinkage, which can manifest itself as shallow, distributed cracks, as well as structural cracks, when exacerbated by external load and internal temperature and moisture-related stresses. The propagation of structural cracks also appears to be accelerated for the RCA pavement sections, which suggests either poor maintenance, volumetric stability issues from shrinkage, reduced fracture resistance, or material-related distresses.

A major difference in performance of these sections can be seen in the level of longitudinal and transverse cracking developed during the life of these pavement sections. As the use of RCA has a dramatic effect on drying shrinkage development in new PCC, the built-in curling in these sections may be significantly greater than through the use of virgin aggregate concrete. High drying shrinkage has been shown to promote alternative fatigue cracking mechanisms in jointed concrete pavements, including longitudinal and corner cracking that increase safety issues in and near the wheelpath (Hiller and Roesler 2006). These alternative cracking modes can lead to more costly and time-consuming repair and rehabilitation options including grouting, stitching, and slab replacements.

Table 2-3. Comparison of performance of RCA and virgin aggregate sections from 1994 to 2006 surveys that have not had rehabilitation after (Sturtevant 2007).

Test	Average RCA Pavement Change (1994 to 2006)	Average Control Pavement Change (1994 to 2006)	Difference in Change (Recycled vs. Control)	Better Performing Section
Transverse Joint Spalling (% Joints)	33%	31%	2%	Control
Transverse Joint Seal Damage (% Joints)	78%	76%	2%	Control
Longitudinal Joint Seal Damage	100%	100%	0%	Equal
D-cracking (% Slabs)	0%	0%	0%	Equal
Pumping (% Slabs)	0%	0%	0%	Equal
Slab/Patch Deterioration (% Slabs)	1%	0%	1%	Control
Avg. Faulting between Panels (mils)	96%	100%	-4%	Recycled
	+11.8 (0.3mm)	+31.5 (0.8mm)	-19.7 (0.5mm)	
Avg. Joint Width (mils)	5%	10%	-5%	Recycled
	+19.7 (0.5mm)	+39.4 (1.0mm)	-19.7 (0.5mm)	
Longitudinal Cracking	25%	0%	25%	Control
Transverse Cracking (% Slabs)	12%	0%	12%	Control
Deteriorated Transverse Cracks	85%	8%	77%	Control
Total Transverse Cracks	35%	7%	28%	Control
IRI	16%	10%	6%	Control

2.7.1 Construction Issues

Many states apply existing virgin aggregate design standards when using RCA in new PCC pavement mixture designs. By doing this, issues such as particle size, density, and water absorption that are essential for a successful mixture are ignored (Chini et al. 1996). Whether the use of RCA in new PCC pavements is economical depends on the local availability of other aggregate sources, disposal costs, and the historical performance of RCA projects (Love 1987).

Economics are predominantly the driving factor in selecting RCA for use in a new PCC pavement. The costs of removal and reconstruction using virgin aggregates can be greater than salvaging, steel separation, and grading specification costs associated with recycling existing PCC pavement. Table 2-4 shows an example of the cost savings from a 16-mile section of rural state highway in Minnesota constructed in 1982. The use of RCA as the aggregate in the new PCC pavement resulted in a savings of nearly 27% (Halverson 1982). These costs are highly dependent on the location of the construction and local experience in recycling concrete.

Table 2-4. Cost savings from recycling concrete on US-59 project after (Halverson 1982).

<i>Item</i>	<i>Quantity</i>	<i>Cost (\$ in 1982)</i>	
		<i>Recycling</i>	<i>Conventional</i>
Remove concrete pavement	229,170 yd ²		401,047
Salvage concrete pavement, crush, and stockpile	229,170 yd ²	595,842	
Stabilizing aggregate	24,238 tons		60,595 ^a
Shouldering ^b			
Class 3	23,114 tons		57,785 ^a
Class 5	21,238 tons		53,095 ^a
Recycled concrete	52,651 yd ³	1,289,950	
Recycled concrete with high early strength	936 yd ³	28,890	
Standard concrete	1,308/53,959 yd ^{3 c}	51,954	2,077,422
Standard concrete with high early strength	31/994 yd ^{3 c}	1,395	43,736
Total		1,968,031	2,693,680

^a Differential cost between recycled material and virgin aggregate.

^b Portion of class for which recycled material was available.

^c Virgin aggregate/total concrete used on the project.

2.7.2 Two-Lift Construction

The use of two-lift paving is common in Austria, France, and Germany with RCA concrete composing the lower lift and higher-quality virgin aggregates utilized in the upper lift. Similar projects have been constructed in the United States, most notably in Iowa (1976) and for the SHRP2 R21 research project. Between 1950 and 1970, two-lift paving using virgin aggregate concrete for both lifts was utilized in Iowa, Wisconsin, Michigan, Pennsylvania, and Minnesota to facilitate placement of mesh in highway construction. Between 1970 and 2000, the U.S. concrete paving industry moved away from a jointed reinforced concrete pavement design and significantly shortened the design length of pavement panels, effectively eliminating the need for two-lift paving (Kuennen 2007).

The use of two-lift paving can control some deficiencies of RCA concrete, including its high propensity for drying shrinkage. With a 2-3 inch (50-75mm) upper lift of higher quality concrete over the RCA concrete, the RCA lift will not experience the low relative humidity levels that exacerbate the volumetric stability issues. The use of fiber-reinforcement in the RCA concrete layer can also lead to increased fracture resistance and help promote sustainability in terms of utilization of existing materials, increased service life, as well as reduction in noise pollution through higher quality top-lift surface construction techniques (including durable exposed aggregate surfaces) as is common in Austria (Tompkins et al. 2009). Construction of the two-lift system can be accomplished through the use of specialized two-lift pavers or two separate pavers providing wet on wet paving as shown in Figure 2-15.



Figure 2-15. Two-lift concrete paving using two pavers after (Fick 2008).

2.8. Michigan Experiences with Recycled Concrete Aggregates

The Michigan Department of Transportation (MDOT) has had varied experiences with RCA in transportation applications. This section looks at MDOT's past experiences using RCA in multiple applications, notes its current policies, and alludes to potential opportunities that exist in using RCA in Michigan's transportation infrastructure.

2.8.1 Recycled Concrete Aggregate in New PCC

MDOT made a significant investment in using RCA in new concrete pavement in the 1980's for over 650 lane-miles on major routes including M-10, I-75, I-94, I-95, and I-96 (FHWA 2008b; Smiley and Parker 1993). Due to poor performance of these high-profile sections including formation of transverse cracking, faulting, and spalling, MDOT put a moratorium on the use of RCA in PCC pavements. During this time, one study by Snyder and Raja (1991) on the performance of concrete pavement shear capacity using different aggregate types noted that blends of RCA and virgin aggregates may not necessarily help in promoting long-term concrete pavement performance in comparison with RCA concretes. Concrete containing RCA exhibited lower strength than concrete using virgin aggregates. Also, aggregate interlock potential was found to be lower and less sustained as compared to other aggregate sources (Snyder and Raja 1991). However, Hansen's work on RCA characterization during this same time period suggested that other underlying causes (base uniformity, sympathy joints, shrinkage cracking) may have led to the early pavement deterioration for these RCA concrete pavement sites (Hansen 1995).

Later studies by Michigan State University (Frabizzio et al. 2000) and Michigan Technological University (Hiller et al. 1999; Van Dam et al. 2002) looked at concrete pavement sites that exhibited transverse cracking. These pavements were examined by field assessment of shear capacity and material-related distresses. These studies shared some field sections that were built using RCA concrete in its surface layer such as the one shown in Figure 2-16. Many of these sections exhibited excessive drying shrinkage cracking and transverse cracks with low load transfer.



Figure 2-16. Concrete pavement containing RCA as aggregate on I-94 WB, West of Kalamazoo.

2.8.1.1 MDOT Specifications for Recycled Concrete Aggregate in New PCC

Due to the poor performance of several high profile freeway sections, MDOT specification 902.03 (MDOT 2003) currently allows RCA production from concrete that originated from MDOT owned facilities and only for the following applications:

- Curb and gutter
- Valley gutter
- Sidewalk
- Concrete barriers
- Driveways
- Temporary pavement
- Interchange ramps with commercial average daily traffic (CADT) less than 250
- Concrete shoulders

To minimize or eliminate poor performing transportation facilities that include RCA, this specification disallows the use of RCA in PCC applications for the following applications:

- Mainline pavements
- Ramps with CADT equal to or greater than 250
- Concrete base course
- Bridges
- Box or slab culverts

- Head walls
- Retaining walls
- Prestressed concrete
- Heavily-reinforced concrete

MDOT specification 902.03 (MDOT 2003) places strict limitations on the processing and quality of the RCA to be utilized in the disallowed PCC applications. Contamination with materials such as joint sealant, asphalt concrete, base material, or subgrade soil must be limited to less than 3% of the particle count of the total aggregate particles. There must not be any contamination from non-MDOT owned material so that the RCA material is of known quality and characteristics. Steel contamination is allowed in the RCA stockpile provided the steel passes the top-size sieve without manipulation by the contractor. Other limitations are put on the material including a liquid limit of less than 25, plasticity index less than 4, freeze-thaw evaluation using Michigan Test Method (MTM) 115 (MDOT 2007), specific gravity uniformity (tests within ± 0.05 from the mean) and absorption capacity uniformity (within $\pm 0.4\%$ from the mean) using ASTM C127, with no apparent segregation.

2.8.1.2 Load Transfer of RCA Concrete Pavements

Due to the non-uniformity of the moisture absorption capacities of recycled aggregates, the bonding characteristics of the new mortar to the aggregate is inherently variable (Raja and Snyder. 1991). These variable bonding characteristics can lead to unpredictable crack face textures and, subsequently, irregular load transfer through aggregate interlock at a joint or crack.

Given that aggregate interlock is a function of the top-size aggregate, crack spacing, and tortuosity of the crack, the results from any study in this area should focus on controlling these factors. Small changes in crack widths have resulted in large changes in the level of load transfer (Buch et al. 2000). For RCA concrete, the additional drying shrinkage can lead to more open cracks and less aggregate interlock. Structural cracks forming through the high mortar content (old and new) of RCA concrete can show less tortuosity than virgin aggregate concrete. This induces high deflections and reduces the ability of the crack or joint to transfer loads to the adjacent slab, resulting in increased crack deterioration as well as faulting and pumping potential.

Core specimens were evaluated using a volumetric surface texture (VST) analysis to characterize aggregate interlock potential from aggregate tortuosity (Buch et al. 2000). The VST procedure involves testing a 25 in² (161cm²) area of a crack face in order to quantify the volume of texture per surface area on the specimen. A high volumetric surface texture ratio (VSTR) indicates a rough surface texture and high potential for load transfer by aggregate interlock, while a low value indicates smooth texture and a lower load transfer potential. Table 2-5 summarizes VSTR values and visual qualitative notes on the crack face surface. The RCA concrete crack faces exhibited extremely variable surface texture between specimens, exhibiting both higher and lower VSTR values in comparison to other coarse aggregate concretes. One constant in the RCA concrete specimens was that the cracks propagated through the aggregate, which would suggest the bond interface between the aggregate and paste tended to be strong.

Another study (Wade et al. 1997) of RCA concrete crack face roughness indicated that VSTR values of recycled aggregates equal that of virgin aggregates provided the old mortar content is low. This would allow for the original coarse aggregate to be involved in load transfer across fairly tight cracks and less reliant on the mortar for point-to-point contact. This original aggregate point-to-point contact can be achieved through proper concrete crushing operations in most cases, but can limit the usable yield of the old concrete.

A Kansas study of RCA concrete pavement (Cross et al. 1996) showed that recycled PCC sections had load transfer efficiencies (LTE) near that of the control sections containing virgin aggregates. While the sample size for this project was small, it does show load transfer can be productive in reducing stresses in concrete pavements. However, the RCA concrete did seem to be more temperature-susceptible with respect to load transfer.

In laboratory studies (Buch et al. 2000; Snyder and Raja 1991) of large-scale slabs, RCA concrete slabs tended to show reduced performance with respect to load transfer efficiency than virgin aggregate concrete slabs. Table 2-6 presents a comparative look at laboratory slabs' performance in load transfer. Slabs 3 and 4, which contained a recycled gravel as coarse aggregate, were reduced from levels above 95% to a load transfer efficiency level of 70% after a lower number of repetitions of a 9,000 lb simulated wheel load compared to carbonate aggregate concrete slabs. Slab 4 included a combination of recycled aggregate and larger-sized virgin carbonate aggregates in an effort to produce better load transfer durability with little success. It should be noted that these tests were conducted for one slab with unknown repeatability.

Table 2-5. Volumetric surface texture test results after (Buch et al. 2000).

<i>Specimen Name</i>	<i>Aggregate Type</i>	<i>Microtexture VSTR (cm³/cm²)</i>	<i>Microtexture</i>	<i>Mode of Fracture (T)hrough / (A)round</i>
CARB-1	Carbonate	0.0678	Smooth	90%T
CARB-2	Carbonate	0.0767	Smooth	99%T
CARB-3	Carbonate	0.0958	Smooth	Poor Visibility ^a
CARB-4	Carbonate	0.0691	Smooth	98%A
CARB-5	Carbonate	0.0429	Smooth-Moderate	99%T
NG-1	Natural gravel	0.1624	Rough	95%A
NG-2	Natural gravel	0.1238	Rough	60%A
NG-3	Natural gravel	0.2498	Moderate	90%A
NG-4	Natural gravel	0.1406	Moderate	80%A
NG-5	Natural gravel	0.055	Moderate	98%A
RCA-1	Recycled Concrete	0.1426	Rough	80%T
RCA-2	Recycled Concrete	0.0419	Smooth	99%T
RCA-3	Recycled Concrete	0.1699	Moderate	85%T
RCA-4	Recycled Concrete	0.0878	Moderate	90%T
RCA-5	Recycled Concrete	0.0635	Smooth	95%T
SLAG-1	Slag	0.0663	Smooth	70%T
SLAG-2	Slag	0.0781	Smooth	99%T
SLAG-3	Slag	0.0659	Smooth-Moderate	95%A

^a Was unable to tell whether the fractures went through or around the aggregate particles.

Another study in Michigan over a three year period (Frabizzio et al. 2000) included extensive field testing of load transfer for concrete pavements using different coarse aggregate types. Figure 2-17 exhibits LTE and its associated deterioration for transverse cracks measured over a year and a half period on a RCA concrete pavement site on I-94 near Battle Creek, Michigan (constructed in 1986). A large range of LTE values can be seen at this site with the low LTE cracks exhibiting large crack widths (0.01-0.03 inches, or 0.30–0.70mm), faulting exceeding 0.16 inches (4mm), and spalling in some areas. The pavement exhibited many shrinkage cracks and large structural cracks, which were attributed to the high drying shrinkage and high mortar contents of the recycled aggregates.

Table 2-6. Performance summary as a function of aggregate type, size, and treatment after (Frabizzio et al. 2000).

	Slab No.	Aggregate Treatment	Load Cycles to 70% LTE
Set 1	1	6A Slag	100,000
	2	60% 6A ^a Slag / 40% 4A ^b Slag	200,000
Set 2	3	6A Recycled Gravel	150,000
	4	50% 6A Recycled Gravel/50% 4A Carbonate	90,000
Set 3	5	4A Carbonate	205,000
	6	6A Carbonate	1,000,000
	7	40% 4A Carbonate / 60% 6A Carbonate	400,000
	8	60% 4A Carbonate / 40% 6A Carbonate	300,000

^a MDOT gradation specification, maximum nominal aggregate size = 1 inch.

^b MDOT gradation specification, maximum nominal aggregate size = 2 inches.

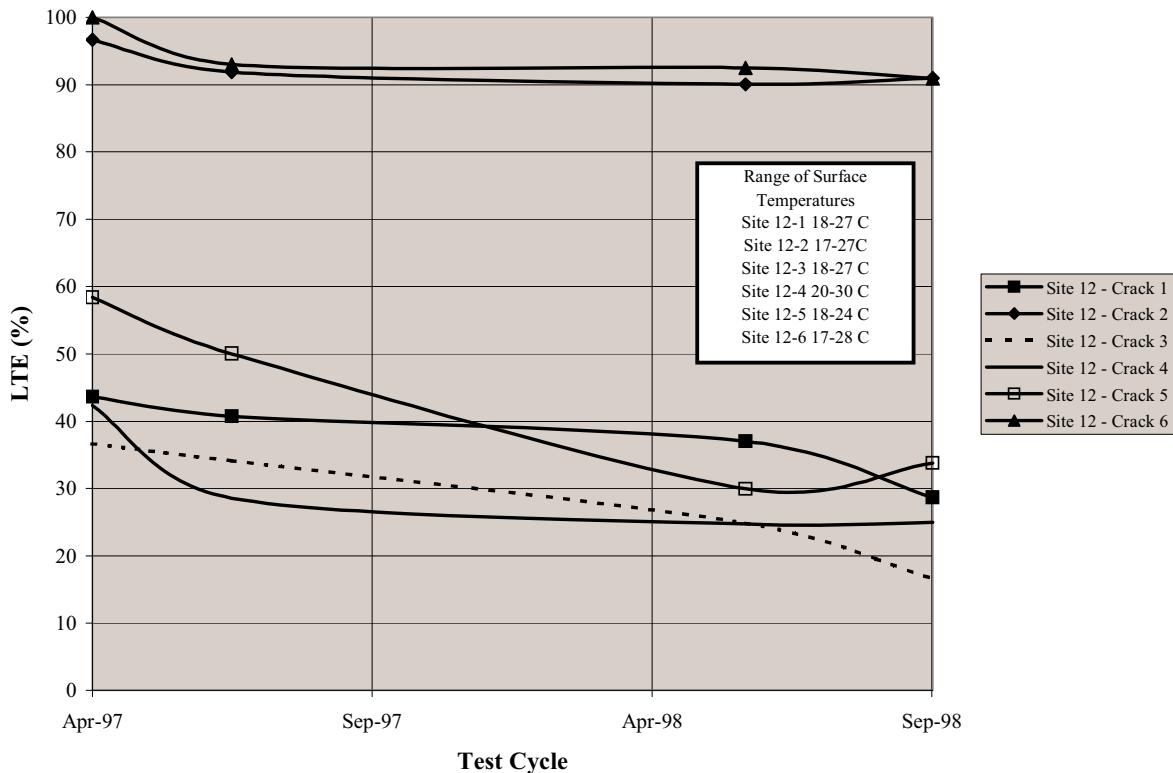


Figure 2-17. RCA concrete pavement LTE deterioration in southwest region of Michigan, Site 12 after (Frabizzio et al. 2000).

2.8.1.3 Other RCA Concrete Pavement Performance Parameters

Many projects that utilized small-sized RCA have quickly developed transverse cracks and have deteriorated rapidly in terms of load transfer capability (Raja and Snyder. 1991). Larger nominal top-sized RCA has historically not been used due to the D-cracking potential of the larger original aggregates. As seen in Figure 2-18 for jointed reinforced concrete pavements in Michigan, Frabizzio et al. (2000) showed that RCA pavements had a larger number of structural cracks on average in comparison to concrete slabs that used other coarse aggregate types. The high shrinkage levels in combination with longer joint spacing tended to produce shrinkage cracks that manifested into larger structural cracks on the sites in this study.

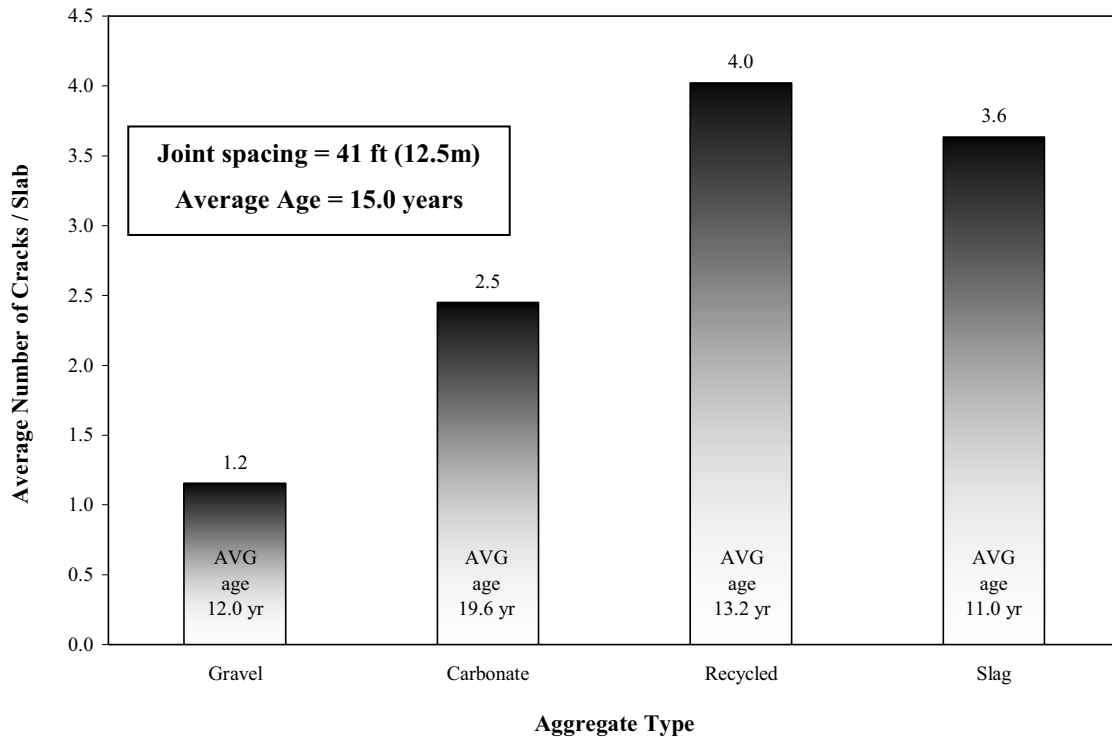


Figure 2-18. Effect of coarse aggregate type on number of cracks per slab for 41 foot (12.5m) joint spacing after (Frabizzio et al. 2000).

2.8.2 *Recycled Concrete Aggregate as Base Material*

Due to issues with the potential for leachate to clog pavement sub-surface edge drains and outlets, MDOT does not permit the use of RCA as a base material near these drainage structures at the time of this report. As many PCC pavements rely on an open-graded edge drain system, the use of RCA in the base or subbase layer is not permitted. This is also true for open-

graded drainage courses used in asphalt pavements. However, specification subsection 902.06B and specification 902.7 of the MDOT Standard Specifications for Construction (MDOT 2003) allows for the use of RCA as base or separation layer for dense and open-graded materials, respectively, for the following conditions:

- The pavement layer does not drain directly to an underdrain or when 12+ inches (30.5+ cm) of non-cementitious granular materials are between the crushed concrete and the underdrain.
- RCA is coated with asphalt or emulsified material
- A barrier (geotextile or blocking membrane) is utilized to prevent leachate directly entering the underdrain

2.8.3 Recycled Concrete Aggregate in Asphalt Concrete

MDOT specification 902.04 (MDOT 2003) currently permits the use of RCA in hot-mix asphalt concrete (HMAC) pavement mixtures. A study of RCA in HMA applications was recently conducted at Michigan Technological University (Mills-Beale and You 2010). This study concluded that RCA can be substituted for virgin aggregate at levels approaching 75%. RCA HMAC mixtures did not perform as well as 100% virgin aggregate HMAC mixtures for most laboratory tests, particularly in the dynamic modulus, rutting (i.e. Asphalt Pavement Analyzer), and moisture susceptibility (i.e. indirect tensile strength) tests. However, RCA HMAC mixtures were produced that met all Superpave specifications with only some difficulty in attaining the required air void contents. This same study also concluded that significant energy savings during the compaction process could be realized by using RCA instead of virgin aggregates solely through the use of the Construction Energy Index, as first proposed by Mahmoud and Bahia (2004). The results of Mills-Beale and You (2010) agreed with results attained by others (Paranavithana and Mohajerani 2006; Robinson Jr et al. 2004; Wong et al. 2007).

2.8.4 Issues and Opportunities for Utilization of Recycled Concrete Aggregate in Michigan

While the use of RCA in PCC applications presents many challenges, understanding the key issues and proper characterization of the RCA material can allow for its use in high performance functions. The use of RCA in PCC with reinforcing steel should be limited due to increased chlorides from the RCA contributing to corrosion. Characterization of the RCA

concrete material in terms of drying shrinkage, creep, coefficient of thermal expansion, and other standard index properties can help provide better understanding of the material and how it works in conjunction with the design of the structure to promote good long-term performance. Material and design collaboration may require planning changes as material selection and design functions are typically done separately and under different timelines. The advent of the Mechanistic-Empirical Pavement Design Guide (MEPDG) allows engineers to bring site-specific climate, specifications, support conditions, and even material characteristics into the design of pavement structures (ARA 2007). The MEPDG presents an opportunity for transportation agencies to consider the use of materials that have previously been discarded. Structural pavement design changes can be implemented effectively, whereas empirical pavement design methods do not have the ability to address the pavement/material interactions directly.

The use of RCA in tied PCC shoulder applications should be carefully examined due to differences in drying shrinkage and CTE between the shoulder and mainline pavement concrete. These differences in volumetric stability could lead to unintended cracking and premature failure of the mainline pavement system. Proper care should be taken to assure similarities in slab response between these materials with respect to time.

MDOT has recently addressed the use of RCA in dense and open-graded base applications with changes to its specifications that are intended to limit the leachate's potential for underdrain clogging. This is a case where a transportation agency realized that, while not a perfect material, RCA can be used in transportation applications by engineering effective solutions. Tools now exist to apply these same principles to RCA use in new PCC and provide the desired performance through material characterization, understanding the differences and issues, appropriate construction techniques, and proper engineering of both the material and the transportation structure.

2.9. Summary

While recycled concrete aggregates have been shown to have deficiencies in many areas, proper characterization of the mechanical properties of the aggregates can lead to successful reuse in a variety of applications. Current standards for recycled aggregates in new PCC pavement are not well defined and many times these aggregates are held to the same standards as their virgin counterparts. Since recycled aggregates have distinct characteristics which separate

them from virgin aggregates, issues such as drying shrinkage, absorption, expansion, load transfer efficiency variability, and material-related distress potentials should be investigated accordingly in both the mixture and structural design of a new PCC pavement, HMAC pavement, underlying support layers, or other transportation infrastructure applications.

CHAPTER 3. SPECIFIC GRAVITY AND ABSORPTION CAPACITY OF RECYCLED CONCRETE AGGREGATE

3.1. Introduction

Characterization of aggregates prior to use in concrete production is important from a durability standpoint and has long been performed for virgin aggregates. In general, aggregates are characterized by their internal void space or pore volume, particle shape and size, and mineralogical properties. The volume of voids in the individual particles of an aggregate used for making concrete, and the size distribution of those voids, is an important characteristic of any aggregate. Voids in an aggregate can be divided into two classes: those that are accessible from the surface (i.e. surface pores) and those that are isolated and are completely surrounded by solid material (i.e. internal pores) (Winslow 1994). Both types of pores can affect the specific gravity and absorption capacity of an aggregate, which are both critical information for the development of satisfactory mixture proportions of concrete. Furthermore, internal pores play an important role in determining some of the key long term properties of concrete such as thermal expansion, elastic moduli and resistance to cyclic freezing and thawing. Relative to absorption, a key characteristic of the aggregate void system is the degree to which the various voids are interconnected. Obviously, the more internal voids are interconnected and connected to surface pores, the higher the degree of saturation of the aggregate that can be achieved.

The volume of water absorbed by the aggregates during the concrete mixing process affects the fresh and long term properties of concrete (Al-Negheimish and Alhozaimy 2008; Deshpande 2006). Aggregate absorption, unaccounted for as part of the mixture design, can result in insufficient or excess water content for properly hydrating the cement in the mixture. Further, water absorption in the first 15 minutes after the start of mixing can result in slump loss leading to pumpability or other placement issues. Therefore, it is necessary that the absorption capacity of an aggregate material be correctly established in advance to ensure that an accurate concrete mixture design and proper proportioning can be achieved.

Currently, ASTM C127 (2008) is the common test method used for measuring the specific gravity and absorption capacity of aggregates. The validity and accuracy of measuring aggregate specific gravity and absorption capacity using this method has been discussed in detail in the literature (Winslow 1994). Several alternative test procedures to determine specific

gravity and absorption have been proposed by several researchers (Black 1986; Saxer 1956). One issue with ASTM C127 is the process of achieving a saturated-surface dry (SSD) condition for the aggregate being tested. ASTM C127 states that achieving the SSD condition is accomplished through use of an absorbent cloth and drying of the aggregate surfaces ‘until all visible films of water’ are removed. This is a subjective measure and relies on one’s ability to characterize the change in appearance or color at the point of SSD as defined by the test method.

RCA is typically more absorptive than are virgin aggregates due to a larger volume of pores, primarily associated with the residual mortar present. Studies have shown that current methods used for measuring porosity of RCA aggregates may not be accurate due to the presence of mortar on the aggregate, especially the high level of surface porosity (Tam et al. 2008). In fact, ASTM C127 specifies that the test method is not suitable for measurement of the absorption capacity of highly porous aggregates, such as light-weight aggregates (LWA) due to the aggregates inability to achieve maximum absorption capacity in 24 hours (ASTM-C127 2008). Submersion of RCA in water for 24 hours can lead to removal of loose mortar from the aggregates, which may also affect the measured values of absorption and specific gravity.

3.2. Experimental Procedures

In this study, characterization of the specific gravity of RCA and low porosity natural gravel was performed using bulk flow and helium pycnometry (Vitton et al. 1998). The envelope density analyzer (EDA) was used to measure the bulk specific gravity (G_B) and an automated helium pycnometer was used to determine the apparent specific gravity of the coarse aggregates (G_S). Figure 3-1a shows an image of the EDA used in this study. An automated helium pycnometer is shown in Figure 3-1b.



Figure 3-1a. EDA (GeoPyc).



Figure 3-1b. Helium pycnometer (AccuPyc).

The EDA determines the bulk volume of a sample, and given the sample mass, calculates the material's bulk specific gravity, G_B . This is accomplished by initially compacting a micro-grained material in the sample chamber of the EDA with a plunger. After compaction, the plunger is retracted and the aggregate sample is placed in the cylinder, as shown in Figure 3-2. The plunger is then re-inserted into the chamber and the combined micro-grained material and aggregate sample are again compacted to the previous compaction pressure. The difference in volume between the two tests provides an estimate of the bulk volume of the sample.

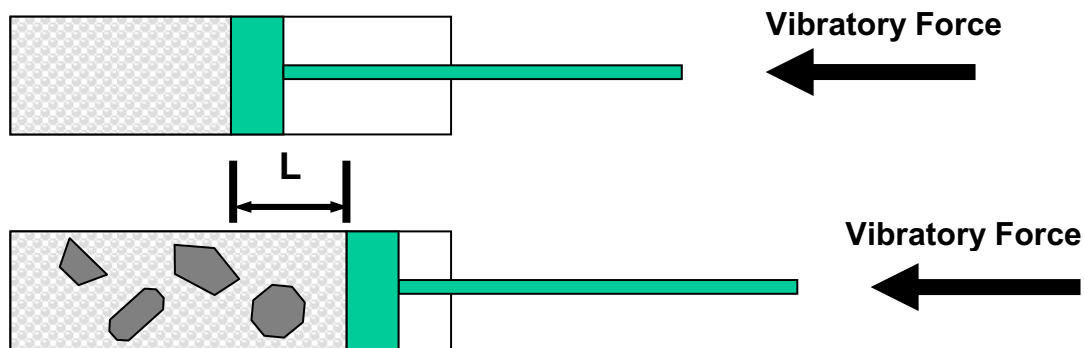


Figure 3-2. Schematic of EDA adopted from (Vitton et al. 1998).

The automated helium pycnometer also measures the volume of the aggregate particles but does so by using the volume of helium that enters a calibrated measuring cell. The helium can penetrate into the aggregates and therefore the resulting volume measured is the apparent volume (discounting surface voids in the volume determination). Dividing the sample mass by its apparent volume gives its apparent specific gravity, G_S . The sample cell volume is 100 cm^3 making this device most suitable for smaller aggregate samples. Each aggregate type tested was randomly sampled at numerous sieve sizes to be measured in the helium pycnometer. The average value of five aggregate specimens for each sieve size was then calculated.

Helium gas, due to being inert and each gas atom having a relatively small atomic radius, can easily penetrate into an aggregate's surface and inter-connected internal pore space as well as some internal pore space. Therefore, helium pycnometry offers the advantage of more completely accounting for all void space in an aggregate and providing an accurate measure of an aggregate's apparent volume. The test time for one sample is relatively short and ranges between 20-60 minutes.

The EDA and automated helium pycnometer use volumetric and mass relationships to calculate porosity (n) and absorption (A) of the aggregate sample. These volumetric relationships are shown in equations 3-1 and 3-2 below (Vitton et al. 1998).

$$n = \left[1 - \frac{G_B}{G_S} \right] \times 100 \quad (3-1)$$

$$A = \frac{n}{G_B} \quad (3-2)$$

In general, the relationship between absorption and porosity also depends upon whether or not the pores are interconnected or connected to the surface, and also the tortuosity and diameter of the connecting passages. Particularly when comparing helium pycnometer results to ASTM C127, it must be noted that helium may penetrate portions of the aggregate that water cannot, thereby affecting the calculated apparent specific gravity. Therefore, the helium pycnometer is not a standard protocol for assessing aggregates for concrete mixture design.

3.2.1 *Thin Sections of Aggregates*

In this study, in addition to determining the porosity based upon the measured specific gravity, an additional measure of porosity and pore sizes of selected aggregates was performed using image analysis. For the purpose of determining porosity in aggregates using image analysis, thin sections of selected aggregate samples were prepared. This process allows characterization of the porosity of the samples as well as the distribution of pore sizes to better understand the potential water transport properties of the aggregates.

The aggregate samples were chosen randomly with the exception of size. It was important to choose samples of an appropriate size to match the sample preparation equipment (i.e. approximately 1 by 1.75 inches, or 25 by 45 mm). Five samples of each aggregate type were selected for examination. The samples were oven dried and placed in a vacuum to remove water and air. The samples were then impregnated with epoxy and coarse silica sand around the particle exterior to reduce the necessary epoxy resin used in the embedding process. This sand accounts for the noticeably rounded material surrounding each sample shown in Figure 3-3 and Figure 3-4. The samples were first impregnated in a blue colored epoxy resin with a viscosity of 100 cP (centipoise) under atmospheric pressure.

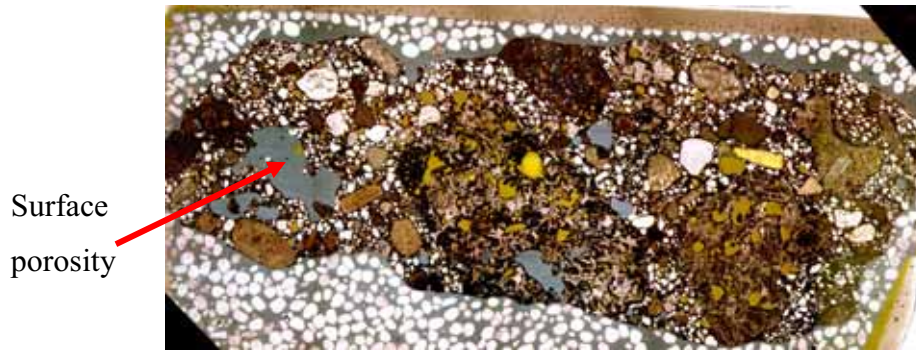


Figure 3-3. Thin section of slag RCA.

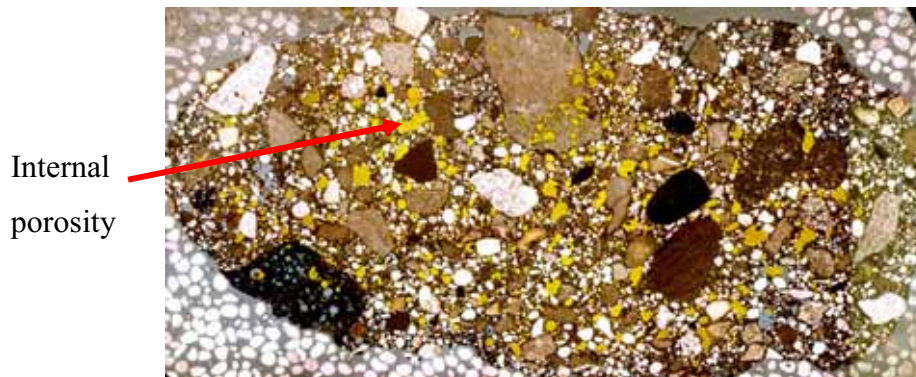


Figure 3-4. Thin section of limestone RCA.

After the initial impregnation with blue epoxy, the sample was cured for 24 hours. The samples were then ground to a flat polished surface and the exposed face was again impregnated with a yellow colored epoxy resin following similar drying and vacuuming procedures as before. Figure 3-3 and Figure 3-4 show thin sections of slag RCA and limestone RCA investigated in this study. The blue colored epoxy resin can easily penetrate the surface pores and these pores are clearly visible when the sample is prepared in thin section, as seen in Figure 3-3 and Figure 3-4. The second impregnation of the sample with yellow epoxy highlights the internal porosity of the aggregate. All cutting and grinding of samples was performed using a kerosene cooled saw and grinder to eliminate hydration of cementitious particles present in the aggregate. The samples were cured, ground, and polished to the final viewing thickness and observed under an optical microscope.

3.2.2 *Image Analysis*

The prepared aggregate samples were scanned on a high-resolution 0.1 x 0.3 mil (3 μ m x 8 μ m) flat bed scanner with a gray scale resolution of 8 bits using transmitted light. Figure 3-5

shows a typical section of a scanned image in a software program for performing segmentation of the images based upon the void type (i.e. external-blue color, internal-yellow color).

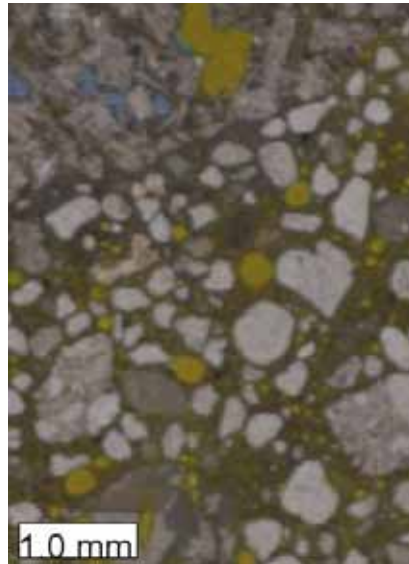


Figure 3-5. Section of scanned image.

Figure 3-6 provides a schematic of the methodology adopted for conducting the image analysis. In the imaging software, a training algorithm was developed to classify different voids based upon the color segmentation. The resulting image was then converted to a grayscale image and then converted into a binary image showing pore type. The porosity in the sample was determined as a percentage of the total area of the sample.



Scanned image
(1 pixel= 10 μ m)



Processed image for yellow color
resin to analyze interior pores



Processed image for blue color
resin to analyze surface pores

Figure 3-6. Methodology adopted for image analysis.

The resulting images were further analyzed to characterize the pores in terms of their radius, area and the threshold diameter. For this purpose, the cross-sectional pore area (A_p) and the perimeter (P_p) of the pore cross section was expressed in terms of the circularity C of the pore as seen in equation 3-3:

$$C = \frac{4\pi A_p}{P_p^2} \quad (3-3)$$

The diameter of the pores was estimated by using the Feret diameter (Walton 1948), which is the maximum chord length measured in a pore, in a fixed direction. Frequency distribution plots were developed based on the estimated pore diameter

3.3. Results and Analysis

The coarse aggregate specific gravity as measured using the helium pycnometer, EDA, and ASTM C127 are shown in Table 3-1. Values in parentheses are the standard deviations. Four types of aggregates were used in this study, including one low porosity virgin aggregate (crushed gravel) and three RCA sources (blast furnace slag, limestone and crushed gravel as the original aggregate types). The three types of RCA were obtained from different pavement concretes in Michigan. Due to variation in the original concretes and crushing operations, the mortar adhering to the recycled concrete aggregates varied considerably. This uncontrolled factor resulted in varying air content. Among all recycled concrete aggregates studied in this project, the slag-based RCA exhibited the highest absorption capacity using any of the test methods. While blast furnace slag is inherently a porous material, using this aggregate type from a recycled concrete material only adds to its porosity. The absorption capacity of limestone RCA and crushed gravel RCA is also high, though neither of these aggregates inherently exhibits a highly porous nature in its virgin form.

The reason for consistently lower absorption values in the ASTM C127 test could be related to issues associated with determining the SSD condition for the aggregates. Another reason for differing measured absorption capacity values can be related to the ability of helium gas to penetrate smaller voids and cracks in aggregate more effectively than water. This increased absorption through helium pycnometry was especially true for porous aggregates (slag RCA) or aggregates with larger percentage of mortar adhering (crushed gravel RCA) to the

original aggregate. However, this method may not properly assess the transport of water through the same aggregate as helium penetrates the pore structure of an aggregate to a greater degree.

Table 3-1. Specific gravity and absorption by different test methods.

Aggregate Type	Using helium pycnometer and EDA			ASTM C 127		
	G_S	G_B	Absorption Capacity (%)	G_S	G_B	Absorption Capacity (%)
Crushed Gravel	2.8 (0.07)	2.78 (0.09)	0.82 (0.02)	2.78 (0.05)	2.71 (0.01)	0.94 (0.05)
Slag RCA	2.66 (0.07)	2.21 (0.09)	7.78 (0.05)	2.46 (0.05)	2.22 (0.62)	4.30 (0.86)
Limestone RCA	2.60 (0.03)	2.34 (0.08)	4.23 (0.15)	2.56 (0.02)	2.34 (0.06)	3.64 (0.86)
Crushed Gravel RCA	2.69 (0.06)	2.41 (0.08)	4.52 (0.09)	2.63 (0.01)	2.45 (0.06)	2.75 (0.22)

Properly characterizing the actual water absorption in aggregates is extremely important in terms of concrete mixture design. A 1% difference higher than the actual absorption capacity of the coarse aggregates can cause a change in the w/c ratio from the intended 0.42 to 0.45 as some water intended for absorption by the aggregate may not be soaked up. This error in characterizing the coarse aggregate's absorption capacity will affect the long-term properties of the concrete including strength and drying shrinkage. Conversely, a 1% difference lower than the actual absorption capacity of the coarse aggregates would modify the w/c ratio to 0.39, affecting workability and potentially causing placement issues. As both the ASTM C127 and helium pycnometer/EDA have some issues in characterizing highly porous materials for different reasons, it is imperative that operators of these tests understand these concerns and the potential impacts of errors on the resulting concrete mixture.

The effectiveness of an automated system to determine the amount of voids is confirmed to some degree by image analysis. Figure 3-7 compares the porosity of different types of aggregates determined by different test methods. The ASTM C127 method consistently showed the lowest porosity values in comparison to the helium pycnometer/EDA and image analysis

methods except for the low-porosity virgin crushed gravel aggregates. Low values of porosity from the image analysis method could be related to the inability of the imaging software to distinctively separate the colors for the gravel aggregate. The epoxy colors and the surrounding color of some gravel aggregate were similar and selection of pixels to train the software for identifying voids was difficult. Therefore, the color threshold for determining voids and gravel aggregates required careful selection. The difference in porosity values between both automated methods and ASTM C127 was highest for slag RCA.

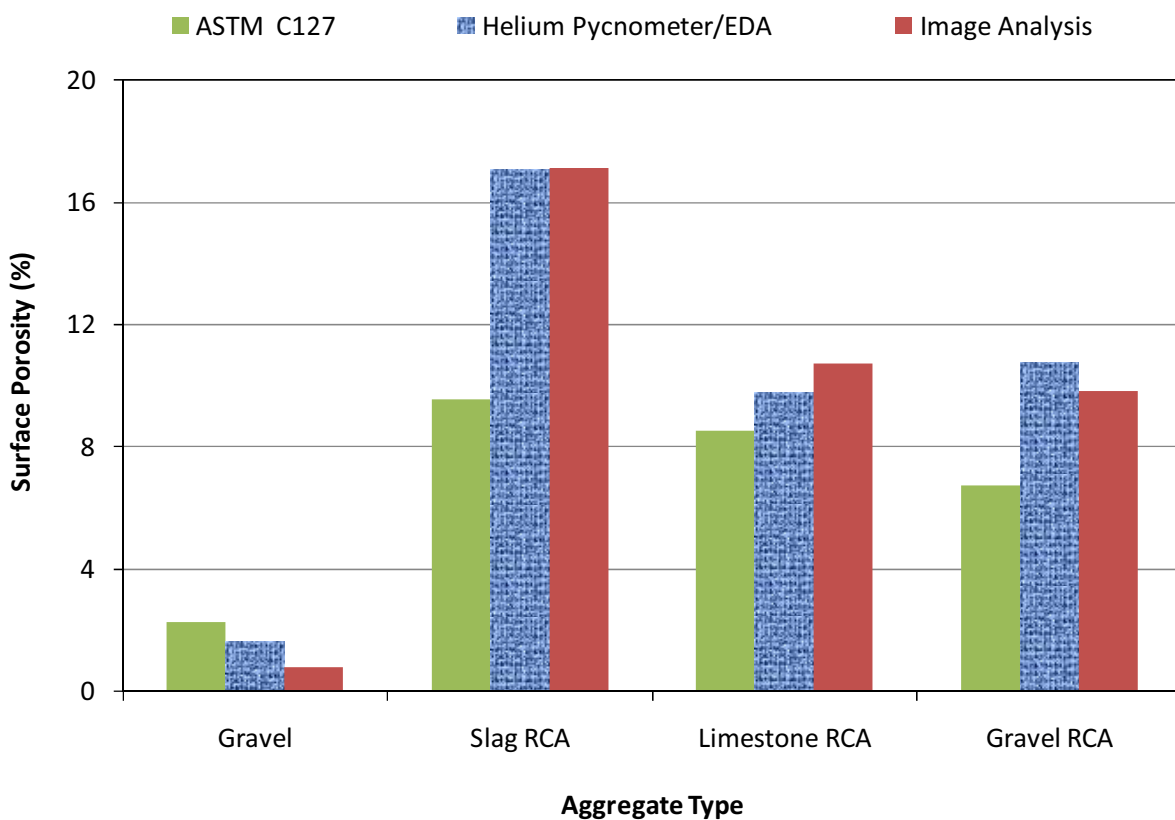


Figure 3-7. Comparison of porosity by different test techniques.

3.4. Pore size distribution comparison using image analysis

Pore sizes and their associated distributions are a significant characteristic of porosity of aggregates. Figure 3-8a and b shows the frequency distribution of pore diameter for surface pores measured for each aggregate type. These surface pores are more likely to contribute to the aggregate's water absorption as they have access to external water sources. Crushed gravel aggregate exhibits a higher frequency of pores in the smaller pore sizes and consequently less

pores in the larger diameter range. However, the number of pores in the virgin crushed gravel aggregate at any diameter is quite small, as seen from Figure 3-9, in comparison to crushed gravel RCA (Figure 3-10). Both of these gravels were originally mined from the same location on the Keweenaw Peninsula and therefore exhibit similar mineralogy, although the original crushed gravel in the RCA was utilized over 40 years ago. The crushed gravel RCA in Figure 3-10 exhibits a large amount of pores from the attached mortar, which affect porosity and water demand in comparison with its virgin gravel counterpart in Figure 3-9. More examples of the image analysis for all aggregate types can be found in Appendix A of this report. Slag RCA exhibits more larger sized pores (0.0069 to 0.0694 inches, as shown in Figure 3-8b, due to the original slag aggregate’s pore structure in addition to the voids of its attached mortar phase.

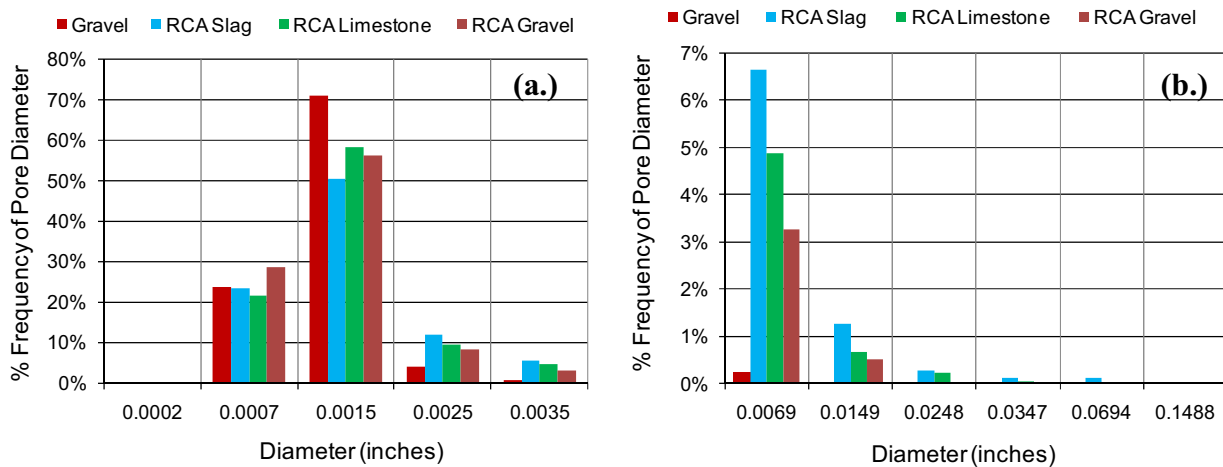


Figure 3-8. Percentage frequency of pore diameter for surface porosity using image analysis for (a) smaller pores and (b) larger pores.

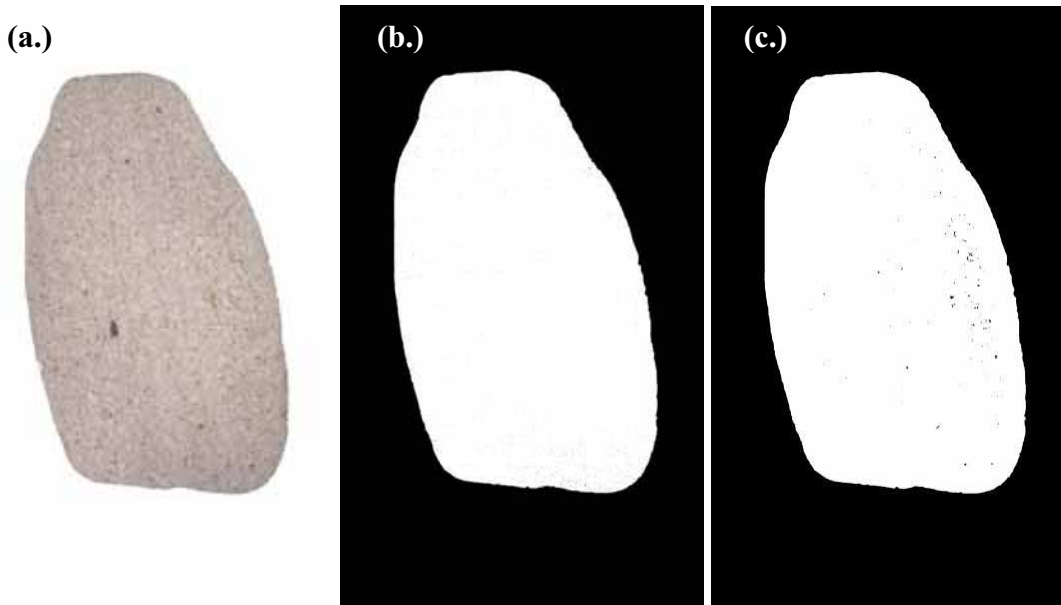


Figure 3-9. Image Analysis for Crushed Gravel Sample for (a.) Original Image, (b.) Image Processed for Blue Resin (Surface Porosity), and (c.) Image Processed for Yellow Resin (Internal Porosity).

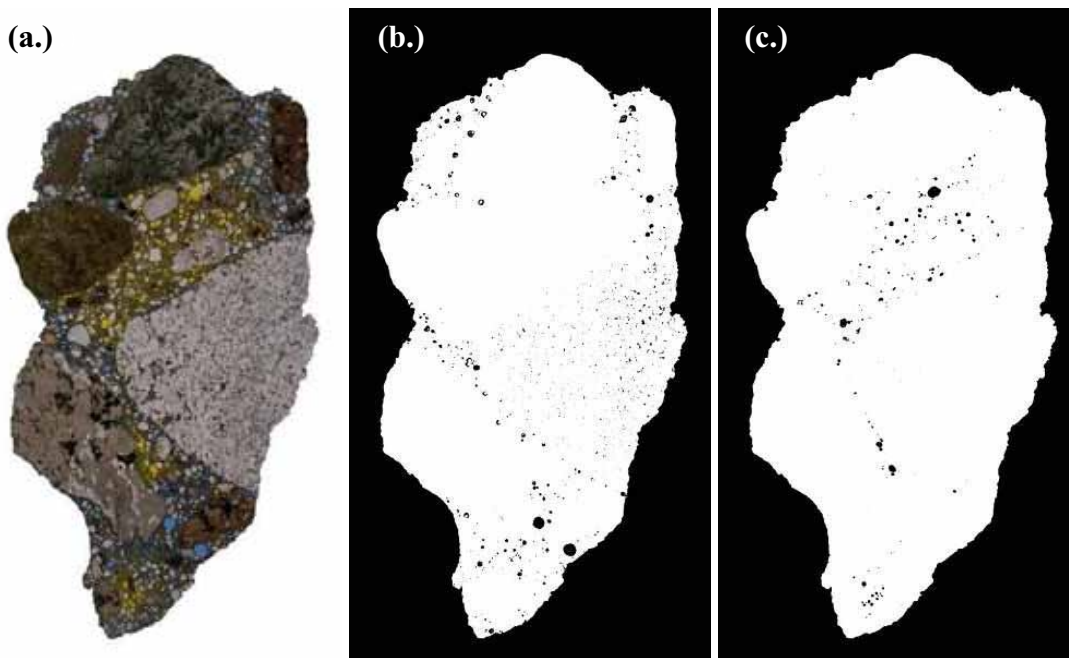


Figure 3-10. Image Analysis for Crushed Gravel RCA Sample for (a.) Original Image, (b.) Image Processed for Blue Resin (Surface Porosity), and (c.) Image Processed for Yellow Resin (Internal Porosity).

Figure 3-11 provides information concerning the type of pores for a particular pore diameter in concrete. The surface pore size distribution in Figure 3-8 shows a significant difference in the frequency of larger pore sizes (0.0069 to 0.0694 inches), which is indicative of

entrained air from the attached mortar. While this image analysis cannot show extremely small voids, it should be noted that the RCA does contain additional capillary and interparticle gel pores from the attached mortar phase of the aggregate.

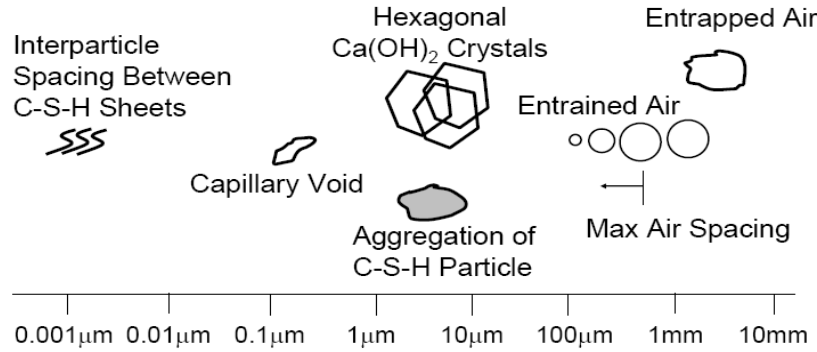


Figure 3-11. Characterization of pore sizes and type in Portland cement-based materials (1 inch = 25.4 mm = 25,400 μm).

Figure 3-12 shows the percentage frequency distribution of measured pore diameter of internal pores for all aggregates in this study. These internal pores contribute less to the water absorption of the aggregates, but more so to the strength and deformation characteristics of the aggregate. The values of pore diameter for the virgin crushed gravel aggregate, though higher for some cases, need to be considered with a caution due to the color matching of the impregnated yellow dye and the yellowish color of the crushed gravel aggregate sample.

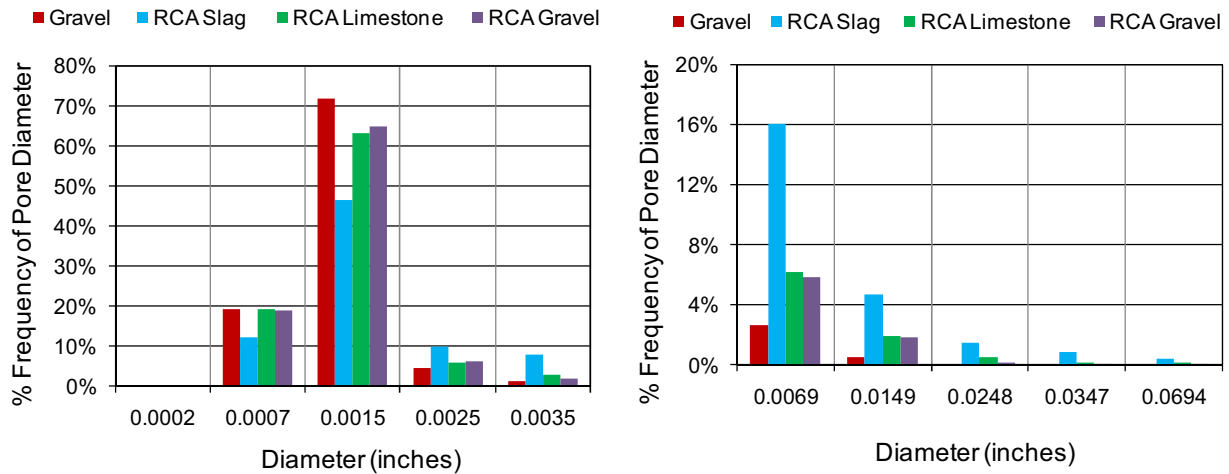


Figure 3-12. Percentage frequency of pore diameter for internal porosity using image analysis.

3.5. Significance of Pore System for RCA

The porosity in the mortar adhering to RCA can be classified as 1) porosity of the virgin aggregate, 2) water and air-filled voids formed during consolidation and final set, and 3) water and air-filled voids formed after partial hydration of cement (Hearn et al. 1994). The pore size and distribution affect many of the engineering properties of concrete such as strength, durability, shrinkage, and creep.

Most studies have concluded that the addition of RCA affects the compressive strength of concrete (ACPA 2009). Loss of strength is directly related to the amount and size of pores in the mortar adhering to the aggregate in addition to its bond with the new mortar. For virgin aggregate concrete, a one percent increase of air voids has been shown to reduce the 28-day compressive strength of concrete by approximately five percent (Mindess et al. 2002). While this rule of thumb is not proven for RCA concrete, the additional air voids from the old mortar are significant in RCA and may help explain the typical reduction in concrete strength and elastic modulus.

Conflicting results on the durability of RCA concretes under freezing and thawing cycles have been reported in the literature (Ajdukiewicz and Kliszczewicz 2002; Zaharieva et al. 2004). In general, it is observed that an increase of RCA substitution in concrete results in reduced resistance to cyclic freezing and thawing. The pore size characterization performed in this study indicates that the amount of pore space available in RCA is high. The pore characterization indicates that RCA has a high percentage of pores (56- 65%) in the range of 1.5 to 7 mils (40-175 μ m), which is indicative of smaller air-entrained voids. If the pores in the mortar adhering to the RCA contain water, it is essential that the pores have sufficient connectivity for water to expand freely into the available pore space as freezing occurs. If the surrounding new concrete is less permeable than the mortar adhering to the RCA or the air void-paste system in the new concrete is not adequate in terms of pore-size distribution and spacing, then the expanding frozen water can increase the internal stresses in the RCA concrete pores and cause cracking. For example, the crushed gravel aggregate RCA used in this study exhibited a low pore volume as compared to the other two recycled concrete aggregates studied. It also had a lower percentage of pores in the range of 1.5 to 7 mils (40-175 μ m), indicating a possibility of an inadequate air-void system in the old attached mortar. Therefore, use of this RCA in concrete would present concerns relative to the concrete's freeze-thaw resistance. Therefore, further evaluation of its

pore structure is necessary to assure air-void connectivity for a quality air void system and freeze-thaw performance. This assessment could be accomplished through freeze-thaw testing using ASTM C666 (2008) using a proposed project-specific concrete mix.

3.6. Summary and Conclusions

In this study, characterization of aggregates was performed using automated as well as ASTM standard test methods. Two automated test equipments – helium pycnometer and EDA were used to measure specific gravity, absorption capacity and porosity. Results were compared with ASTM C 127 test method based measurements. Porosity of aggregates was also determined by performing image analysis of high resolution images of the aggregates. The conclusions are summarized below:

1. Automated tests such as the helium pycnometer and EDA provide different results for the specific gravity and absorption of RCA as compared to ASTM C127. The results from the helium pycnometer and EDA typically have a lower standard deviation in comparison with ASTM C127 measurements. However, this study did not fully assess whether helium pycnometry/EDA can accurately represent the absorption of water that occurs during the concrete mixing process.
2. Absorption capacities and porosity of RCA was significantly higher than typical virgin aggregates sources, which may lead to difficulties in assuring proper moisture absorption during concrete mixing.
3. High resolution images and image analysis techniques were adopted to quantify pore structure of RCA and were useful in better understanding the porosity and void distribution. This void distribution is important to understand as the connectivity and similarity to the new concrete mortar's air void system may be required to assure adequate durability.
4. For all aggregates, porosity measurements obtained from image analysis and helium pycnometry/EDA were comparable and typically greater than that measured by ASTM C127.
5. Slag RCA exhibited the highest percentage of surface porosity for pore diameters greater than 0.1 mm as both the original aggregate and attached mortar contributed to these larger pore sizes.

6. While virgin crushed gravel aggregates had a large percentage of its porosity from smaller pore sizes, the total number and volume of pores in these virgin aggregates was far less than all types of RCA characterized in this project.

CHAPTER 4. LABORATORY INVESTIGATION OF RCA IN CONCRETE

4.1. Introduction

Volumetric stability of concrete is an important parameter and is linked closely to durability and long term performance of concrete. Studies of jointed concrete pavements in the USA have shown excessive shrinkage cracking and premature deterioration of sections containing RCA as the sole aggregates in the concrete slabs (Buch et al. 2000). The effect of RCA on concrete properties is related to various factors such as the type of virgin aggregate used in the original concrete, age of crushed concrete, amount and type of mortar adhering to the aggregates (Berndt 2009; Tam et al. 2008). All these factors directly affect the porosity and the absorption capacity of the RCA. Higher porosity and absorption capacity in turn affects the workability, compressive strength, and other mechanical properties of the RCA concrete.

In this project, different types of recycled concrete aggregates were evaluated in terms of physical characteristics as well as their effect on fresh and hardened properties of concrete. The effect of RCA on the volumetric stability of the concrete was evaluated based on the porosity and absorption capacity as discussed in Chapter 3.

4.2. Experimental Methods

4.2.1 *Material*

In this study, eight mixtures with a target water to cement ratio (w/c) of 0.42 were cast using five different types of aggregates. The aggregate blends used are shown in Table 4-1. Since some concrete samples were cast using characteristics of the different absorption capacity and specific gravity methods, presented in Chapter 3.

Table 4-2 details the concrete mixture matrix adopted for both virgin and RCA sources based on the specific gravity characterization technique.

Table 4-1. Aggregate types used in laboratory assessment.

Aggregate Type	Source	Control Section
Virgin crushed gravel	Superior Sand and Gravel in Houghton County	n/a – virgin aggregate
Blast furnace slag RCA	I-69 eastbound between Peacock Road and Shaftsburg Road in Shiawassee County	76024
Limestone RCA	I-75 southbound near Birch Run in Saginaw County	73171
Crushed gravel RCA	US-41 northbound near Michigan Tech University campus in Houghton County	31051
Recycled crushed gravel RCA or third generation (3rdGen) aggregate	US-131BR in Kalamazoo County	39051

Table 4-2. Matrix of concrete mixtures prepared in the project.

ASTM C127	Helium Pycnometer and EDA
Crushed Gravel	Crushed Gravel
---	Blast Furnace Slag RCA
----	Limestone RCA
Crushed Gravel RCA	Crushed Gravel RCA
3rdGen	--

The crushed gravel virgin aggregate mixtures were prepared for comparison with normal concrete and RCA concretes. All RCA concretes were made with 100% RCA coarse aggregate substitution. The fresh and hardened properties of the RCA concretes were compared with crushed gravel virgin aggregate concrete. Mixture designs were prepared using two different specific gravity and water absorption measurement techniques. A central emphasis of this

portion of the research was to study the effect of availability of water in the mixture on the volumetric stability of RCA concretes.

The coarse aggregate grading used for this study was Michigan Department of Transportation (MDOT) Standard Specification Series/Class 6AAA, and a local virgin sand source conforming to MDOT Standard Specification Series 2NS was used as the fine aggregate. Sieve-specific grading of the coarse and fine aggregates was maintained to assure a particle size distribution representing the middle of the upper and lower specification. The gradation of the coarse and fine aggregates used for all concrete mixtures is shown graphically in Figure 4-1.

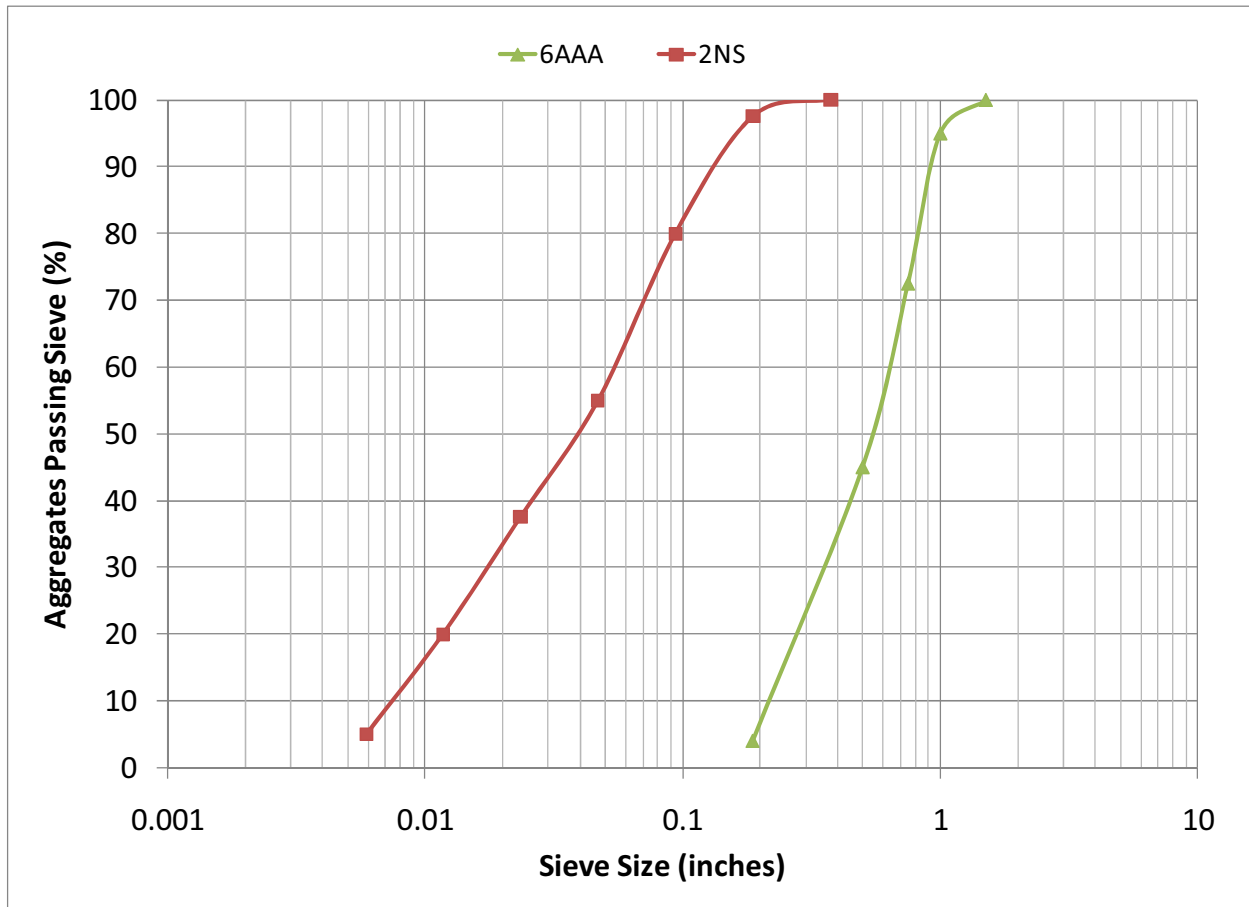


Figure 4-1. Gradation of aggregates used in the study.

The specific gravity and absorption capacity of the fine aggregate used in this study was measured in accordance with ASTM C128 (2008). The cement used in this study was an ASTM C150 Type I Portland cement (ASTM-C150 2008). For developing the mixture proportions, specific gravity and absorption capacity of coarse aggregates was measured using either the ASTM C127 or the helium pycnometer/EDA, as discussed previously. Table 4-3 provides the

proportions for the different mixtures used in this study. The bulk volume of coarse aggregate per unit volume of concrete (b/b_0) used in each mixture was kept constant at 72% to adhere to MDOT concrete paving specifications (MDOT 2003). An air entraining agent (AEA) conforming to ASTM C260 (2008) proportioned at 0.8% by weight of cement (as prescribed by the admixture manufacturer) was used to ensure an adequate air-void system in the mixtures.

Table 4-3 Mixture proportions of concretes (in lb/yd³ of concrete).

Material (lb/yd³ of concrete)	Crushed Gravel	Slag RCA	Limestone RCA	Crushed Gravel RCA	3rdGen
Type I Cement	610	610	610	610	610
Water	260	260	260	260	260
Coarse Aggregate	1965	1807	1836	1930	1793
Fine Aggregate	1160	834	957	981	1048

4.2.2 *Mixing Methodology*

A 4 ft³ capacity rotating drum mixer was used for mixing the concrete. In field conditions, the RCA is typically dry and exposed to ambient atmosphere for long periods of time. In order to ensure dryness of the coarse aggregate and to aid the grading process to assure middle-specification gradation, the RCA was conditioned in an oven at 120°F for 24 hours prior to mixing. This was done to more closely mimic typical concrete mixing operations (above or below SSD conditions, but not oven-dry), to eliminate issues of high alkalinity in the initial mixing water, and to attempt to reduce excess bleeding from the aggregates from a high localized w/c ratio. The mixing methodology adopted was as follows:

- RCA + water required to bring the RCA to SSD condition
- Mix for 1 minute
- Sand + air entraining agent + Type I cement + remaining water
- Mix for 3 minutes

- Mixer stopped for 2 minutes
- Mix for 2 minutes

4.2.3 *Testing Procedures*

In this section, test procedures adopted for the study are discussed. Details about the petrographic methodology and non-standardized methods of determining specific gravity and absorption capacity are provided in detail in Chapter 3.

The fresh properties measured for all concretes were slump, unit weight, and air content. The air content of the fresh concrete was measured in accordance with ASTM C231 (2008) using the pressure method. The hardened concrete properties measured were compressive strength, modulus of rupture, elastic modulus, rapid chloride penetrability, as well as autogenous and drying shrinkage. Air content of hardened concrete was measured in accordance with ASTM C457 (2008) using petrographic methods.

For the hardened concrete air content analysis, one sample for each mixture design was tested at 56 days. The procedure used for the characterization of the air-void system of the hardened concrete works on the same principle of contrast enhancement and digital analysis first described by Chatterji and Gudmundsson (1977; Gudmundsson et al. 1979). The procedure used here can be broken into four basic steps:

- Preparation of lapped slabs
- Black and white contrast enhancement procedure
- Image collection
- Automated ASTM C457 air-void characterization

4.2.3.1 Preparation of Lapped Slabs

Each slab was trimmed to a width of 3 inches (76mm) and a height of 4 inches (100mm) to accommodate the dimensions of the retaining rings of the automated lapping equipment. The slabs were ground flat using hand pressure on a water-cooled rotating wheel topped with a 60 grit metal-bonded diamond platen, followed by 24 minutes with an 800 grit SiC water slurry on the lapping equipment. The flatness of the lap was monitored and maintained within ± 0.1 mils (2.5 μ m). The surfaces were cleaned between steps with a gentle pressurized water spray followed by a short ultrasonic water bath. The slabs were oven-dried at 120°F followed by the

application of a 5:1 by volume solution of acetone and clear fingernail hardener (Roberts and Scali 1984). The solution was brushed onto the lapped surfaces in two coats. After the hardener had set, the slabs were briefly polished using hand pressure on the water-cooled rotating iron wheel topped with 600 grit adhesive backed SiC paper and cleaned as described previously.

4.2.3.2 Black and White Contrast Enhancement Procedure

Contrast enhancement was achieved by drawing slightly overlapping parallel lines with a wide tipped black permanent marker. Three coats of permanent marker were applied, changing the orientation 90 between each coat. After the ink dried, a few tablespoons of 0.8 mil (2 μ m) median size white powder were worked into the samples using the flat face of a glass slide. A razor blade was used to scrape away excess powder, leaving behind powder pressed into voids. Residual powder was removed by wiping with a clean and lightly oiled fingertip. A fine-tipped black permanent marker was used to darken voids in aggregates in an effort to differentiate between the voids in the mortar.

4.2.3.3 Image Collection

Each slab was scanned individually, and placed as near as possible to the center of each flatbed scanner's glass plate. The images collected were 8-bit grayscale, 3175 dpi, (125 dpm, 8 x 8 μ m pixel). A flat steel plate with applied black and white vinyl electrical tape was included at the top of each scan. The intensity distribution (histogram) of a population of 4 million pixels covering equal areas of the black and white tape was recorded for each scan in order to calibrate the scanner using enhanced imaging software. To compensate for minor differences in gain between scans, a linear stretch was performed on the entirety of each scanned image.

4.2.3.4 Automated ASTM C457

A Visual Basic script developed at Michigan Technological University was used to compute paste volumes based on mixture design information provided with the concrete samples according to the simple formula:

$$P = (100 - A) \left[\frac{P_m / \text{Agg}_m}{1 - P_m / \text{Agg}_m} \right] \quad (4-1)$$

where:

P = Vol. % paste in sample.

A = Vol. % air determined from the automated procedure.

P_m = Paste volume computed from mixture design.

Agg_m = Aggregate volume computed from mixture design.

Alternatively, the Visual Basic script also allows paste content to be input directly for each sample. A third option available in the script allows for a manual point count to be performed on an image scanned from the polished sample before the black and white treatment. The script divides up the image into frames, and the operator answers either yes or no as to whether the cross-hairs fell on an aggregate particle or not. The paste volume is then computed according to the simple formula:

$$P=100-Agg-A \quad (4-2)$$

where:

A = Vol. % air determined from the automated procedure.

Agg = Vol. % aggregate computed from the point count data.

The script utilizes imaging software to select the areas on the images to be analyzed, to extract the traverse lines, and to apply the threshold levels. The script also utilizes spreadsheet and word processing software to perform air void calculations and to generate reports. The script has the option of whether or not to report an air-void chord length distribution.

4.3. Hardened Properties Testing Plan

To evaluate hardened concrete properties, a suite of samples was produced from each mixture. Unless otherwise indicated, all hardened concrete tests were performed in triplicate (i.e. 3 samples per test). Compressive strength and elastic modulus were measured at 28 days following ASTM C39 and ASTM C469, respectively (ASTM-C39 2008; ASTM-C469 2008). Chloride penetrability of each mixture was measured at 56 days in accordance with ASTM C1202 (2008). For compressive strength, elastic modulus and chloride penetrability, three 4 by 8 inch (10 by 20cm) cylindrical specimens were cast per mixture. The molded specimens were covered with a lid after consolidation to avoid any water loss due to evaporation. The samples were demolded after 24 hours and placed in a moist cure room at 100% relative humidity (RH).

Free shrinkage of concrete prism samples were prepared, cured, and measured in accordance with ASTM C157 (2008) under the following conditions:

- Unsealed prisms at 100% RH and 23°C

- Unsealed prisms at 50% RH and 23°C
- Sealed prisms (with aluminum tape on all sides) at 50% RH and 23°C

The first measurements were taken 18 hours and 24 hours after addition of mixture water to the concrete and continued for several months at daily and then weekly intervals. Sealed specimens were cast to give an indication of the level of autogenous chemical shrinkage that is occurring in the concrete. The length change difference between the unsealed and sealed specimens in the same curing conditions indicated the level of drying shrinkage the concrete has undergone at a given time. Unsealed specimens were also placed in the 100% RH environment to ascertain the level of moisture transport potential of each particular concrete mixture. Cracking susceptibility of the concrete mixtures were determined following AASHTO PP 34 (AASHTO-PP-34 2005) by casting concrete around a ring as shown in Figure 4-2. Each ring had 4 strain gages mounted inside the steel ring and three replicates were made for each concrete type. These ring specimens were maintained in a 50% RH and 73°F chamber during the entire duration of the test. Initial readings were taken within 20 minutes of addition of mixture water to the concrete mixture. The rings were sealed with aluminum tape at the top and bottom of the specimens as shown in Figure 4-2 to allow moisture movement only from the sides. Measurements of the compressive strain inside the steel ring core were made in 30 minute intervals using strain gages epoxyed to the inside of the steel ring for the duration of the test.



Figure 4-2. Unsealed, sealed, and restrained shrinkage specimens.

4.4. Fresh Concrete Properties Results

The properties of the fresh concrete mixtures are presented in Table 4-4. The slump was lowest for the concrete mixture containing crushed gravel aggregates and was highest for the mixture made with slag RCA. The high slump values of the slag RCA mixture were most likely

due to excess water in the mixture as a result of establishing the mixture design using absorption values determined by helium pycnometry/EDA. For mixtures cast using water corrections determined using the helium pycnometer/EDA, in comparison to the ASTM methods, the slump values were consistently high (Figure 4-3).

Table 4-4. Fresh properties of concrete mixtures.

Fresh Property	Crushed Gravel (ASTM C127)	Crushed Gravel (He Pyc)	Slag RCA	Limestone RCA	Crushed Gravel RCA (ASTM C127)	Crushed Gravel RCA (He Pyc)
Slump (in)	2.5	4	9	7	3	8
Air content (%)	6.25	4.5	3.5	5.75	5.5	6
Unit Weight (lb/ft³)	147.7	152.0	132.2	136.9	149.0	138.9

This can most clearly be seen in the mixtures made with crushed gravel aggregate and crushed gravel RCA. The high slump values indicate the extra water added to compensate for aggregate absorption was not absorbed by the aggregates within the mixing time, thereby causing an initial increase in the *w/c* ratio of the paste. The concrete mixture made using the 3rdGen aggregate mixture had zero slump. The air content and the unit weight were not measured for the 3rdGen RCA mixture due to a limited amount of aggregates and inadequate yield of the mixture.

While most of the initial slump values for the RCA concrete mixtures were higher than the specifications, the window of workability was short in all cases. Due to the porous nature of the aggregates, they tended to absorb moisture from the fresh paste even after mixing was completed. Therefore, the RCA concrete mixtures tended to be harsh soon after initial assessment of fresh properties.

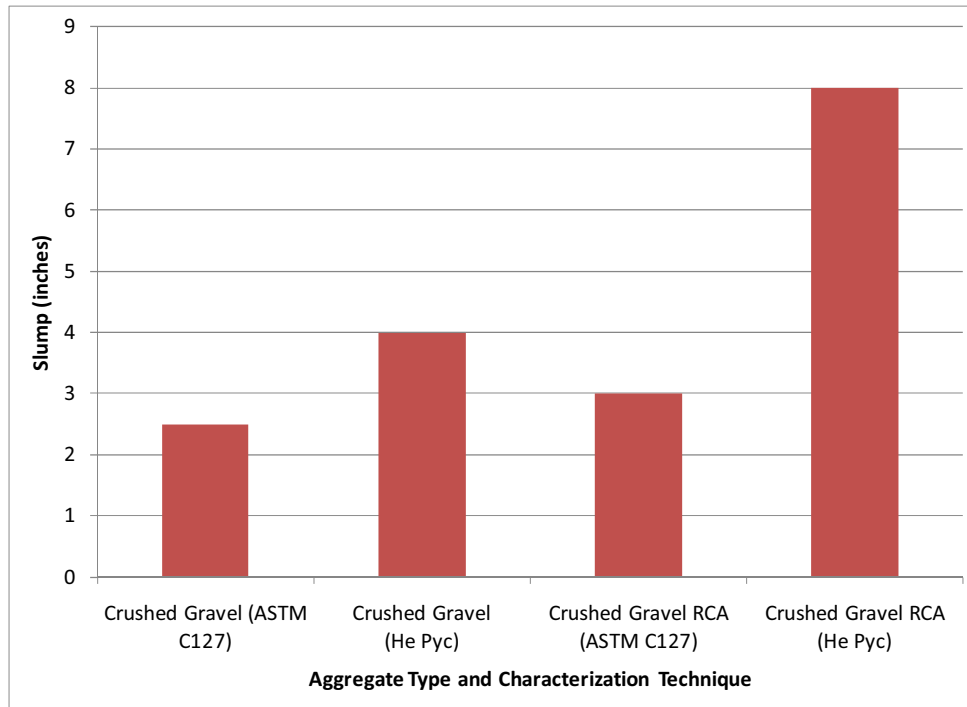


Figure 4-3. Comparison of initial slump using two different specific gravity measurement techniques.

4.5. Hardened Concrete Properties

The 28-day compressive strengths for all the mixtures are shown in Figure 4-4. The solid line represent the 28-day compressive strength specified for acceptance as an MDOT P1 concrete mixture. The lowest compressive strength was measured for the mixture containing slag RCA (He Pyc as absorption and specific gravity assessment method) whereas the highest strength was observed for the virgin crushed gravel (ASTM C127). Overall, the RCA concretes exhibited compressive strengths lower than virgin aggregate concrete made with ASTM C127-based absorption correction process. Mixtures made with the absorption correction based on the helium pycnometer method typically exhibited lower compressive strength values in comparison to those mixtures where absorption capacities were determined by ASTM C127. The water absorption values as predicted by the helium pycnometer were always higher than those predicted by ASTM C127, leading to excess water in the concrete mixture and thereby reducing the compressive strength and creating an artificially higher w/c ratio of the cement paste.

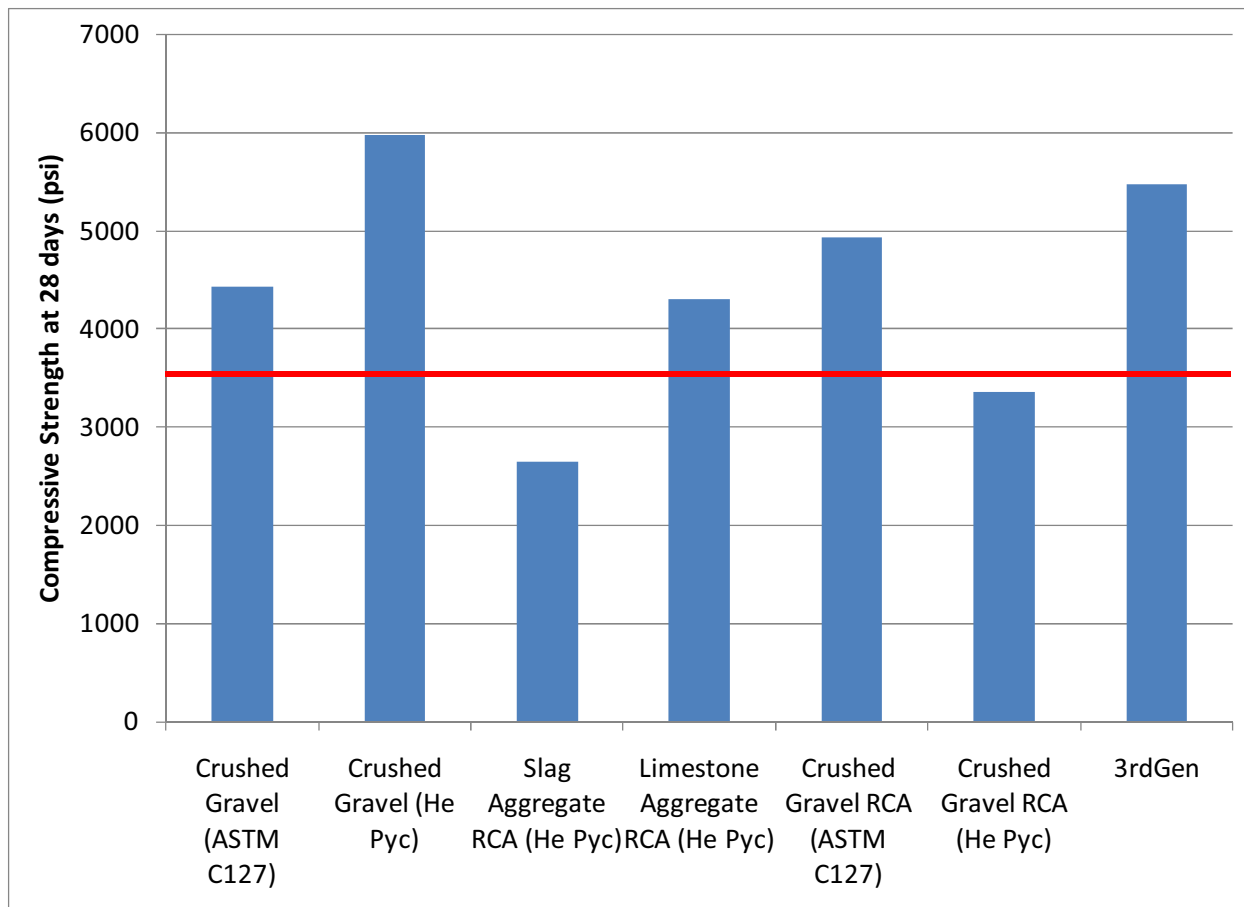


Figure 4-4. Compressive strength at 28 days.

Some studies have shown that higher compressive strengths are achieved in concrete mixtures containing RCA, however, it is dependent upon the maximum size of RCA used in the mixture as well as the amount of mortar adhering to the RCA particles. Domingo-Cabo (Domingo-Cabo et al. 2009) postulates that when completely dry RCA is used, due to the high absorption capacity, the effective water to cement ratio is reduced and the compressive strength is increased. In the study conducted by Domingo-Cabo, it was observed that an increase in the amount of RCA substituted for virgin aggregate resulted in higher compressive strength values.

4.5.1 Modulus of Rupture

The moduli of rupture at 28-days for the concrete mixtures prepared are shown in Figure 4-5. This flexural strength was lower for concrete mixtures with RCA than the comparable mixtures containing virgin aggregates. Failures characterized by cracks propagating through the RCA were observed in the flexural strength specimens of concrete made with slag RCA, but not

the crushed gravel or limestone-based RCA concretes. Due to the brittle nature of slag aggregates and their high surface porosity, the plane of weakness generally is through and not around coarse aggregates (Buch et al. 2000).

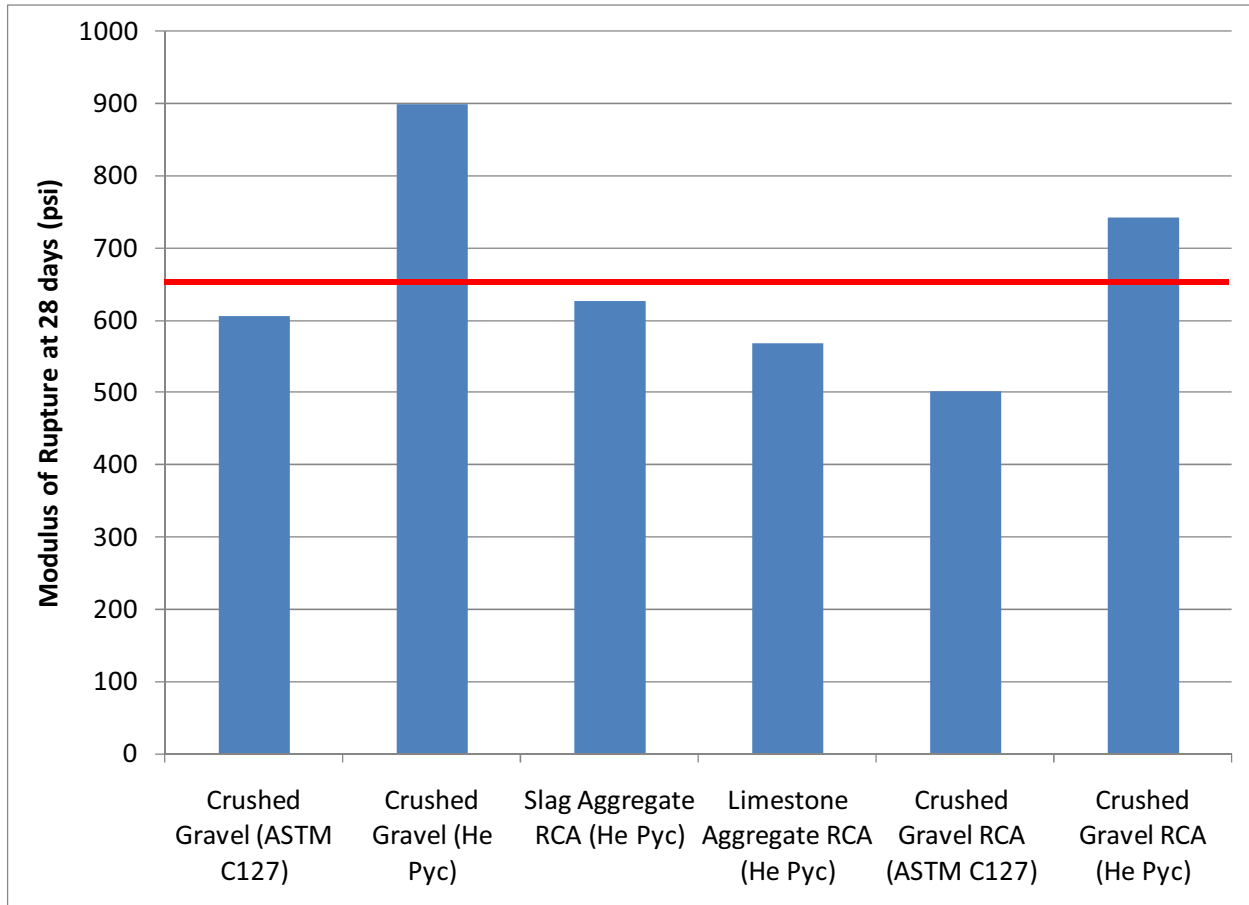


Figure 4-5. Modulus of rupture at 28 days.

4.5.2 Elastic Modulus

Elastic modulus values for all concretes mixtures were assessed at 56-days and are shown in Figure 4-6. The elastic moduli values of the RCA-based mixtures are comparable with each other, but are about 20% lower than the mixture containing virgin crushed gravel aggregate. In this study, all elastic moduli values were found to be consistently lower than typical virgin aggregate concrete values that are roughly 4.35 million psi (30,000 MPa).

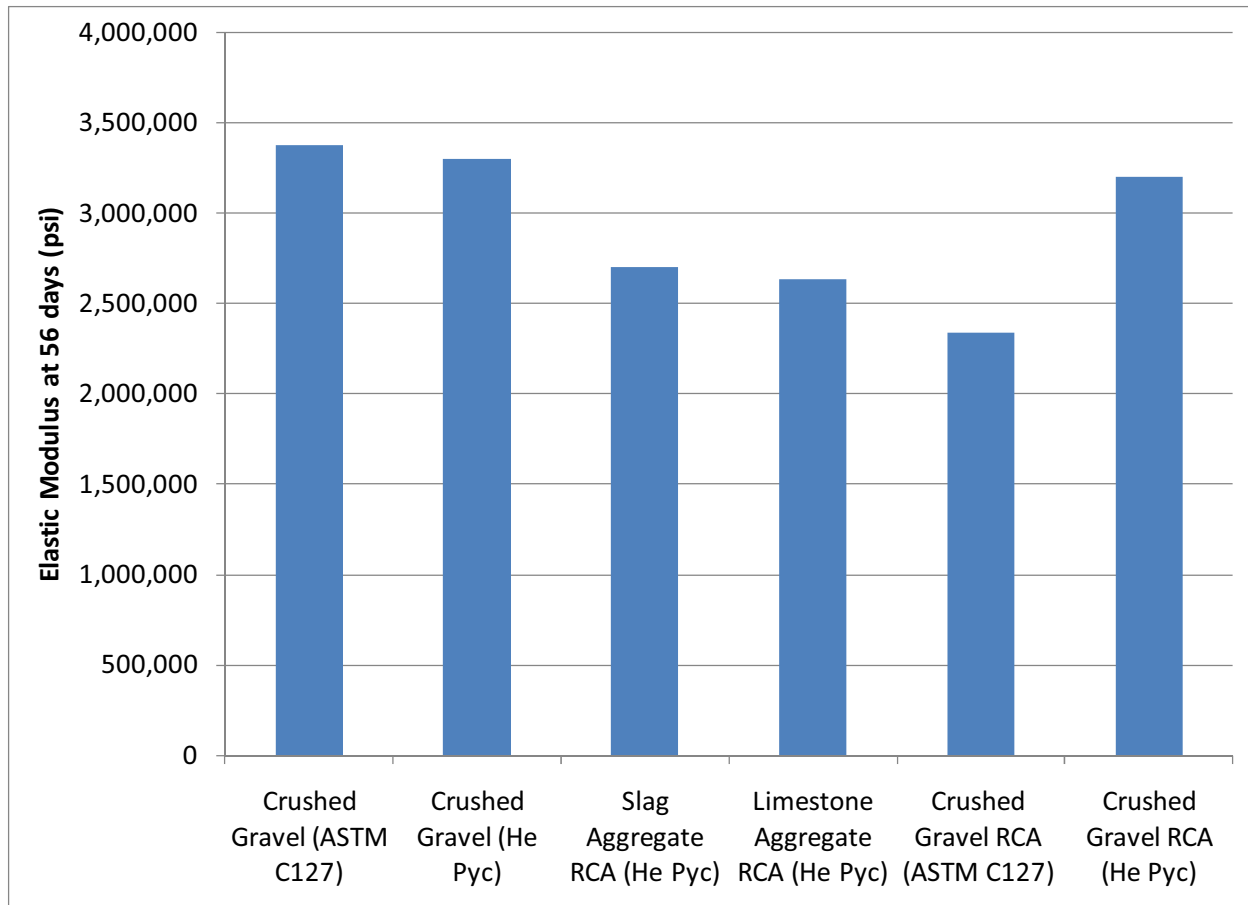


Figure 4-6. Elastic modulus at 56 days.

4.5.3 Rapid Chloride Ion Penetrability

For the mixtures prepared, resistance to chloride ion penetrability was measured as per ASTM C1202 (2008) at the age of 56-days, and results are presented in Figure 4-7. Concrete mixtures made with RCA exhibited very high penetrability to chloride ions in comparison to virgin crushed gravel concrete. Limestone RCA concrete exhibited the highest penetrability values followed by slag RCA concrete, which fall in the range of having high chloride ion penetrability. Crushed gravel RCA concrete exhibited low to moderate chloride ion penetrability. Table 4-5 provides a qualitative assessment on chloride ion penetrability based on the charge passed as per ASTM C1202.

In addition to the quality of the new mortar, chloride ion penetrability is also dependent upon the quality of the old mortar adhering to the virgin aggregate in the RCA. Residual mortar in RCA has previously been suggested as a conduit for water transport (Kakizaki et al. 1988; Tam et al. 2009). Figure 4-7 shows that a conclusive correlation between water absorption and

chloride ion penetrability cannot be drawn from this study. The results indicate the quality and air void system of the old mortar present on the RCA plays an important role in chloride ion penetrability, rather than water absorption capacity or the amount of mortar present on the aggregate. As evidence, limestone RCA concrete had a lower absorption than slag RCA concrete while the slag RCA had higher percentage of residual mortar.

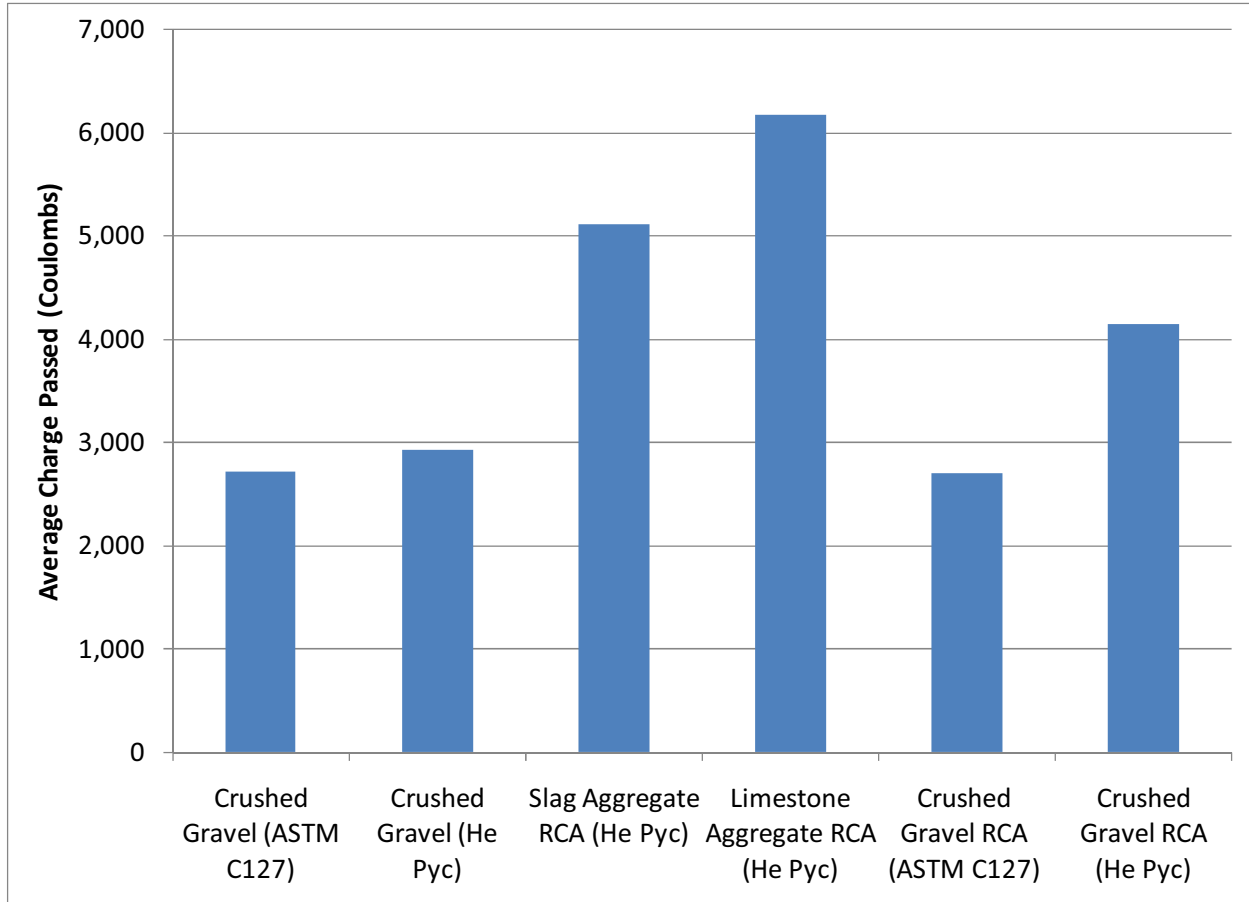


Figure 4-7. Chloride ion penetrability at 56 days.

Table 4-5. Concrete chloride ion penetrability based on charge passed as per ASTM 1202.

Charge Passed (Coulombs)	Chloride Ion Penetrability	Typical of – (According to AASHTO T277)
> 4000	High	High w/c ratio (> 0.60) in conventional PCC
2000 - 4000	Moderate	Moderate w/c ratio (0.40 - 0.50) in conventional PCC
1000 - 2000	Low	Low w/c ratio (< 0.40) in conventional PCC
100 - 1000	Very Low	Latex-modified concrete or internally-sealed concrete
< 100	Negligible	Polymer-impregnated concrete, Polymer concrete

4.5.4 Hardened Air Content

Figure 4-8 shows a comparison of the hardened concrete air content versus the air content of the mortar in the RCA. The hardened concrete air content was measured in accordance with ASTM C457 whereas the air content in the mortar of RCA was determined from image analysis measurements as a summation of the area average of all pores larger than 0.04 inch (0.1mm) diameter. All RCA concretes exhibited significantly higher hardened concrete air content than the target air content of 6% (-1% to +2% as shown by the solid lines in Figure 4-8). This figure indicates that to create an adequate air-void system in RCA mixtures, the entrained air could be potentially reduced depending upon the air content of the mortar fraction of the RCA. However, it is not known whether the combined air void systems of the attached mortar on the RCA and the new mortar are sufficiently well-connected to contribute to the overall freeze-thaw protection of the concrete. Hypothetically, if this air void system was well-connected to allow for pore pressure build-up under freezing, this reduction in entrained air may help compensate for the reduced compressive and flexural strength, and elastic modulus of RCA concretes.

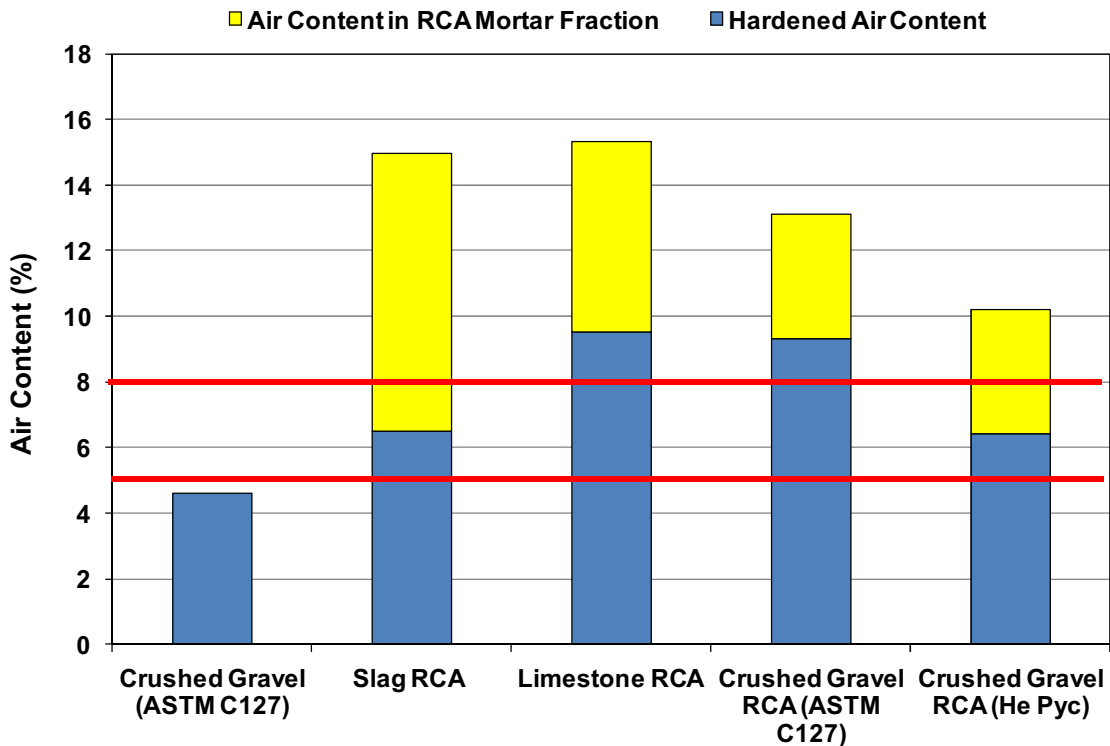


Figure 4-8. Comparison of hardened air-content in concrete and air-content of RCA mortar fraction.

The critical parameters that define a satisfactory air-void system for freeze-thaw durability of concrete are the specific surface area, void frequency, and spacing factor. Table 4-6 provides information on these characteristics for concrete mixtures made in this study. Specific surface area and void frequency are inter-related and reflect the mean size of the air bubbles. Specific surface is the ratio of the surface area of air voids (in²) to their volume (in³). For a protective air void system, the specific surface area should not be less than 600 inch⁻¹ (24mm⁻¹) and the void frequency should be within 7.6 to 15.2 per inch (0.3 to 0.6 per mm). Smaller voids have higher specific surface and tend to have a higher void frequency as well. The spacing factor is conceptually, but not actually, the average distance between any point in the paste to the edge of an air void. Typically, this should not exceed 0.008 inches (0.2mm) for adequate resistance to freezing and thawing. None of the RCA or virgin aggregate mixtures exhibited a completely adequate air-void system by these criteria with the exception of the crushed gravel RCA (He Pyc) concrete. This may have been true due to the high amount of properly air-entrained attached mortar for these aggregates as the ASTM C127 version of this mix was also quite close to passing these criteria. While this is true for these mixes, changes in the mixing and mix design process may lead to a better quality air void system in concretes using RCA.

Table 4-6. Spacing details of hardened air content in concrete (1 inch=25.4mm).

Coarse Aggregate	Void Frequency (per inch)	Within Criteria	Specific Surface Area (inch⁻¹)	Within Criteria	Spacing Factor (inches)	Within Criteria
Crushed Gravel (ASTM C127)	4.75	N	414	N	0.0119	N
Slag RCA	8.61	Y	467	N	0.0093	N
Limestone RCA	13.26	Y	605	N	0.0055	Y
Crushed Gravel RCA (ASTM C127)	16.94	N	714	Y	0.0047	Y
Crushed Gravel RCA (He Pyc)	12.93	Y	757	Y	0.0060	Y

4.5.5 Volumetric Stability of RCA Concretes

As volumetric stability issues were found to be a major concern through both literature review and previous failures of RCA concrete pavements, this study looked at characterizing autogenous, drying, and total shrinkage of these concretes in comparison with more standard aggregate concretes. This study also looked at restrained shrinkage of RCA concrete to assess its potential for mitigating some shrinkage strains through creep mechanisms, which RCA concrete has been demonstrated to possess by other researchers.

4.5.5.1 Unsealed Prisms in 100% Relative Humidity

In Figure 4-9, the measured length change values of concrete prism samples placed in a 100% RH moist curing room are shown. These samples were unsealed to allow water to be absorbed into the concrete for continued hydration. The first length measurement was taken 18 hours after addition of mixture water. A significant level of expansion was observed in the concretes made with RCA in comparison to concrete made with virgin crushed gravel. Higher strains and weight gain (negative weight loss) were observed in concrete made with slag RCA (Refer to Figure 4-9 and Figure 4-10) in comparison to the other concretes. All mixtures show a reduced rate of length change after a period of 30 days in 100% RH, but a weight gain is typically observed beyond this time period for all mixtures. This trend indicates that the concrete continues to hydrate in the presence of moisture but it does not result in considerable length change.

Typically, mixtures made with absorbed water corrections established using the helium pycnometer resulted in lower weight gain and lower shrinkage strain in comparison to the ASTM C127-based method (Figure 4-10).

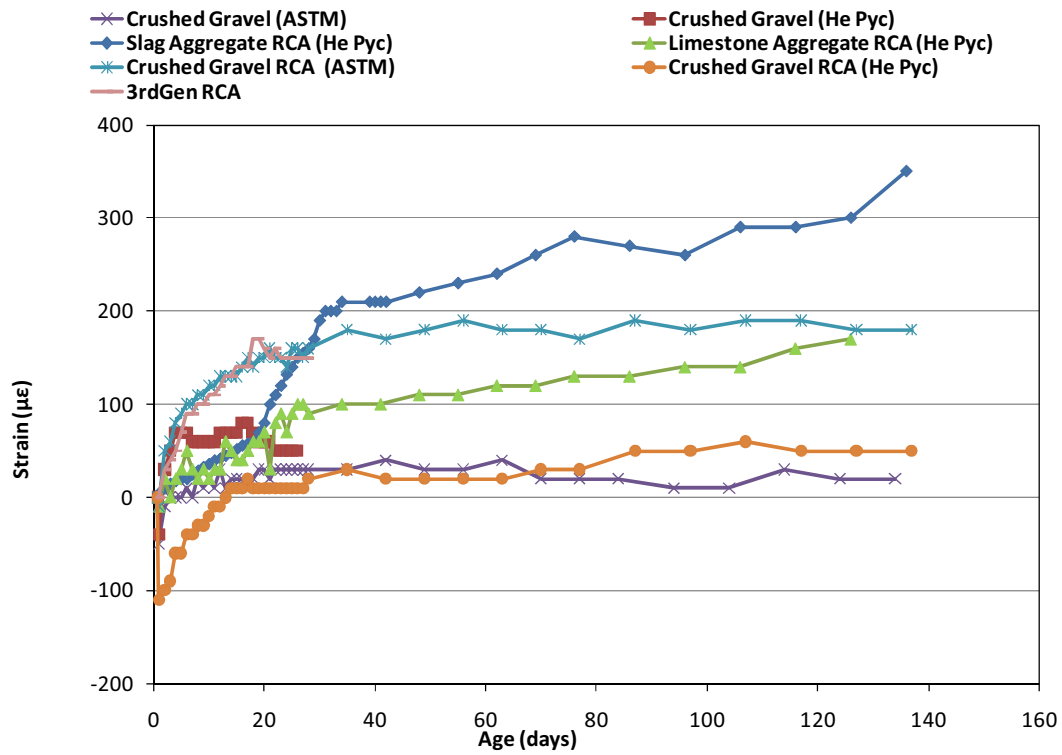


Figure 4-9. Uniaxial shrinkage strains (growth) of prism specimens in 100% RH.

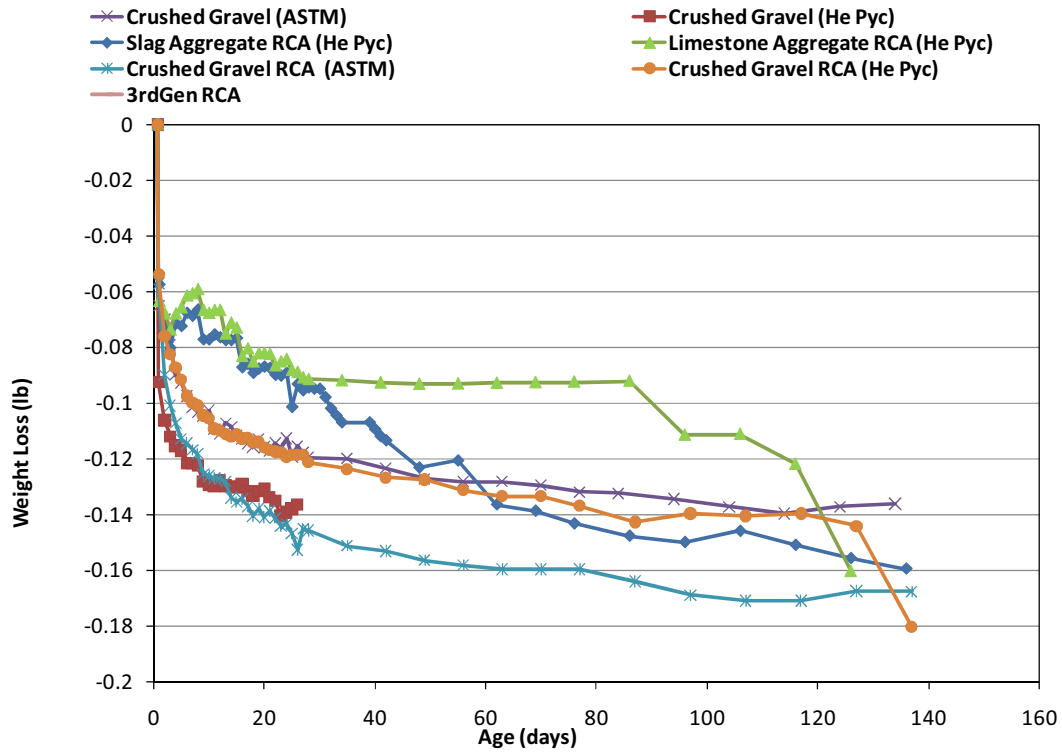


Figure 4-10. Weight loss of shrinkage prism specimens in 100% RH.

4.5.5.2 Unsealed and Sealed Prisms in 50% Relative Humidity

Figure 4-11 shows the measured sealed concrete prism strains to assess the level of autogenous shrinkage, and Figure 4-12 shows the minimal weight loss for the specimens stored at 50% RH at room temperature. Under these sealed conditions, slag RCA concrete exhibited an initial expansion followed by a reduction at later ages. This behavior was attributed to the large interconnected pore structure of the slag RCA that was able to contribute moisture to the hydration process, even when the system was closed to external moisture sources. This behavior was not observed in any of the other mixtures tested. The highest weight loss was observed for slag RCA concrete whereas the lowest weight gain was observed for concrete mixtures with virgin aggregate only.

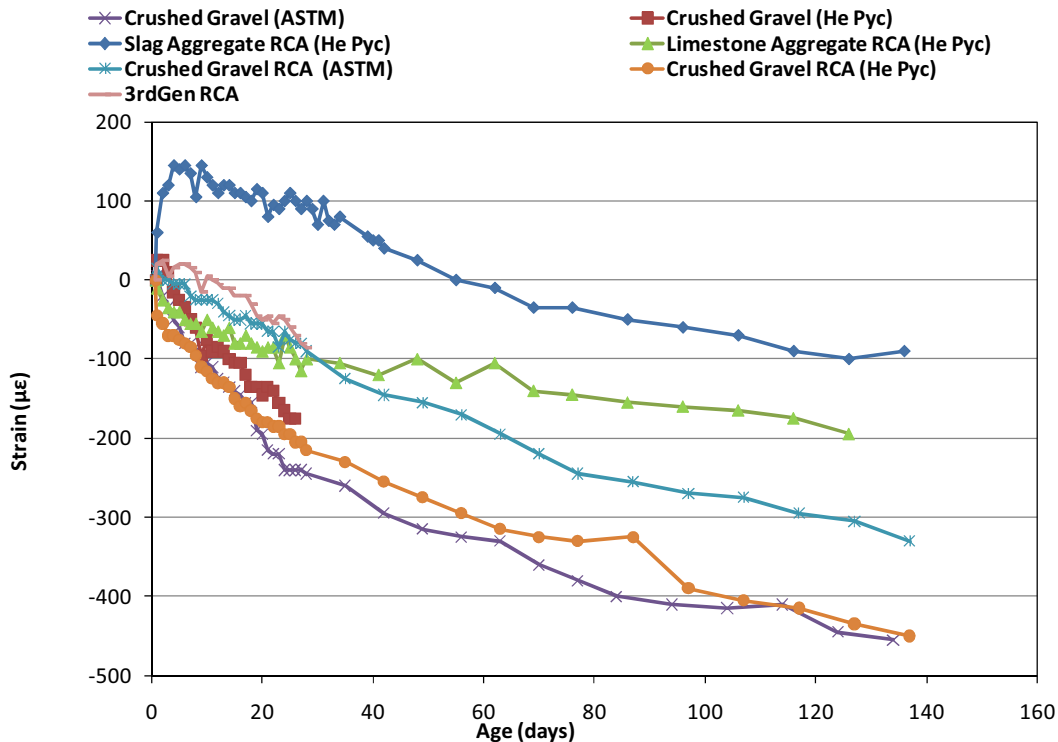


Figure 4-11. Uniaxial shrinkage strains of prism specimens at 50% RH in sealed conditions.

It should be noted that these weight losses were rather insignificant in comparison to their unsealed companion prisms in the same environment. In a completely sealed system, the weight loss should be minimal as water from the mixing process should not exit the system. Likewise, water from the ambient air should not be absorbed into the system if greater than the internal relative humidity.

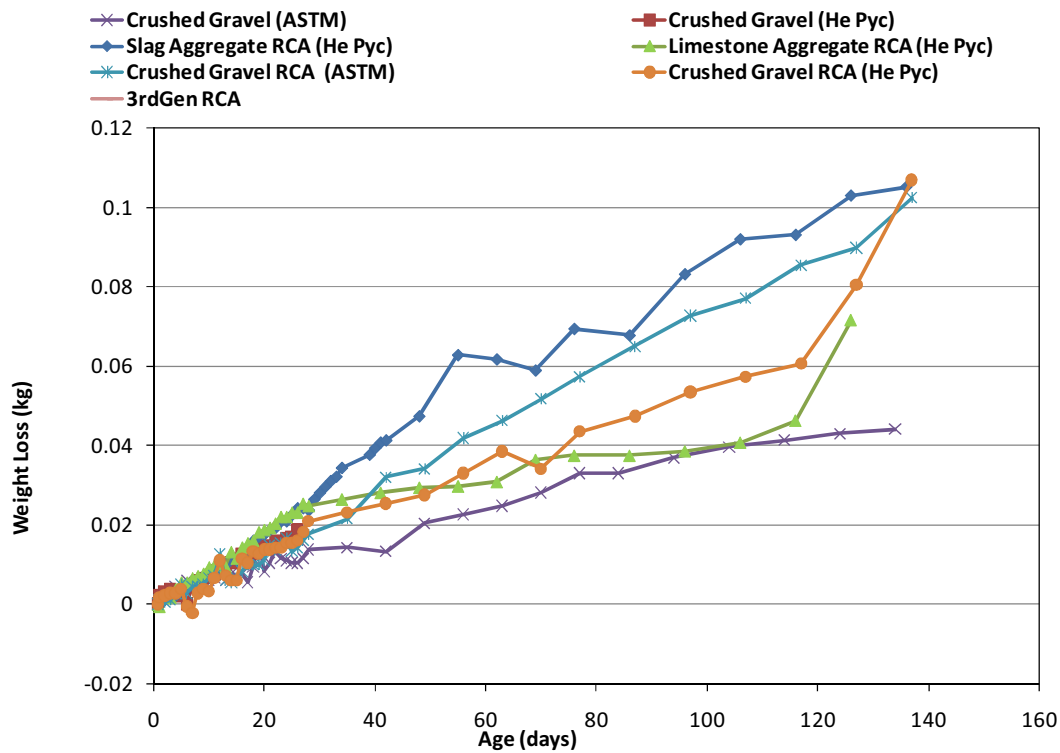


Figure 4-12. Weight loss by prism samples stored at 50% RH in sealed conditions.

The higher porosity slag increased the slag RCA concrete’s ability to store water in pores, or in effect, increased the internal humidity of the concrete in the larger pores. In the case of these more porous concretes under sealed conditions, the rate of moisture loss from the specimens was reduced, leading to reduced autogenous strain development as concrete is more prone to autogenous shrinkage development at lower w/c ratios. Combining these factors with the condition of having excess water in mixtures, the net result was measured reduced strain. Consistent with this fact, it was observed that crushed gravel RCA (He Pyc) and crushed gravel (ASTM C127) exhibited the highest strain.

Image analysis results presented in Chapter 3 indicate that among all the RCAs used in this study, slag RCA is the most porous followed by the limestone RCA. The reduced strain in high-porosity RCA concrete described above is consistent with these image analysis results.

Figure 4-13 and Figure 4-14 show the development of strains and significant weight loss in specimens, respectively, stored at 50 % RH at room temperature under unsealed conditions. The unsealed conditions provide an indication of the cumulative volumetric stability issues including autogenous and drying shrinkage. This unsealed specimen testing is defined as the

“free shrinkage” of a concrete specimen. Typically, a higher rate of increase in strain was observed within the first 30 days followed by a lower rate of strain development for all specimens. The highest strains were measured in crushed gravel RCA concrete specimens, which had lower porosity and therefore absorbed less water.

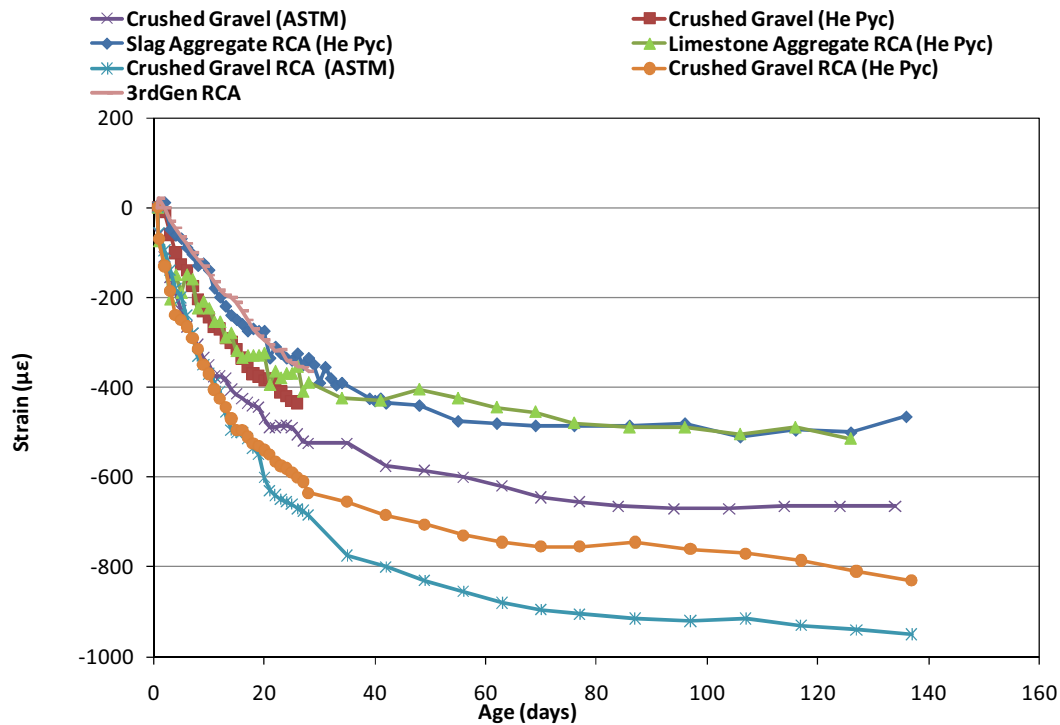


Figure 4-13. Uniaxial shrinkage strains of prism specimens at 50% RH (unsealed).

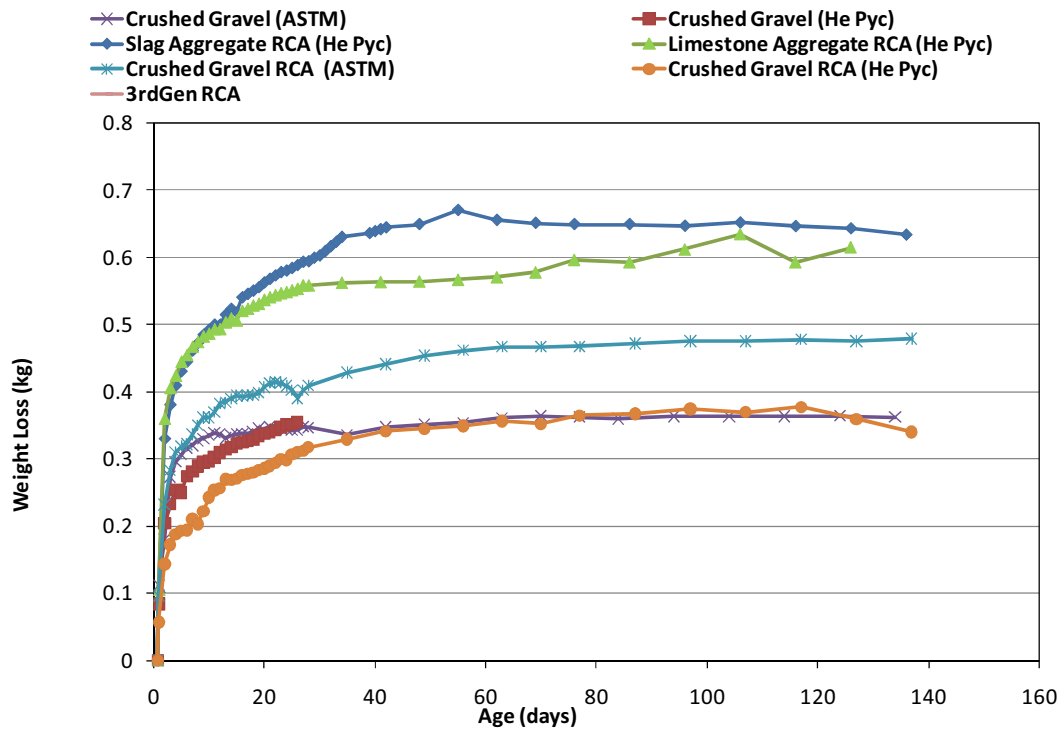


Figure 4-14. Weight loss by prism samples stored at 50% RH in unsealed conditions.

Another reason for higher shrinkages may potentially be related to the amount of unhydrated cement present within the old mortar fraction of some of the RCA. The unhydrated cement particles can undergo rapid hydration when they come in contact with water and artificially lower the intended w/c ratio. In this study, the specific amount of unhydrated cement was not calculated for each RCA. However, optical micrographs of some RCA shows unhydrated cement in the attached mortar phase, as shown for crushed gravel RCA in Figure 4-15. The level of unhydrated cement may be an important factor to consider when recycling older concrete that may have utilized coarser-grained Portland cement (lower Blaine fineness), characteristic of older cements.

Figure 4-16 shows the drying shrinkage measured for concrete samples based on the difference in shrinkage strains developed in sealed and unsealed conditions at 50% RH and 23°C. The highest drying shrinkage strains and weight loss were observed in crushed gravel-based RCA. All RCA-based mixtures exhibited a substantial weight loss until 20 days, after which, a slightly higher weight loss is observed for slag RCA mixture.

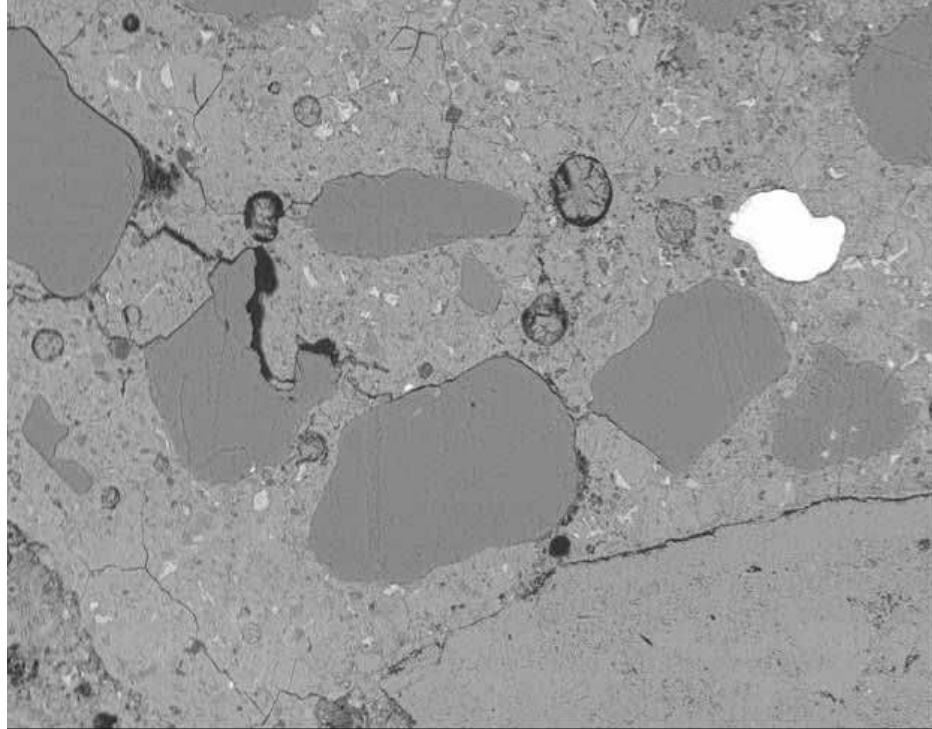


Figure 4-15. Optical micrograph showing unhydrated cement (white particle) in attached mortar phase of RCA.

A rapid change in strains was observed in the initial 30 days followed by a gradual increase in strain for all mixtures. Typically, concrete exposed to ambient conditions experiences about 20% of its ultimate shrinkage in the first 20 days and roughly 80% of the ultimate shrinkage over a period of one year (Neville 1996). Initially, the slag RCA concrete exhibits a modest expansion followed by continued drying shrinkage. Lower drying shrinkage strains at early ages in concrete made with porous aggregates, such as slag RCA concrete, were most likely due to a high water content and open pore structure in the aggregate. Thus, as the weight loss in the slag RCA concrete increased after 28 days, the drying shrinkage strains also increased. Crushed gravel (ASTM C127), crushed gravel RCA (He Pyc), and limestone RCA concretes exhibited an increase in drying shrinkage strains in the first 50 days followed by a drop in the measured strains, indicating that some amount of autogenous shrinkage continued to occur past 50 days. Overall, it was observed that concrete made with absorption corrections based on the helium pycnometer exhibited higher measured strains in comparison to concrete made with water corrections based on ASTM C127 method.

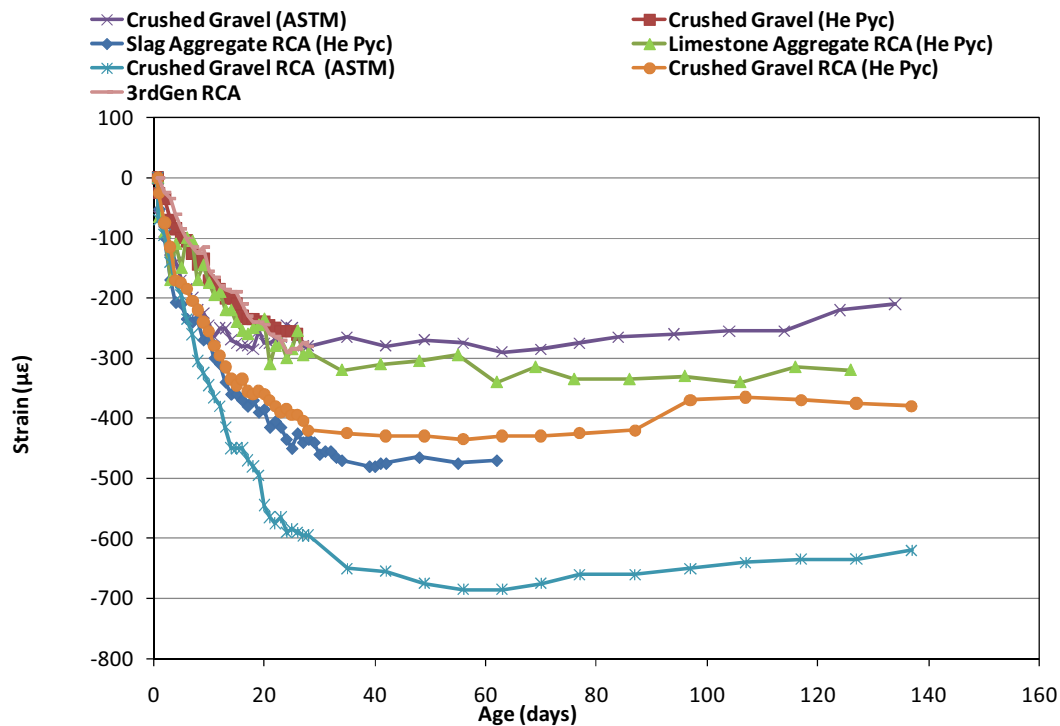


Figure 4-16. Uniaxial drying shrinkage strains of prism specimens at 50% RH.

4.5.5.3 Restrained Shrinkage

Table 4-7 presents the results of tests used to assess the rate of strain development of concrete specimens under restrained conditions. All concrete mixtures exhibited an initial increase in strain in the first 24 hours followed by a rapid drop in strain. The highest strains were measured for the slag RCA concrete. Limestone RCA and crushed gravel aggregate RCA (He Pyc) exhibited lower restrained strain development in comparison to crushed gravel aggregate (ASTM C127) concretes. This observation is contrary to the observed trend for unrestrained drying shrinkage samples where almost all RCA concretes exhibited higher drying shrinkage strains than virgin concretes. The amount of mortar present on the RCA can have an effect on the rate of strain development under restrained conditions. Slag RCA has the highest amount of residual mortar and exhibits higher strains compared to the limestone RCA or crushed gravel RCA mixtures. None of the restrained shrinkage ring concretes cracked even though strain levels observed on the inside of the steel rings were significant. This may be due to the reduced elastic moduli values of these concretes and the resulting lower stresses in the concretes themselves.

Table 4-7. Restrained ring shrinkage strains at 28 days for virgin and RCA MDOT P1 concretes.

Coarse Aggregate Type	Compressive Strain at 28 days ($\mu\epsilon$)
Crushed Gravel (ASTM C127)	82.9
Crushed Gravel (He Pyc/EDA)	72.2
Slag RCA	74.8
Limestone RCA	62.8
Crushed Gravel RCA (ASTM C127)	75.8
Crushed Gravel RCA (He Pyc/EDA)	72.1
3rdGen RCA	65.4

While some differences exist in the restrained shrinkage results at later ages, Table 4-7 shows similar restrained shrinkage strains for all concretes tested. This trend shows that while drying shrinkage is typically much higher for RCA concretes, its creep properties provide some ability to relax these drying shrinkage mechanisms under restrained conditions. Restrained conditions in concrete pavements may include dowels, tie bars, and self-weight that impacts the curling/warping stresses.

Comparably high strain development is observed in slag RCA, crushed gravel RCA, and limestone RCA concretes. The 3rdGen RCA concrete mixture shows good performance in the restrained ring test with the ability to relax strains similar to the first generation recycled aggregate concretes. Comparing the behavior in Table 4-7 and Figure 4-13, it can be observed that though slag RCA concrete exhibits lower free shrinkage strains, under restrained conditions the strain development in the concrete is higher.

4.6. Summary and Conclusions

In this study, five different aggregate sources were used to produce nine different concrete mixtures. The fresh and hardened properties measured were slump, air content, unit weight, hardened air-content, compressive and flexural strength at 28 days, elastic modulus and chloride ion penetrability. Extensive studies on the shrinkage properties of the mixtures were

performed using different test regimes and curing regimes. Observations made in this study are as follows:

1. Accurate and appropriate measurements of the physical characteristics such as absorption capacity and specific gravity affect the fresh and hardened concrete properties for mixtures made using RCA.
2. The total air content in the hardened RCA concretes was higher than the target air content that was achieved in normal aggregate concrete mixtures. The total air content is affected by the amount of mortar adhering to the RCA and the quality of that mortar.
3. In general, the quality and amount of mortar present on the RCA impacts the fresh and hardened concrete properties of mixtures containing RCA.
4. All RCA concretes exhibited workable initial mixtures except the mixture made with 3rdGen RCA, even though most RCA concretes had higher slump than the targeted value. However, the window for good workability for these mixes was often short as the RCA continued to absorb available mix water after the mixing process was complete due to the RCA's inherent porosity. This short window of workability can potentially be addressed through aggregate wetting or soaking in a two-stage mixing process.
5. All RCA concretes exhibited a lower compressive strength and elastic modulus with respect to comparable virgin aggregate concrete mixtures. Mixtures made using the aggregate specific gravity and absorption measured using the Helium pycnometer exhibited lower compressive strength and elastic modulus values than those made with the specific gravity and absorption determined by standard ASTM C127 measurements.
6. Chloride ion penetrability of RCA mixtures is affected by the porosity of the concrete and the quality of the mortar adherent to RCA.
7. The development of shrinkage strains in RCA concrete is dependent upon the environment and the moisture content of the system. Slag RCA concrete exhibited the highest drying shrinkage strain, but was similar to other concretes in restrained conditions. All mixtures containing virgin crushed gravel aggregate exhibited comparable strain development to the RCA concretes under restrained conditions.
8. While drying shrinkage of RCA concretes was often much higher than that of virgin aggregate concretes, the ability of RCA concrete to allow substantially higher creep characteristics tended to produce similar results under restrained conditions.

CHAPTER 5. EXPERIMENTAL TESTING FOR THE LEACHATE CHARACTERISTICS OF BASE AGGREGATES

5.1. Background

Using an open-graded drainage course (OGDC) as a base support layer under concrete pavement has been used for decades in many states. Before its use, bases were constructed using a dense-graded aggregate, providing adequate long-term support, but poor sub-surface drainage characteristics without a designed underdrain system. Poor drainage under the pavement surface layer has been shown to be a major contributor to premature deterioration at joints and cracks, due partly to saturation of the bottom side of the pavement slab leading to loss of underlying support under traffic loading. OGDC bases alleviate the buildup of pore pressure and areas of saturation by quickly draining water away from the pavement's base, directing it into an engineered edge drain system.

Currently, MDOT does not allow RCA in OGDC when a pavement base or subbase is constructed. The Department's "2003 Standard Specifications for Construction" (MDOT 2003) prohibits the use of RCA as OGDC when the subbase of the pavement section is graded to a nearby engineered open-graded base edge drain system. This prohibition reduces the opportunity for recycling old concrete pavement and concrete slabs in new pavement structures, resulting in higher costs related to transportation and landfilling to dispose of concrete debris, and costs for hauling in virgin aggregate for the new construction. The primary reason for this prohibition was to limit leachable cementitious fines from the crushed concrete entering the new edge drains in unbound layers.

In past years, research has been conducted to understand the impacts of RCA as OGDC in pavement construction (Bruinsma 1995; Snyder and Bruinsma 1996; Steffes 1999). These studies found that the pH of the effluent leachate from coarse-graded RCA studied was 9.7-10.5 and from fine-graded RCA the pH was approximately 11-12. High alkaline effluent corroded the rodent guard screen and fine crushed concrete particles leached from RCA open-graded base to cause clogging of the sub-surface drainage system. With respect to the composition of the effluent, Limbachiya *et al* (2007) reported the effluent of coarse RCA contained mainly SiO_2 , Al_2O_3 and CaO .

However, these researchers do not mention whether the pH measurements were conducted intermediately following initial construction or before their final observations 6 years later (Bruinsma 1995; Snyder and Bruinsma 1996; Steffes 1999). Hence, there was no identification whether, in time, leaching diminished to insignificant levels. The Iowa DOT reported measuring the pH of the effluent, which included a qualitative visual assessment of the leachate (Steffes 1999). Their field investigations reported that the alkalinity of the discharged effluent decreased over the first three months, stabilizing at a pH of 11. This level of pH continued for the duration of the study and was expected to remain at these levels for several years thereafter. In addition, this report documented significant quantities of leachate exiting the edge drains. However, it did not recommend removing the outlet screens to alleviate leachate accumulation in the pipe. Some unresolved issues from this research included the following:

- The chemical composition of the leachate from the RCA was not well characterized
- Leaching characteristics of different gradations of RCA was not investigated.

Therefore, further investigation of RCA leaching is needed to establish its suitability for use as OGDC. The objective of this study was to verify the following:

- If leachate from unbound crushed concrete will clog the edge drain system
- If the pH of RCA leachate effluent is below the threshold for being environmentally hazardous, and
- If the leachate contains any components of environmental concern. To fulfill this objective, both field observation and laboratory investigations were conducted.

The field observations assessed the precipitate accumulation at the drain outlets on selected projects after one winter in service. In the laboratory experiments conducted by MDOT, crushed concrete, limestone, natural gravel and blast furnace slag were tested to measure the comparative leachate volumes accumulated. Residual precipitate materials were collected from cyclic testing and sent to Michigan Tech to determine the chemical composition of the leachate.

Each material was separated and recombined into three gradations representing the upper, middle and lower gradation specifications of the MDOT Series/Class 4G base material specification (MDOT 2003) as shown in the 0.45 power gradation chart in Figure 5-1. The deposits were then analyzed using various methods to determine chemical properties.

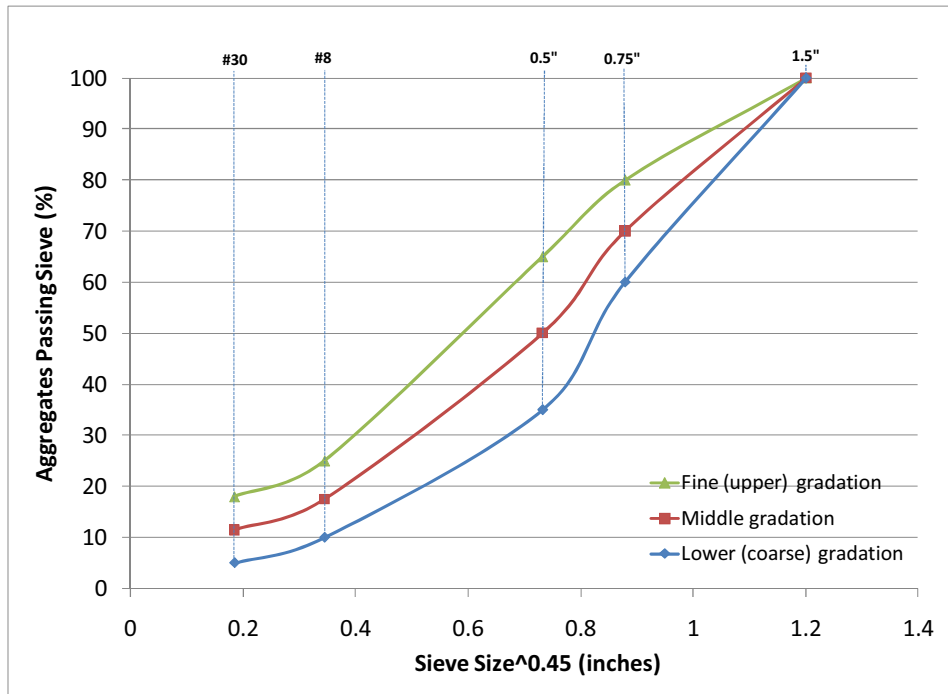


Figure 5-1. 0.45 power gradation chart for MDOT open graded aggregate series 4G.

5.2. Field observations

Field inspections of two recently completed projects were conducted by MDOT materials technicians from the Construction and Technology Division. One project, located on I-69 east of Flint, was completed in 2007 and utilized blast furnace slag in the OGDC layer. Figure 5-2 illustrates a typical edge drain outlet from this project. These pictures show a high degree of corrosion, partial plugging of the rodent screen, and also significant material build up behind the rodent screen extending into the drainage system outlet pipe.



Figure 5-2. I-69 east of Flint; (left) partially plugged rodent screen; (right) blast furnace slag sludge behind screen.

The other project, located on I-75 near Bridgeport, was completed in 2008 and utilized RCA from the old PCC pavements in OGDC directly beneath the PCC shoulders. This RCA contained crushed gravel as its original aggregate source. A virgin limestone OGDC was used directly under the mainline pavement lanes. An additional open-graded edge drain was intentionally installed at a location two feet beyond the outside edge of the shoulder in an effort to capture any leachate. The OGDC material used in this project contained more fines than the current MDOT Series/Class 4G gradation specification permits. Figure 5-3 shows the precipitate from the drains after one winter in service.



Figure 5-3. I-75 near Bridgeport; Precipitate from high fines crushed concrete OGDC under shoulder.

5.3. Laboratory leachate investigation

In this study, MDOT utilized four types of aggregate (i.e. crushed gravel, limestone, RCA, and blast furnace slag) to quantify leachate material resulting from drainage through pavement base material. Each type of aggregate was prepared using three gradations as previously described (i.e. upper, middle, and lower limits of the MDOT Series/Class 4G gradation specification). Each aggregate gradation was subjected to leaching using separate solutions of both deionized water and simulated acid rain. Simulated acid rain was produced using deionized water and H_2SO_4 to achieve a pH of 5.0. At seven day intervals, the pH of each sample was measured prior to decanting 30 in³ (500 mL) of liquid from each container. New

liquid (distilled or acidic water) of volume 30 in³ (500 mL) was then added to the containers to replace the decanted liquid for another 7-day leaching cycle. The liquid from each test was decanted through a 0.1 mil (2.5 µm) filter into aluminum pans. The decanted liquid captured in the pans was then placed in an oven at 180°F (82°C) to evaporate water and to precipitate the dried leached effluents. The process was repeated for 11 weeks, cumulatively resulting in 538 pans with leachate precipitates. For analysis, the precipitated solids were collected by removing the deposits from the pans and categorically combining them from each aggregate type for weeks 1-2, weeks 3-5, and weeks 6-11 to ensure a sample size adequate enough for chemical analysis. This splitting of the samples by weeks also allowed for documentation of whether there was a change in the chemical composition indicating a possible change in precipitate minerals over time. The precipitates were analyzed using a scanning electron microscope (SEM) equipped with an energy dispersive X-ray analyzer (EDXA), X-ray diffraction (XRD), and weighing of the leachate deposits.

5.3.1 Leachate chemical analysis

5.3.1.1 SEM analysis

SEM analysis was used to detect the chemical composition of both blast furnace slag and RCA leachate precipitates. Twelve samples representing the two aggregate types, three gradation specifications, and two leaching solutions were prepared for each time grouping. The preparation was done by taking a 1 gram sample of each precipitate and placing it on a specimen holder. The specimen was then covered with a conductive coating using a "sputter coater". Further details regarding SEM sample preparation can be found in (bama.ua.edu 2006).

Figure 5-4 and Figure 5-5 show SEM micrographs of the RCA and blast furnace slag leachate precipitates, respectively. These micrographs show that the morphology of the leachate precipitates from blast furnace slag is similar with respect to leaching solution (Figure 5-5). On the other hand, Figure 5-4 shows that the leachate morphology of RCA is different with respect to the solution used, particularly for the upper (fine) gradation. Due to its consistency, the SEM was used to analyze the leached chemical composition of blast furnace slag for weeks 1-2, while XRD was used to detect the leached chemical composition of RCA to further investigate.

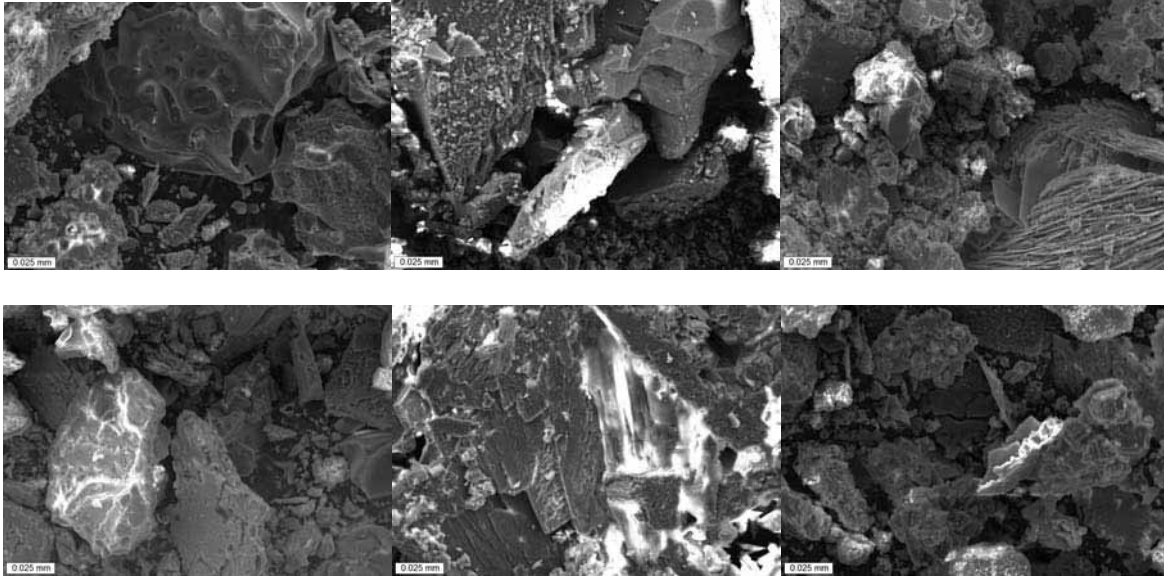


Figure 5-4. SEM images taken from the leachate precipitated deposit of RCA in 1-2 weeks. Note: simulated acid rain water—first row, deionized water—second row; from left to right, upper, middle, lower gradation specification; magnification, 650x.

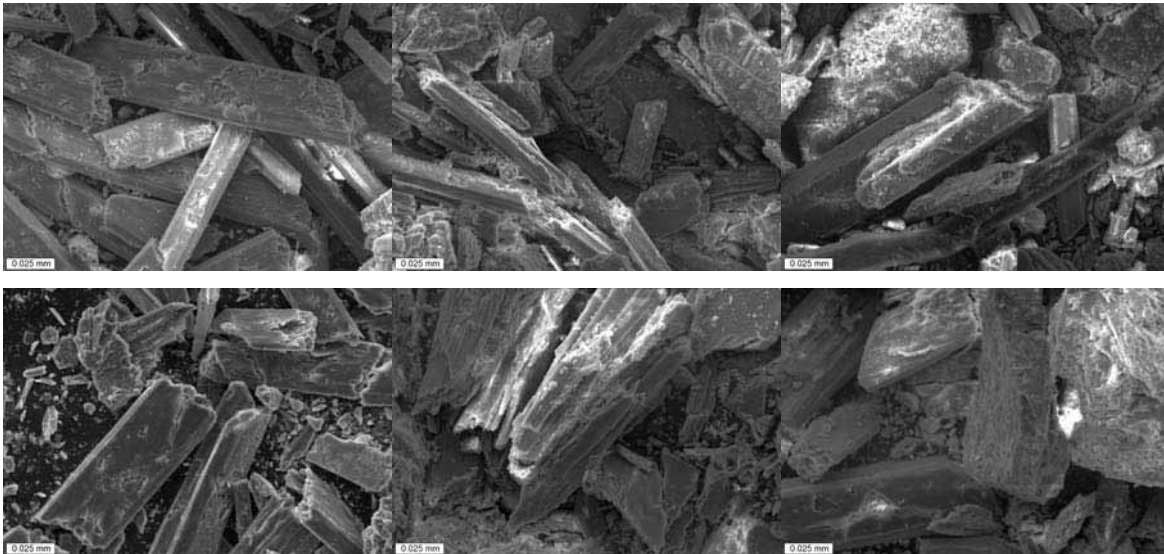


Figure 5-5. SEM images taken from the leachate precipitated deposit of blast furnace slag in 1-2 weeks. Note: simulated acid rain water—first row, deionized water—second row; from left to right, upper, middle, lower gradation specification; magnification, 650x.

Using SEM, the precipitates can be chemically analyzed based upon characteristic X-ray spectrometry through the energy dispersive X-ray analysis (EDXA) (Goldstein et al. 1992). Figure 5-6 shows an example X-ray spectrum obtained from the leachate precipitate from the blast furnace slag. Three analyses were taken from different positions on the specimen surface and the measured intensities were averaged for each element. The measured intensity is

proportional to the concentration so this approach allows for average relative quantities of each chemical to be determined for each specimen. Figure 5-6 illustrates the precipitates are primarily calcium, sulfur, and oxygen, suggesting the precipitates are a form of gypsum (CaSO_4). A quantitative analysis, listed in Table 5-1, was performed by converting the average measured X-ray intensity from three spectra to weight percentage. When comparing the measured x-ray spectrums from Figure 5-6 to the theoretical compositions of the various forms of gypsum, the precipitates were found to be very similar to gypsum with some level of dehydration.

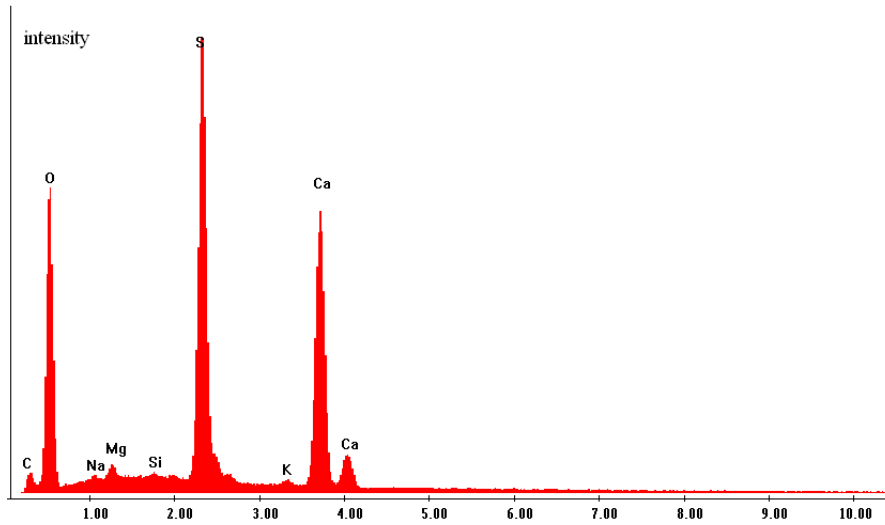


Figure 5-6. Characteristic X-ray spectrum from a blast furnace slag leachate precipitate using SEM.

Table 5-1. Summary of spot analyses from 1-2 week evaporation pan deposits collected from blast furnace slag aggregate.

Element (%)	deionized water			simulated acid water			pure minerals (control)		
	fine	middle	coarse	fine	middle	coarse	anhydrite	hemi-hydrate	gypsum
H	*	*	*	*	*	*	0.00	0.69	2.34
O	*	*	*	*	*	*	47.01	49.60	55.76
C	*	*	*	*	*	*	0.00	0.00	0.00
Na	0.13	0.05	0.16	0.13	0.20	0.16	0.00	0.00	0.00
Mg	0.45	0.12	0.36	0.14	0.21	0.24	0.00	0.00	0.00
Al	0.01	0.01	0.00	0.02	0.01	0.00	0.00	0.00	0.00
Si	0.09	0.02	2.49	0.04	0.01	0.07	0.00	0.00	0.00
P	0.05	0.07	0.03	0.06	0.05	0.05	0.00	0.00	0.00
S	23.12	22.70	20.03	24.00	23.41	19.82	23.55	22.09	18.62
Cl	0.32	0.11	0.27	0.18	0.09	0.06	0.00	0.00	0.00
K	0.25	0.02	0.63	0.16	0.32	0.17	0.00	0.00	0.00
Ca	32.86	32.75	28.38	34.86	33.29	28.57	29.44	27.61	23.28
Ti	0.00	0.00	0.00	0.00	0.00	0.00	0.00	0.00	0.00
Mn	0.03	0.07	0.10	0.10	0.01	0.04	0.00	0.00	0.00
Fe	0.09	0.05	0.03	0.08	0.00	0.02	0.00	0.00	0.00

Note: * signifies the element cannot be detected by SEM.

5.3.1.2 XRD analysis

Each leachate precipitate specimen from blast furnace slag, natural gravel, and limestone was analyzed by XRD to both confirm SEM analysis results and obtain more detailed chemical composition information. For this analysis, the leachate precipitate from each gradation and type of aggregate was combined to provide a large enough sample for XRD analysis. Figure 5-7 shows an overlay of the 8 diffractograms (i.e. diffraction pattern) resulting from the x-ray diffraction analysis of the leachate precipitates from the four types of aggregates. As these 8 spectrums overlap each other, 500*N (N=1, 2, ... to 8) counters were added to each spectrum so that each individual spectrum can clearly be noted. Also, at the top of Figure 5-7, the reference pattern for calcium sulfate hydrate PDF# 41-0225 (ICDD 2009) is plotted. In Figure 5-7, it can be seen that the topologies of the patterns are similar. That is, the diffraction profiles appear at

approximately the same diffraction angle with approximately the same intensity. It should be noted that diffraction peak intensity is proportional to the abundance of a phase in the sample, but can also be affected by numerous other factors such as the orientation of the crystals within the sample. When comparing to the reference pattern for calcium sulfate hydrate, it can be concluded that all precipitates are calcium sulfate hydrate.

According to PDF#41-0225 (ICDD 2009), a special calcium sulfate hydrate is $\text{CaSO}_4 \cdot 0.62\text{H}_2\text{O}$. It should be noted that water in the calcium sulfate hydrate had been partially lost when leachate effluents were heated for evaporation. When the leachate pans were removed from the oven, the precipitated deposit was exposed to room temperature and ambient relative humidity, hence water was re-absorbed to some degree. Such loss and absorption of water from the experimental process makes determination of the exact amount of water in the crystal structure of calcium sulfate hydrate difficult to detect. Regardless, it can be concluded that the leachate precipitates of all type of aggregates studied, regardless the gradation of aggregate, are gypsum products like $\text{CaSO}_4 \cdot 2\text{H}_2\text{O}$; while the leachate precipitate analyzed using x-ray diffraction was found to be closest to $\text{CaSO}_4 \cdot 0.62\text{H}_2\text{O}$ in its tested state. Likely, the original precipitate was $\text{CaSO}_4 \cdot 2\text{H}_2\text{O}$.

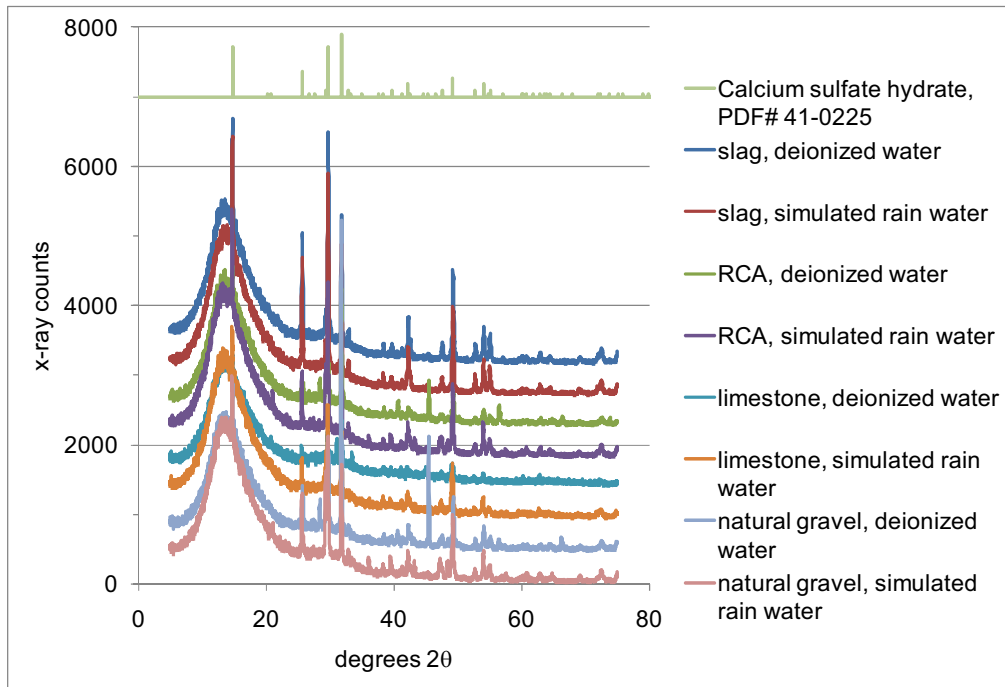


Figure 5-7. X-ray diffraction patterns obtained from the different aggregate precipitates.

5.4. Leachability volume and pH analysis

5.4.1.1 Total cumulative precipitate

The weights of each precipitate obtained from the leaching experiment were measured and tabulated in Table 5-2. For the upper (fine) gradation leached by deionized water, the trends of total cumulative precipitate mass of four types of aggregated are plotted in Figure 5-8. This shows that blast furnace slag generates almost twice as much precipitate as the RCA. These results are consistent with the field investigation previously presented. Extrapolation of the cumulative leachate precipitate mass by using the curve-fitting parameters obtained from obtained from Figure 5-8 tends to demonstrate that the amount of precipitate may potentially level off at some point under these aggressive moisture saturation conditions. This hypothesis is supported by the previously mentioned studies conducted by other state DOT's (Bruinsma 1995; Steffes 1999).

Table 5-2. Mass of leachate deposits (unit: grams).

Aggregate	Leachate solution	Weeks 1-2	Weeks 3-5			Weeks 6-11		
		merged	fine	middle	coarse	fine	middle	coarse
Natural gravel	simulated acid water	7.13	2.5	1.53	1.33	3.1	2.73	2.73
	deionized water	5.13	1.9	0.73	0.53	2.5	1.53	1.13
Limestone	simulated acid water	4.94	2.1	1.78	1.44	2.1	2.61	1.78
	deionized water	2.11	0.9	1.11	0.78	0.6	0.61	0.61
Blast furnace slag	simulated acid water	17.74	6.3	5.85	7.41	9.9	8.96	6.96
	deionized water	16.74	5.7	4.74	7.18	8	7.29	6.52
RCA	simulated acid water	11.78	3.8	3.28	0.78	4.3	2.44	0.78
	deionized water	9.11	2.6	2.61	0.61	2.6	1.86	0.86

Note: To ensure enough deposit available for XRD, three specifications of each type of aggregate were merged in weeks 1-2.

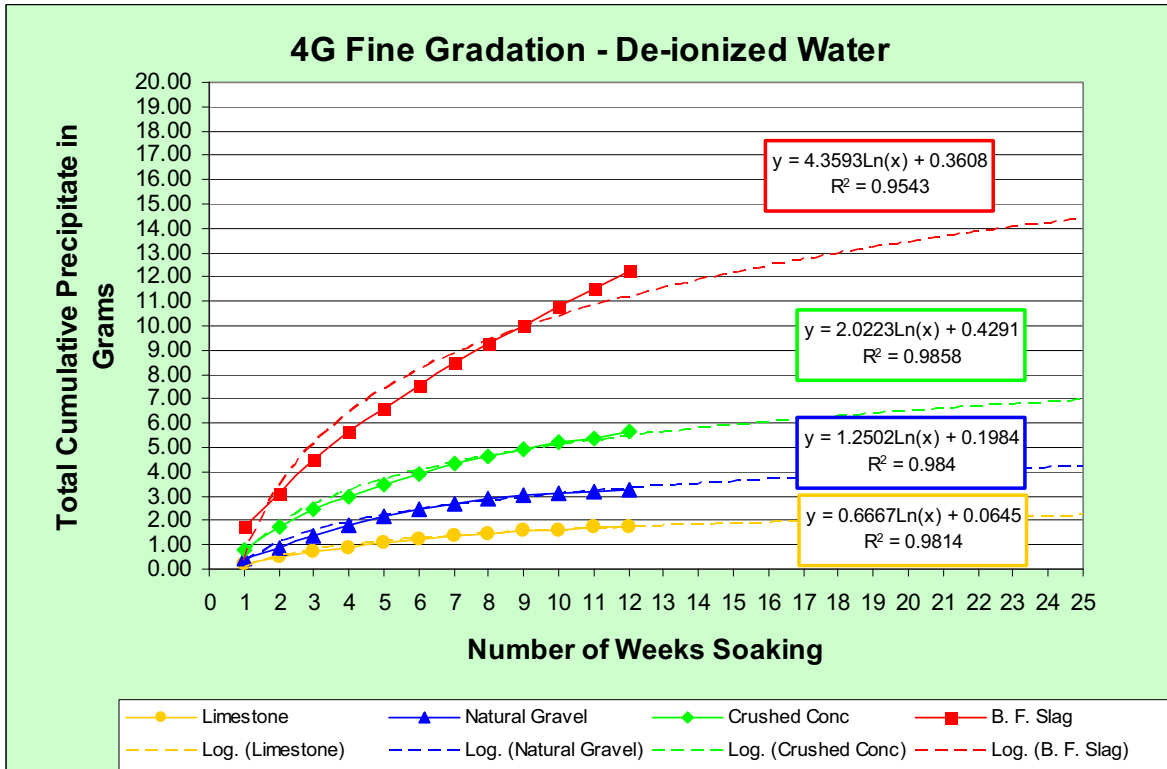


Figure 5-8. Total cumulative precipitate weight vs. number of weeks soaking

5.4.1.2 Leachability of RCA

It is important to examine the weight of leachate precipitate from the different gradation of RCA. The weight of leachate precipitate from RCA is plotted in Figure 5-9. The initial leachate precipitate mass per week (for weeks 1-2) was unaffected by the gradation. However, the leachability of the upper (fine) gradation is significantly greater than both the middle and coarse gradations, particularly at the later stages of the leaching process. This has ramifications in terms of both volumes of leachate as well as its affect on the long-term pH of the leachate effluent.

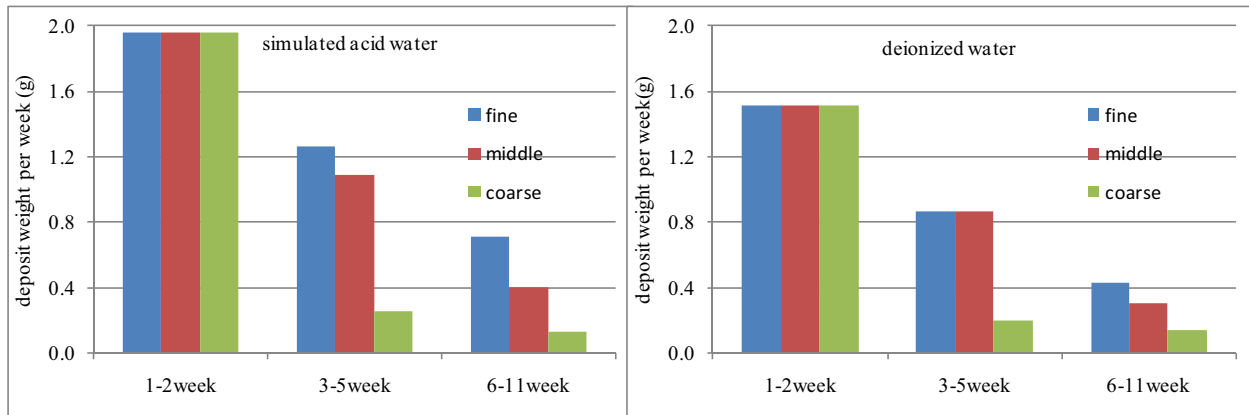


Figure 5-9. The leachate characteristics of RCA for acidic and de-ionized water sources.

5.4.2 Leachate pH analysis

As discussed earlier, the Iowa DOT's investigation of the alkalinity of OGDC effluent reported the long-term pH levels to be 11 for the effluent from a crushed concrete OGDC (Steffes 1999). The synopsis of their field measurements is this pH level would be expected after three months in-service, and would be expected to remain so for several years thereafter. In this research, the pH of the leachate from each type of aggregate was measured before decanting the leachate effluent from the container. Figure 5-10 presents the measured pH values for deionized water leachate over 10 weeks. This analysis confirms the leachate of coarse RCA is highly alkaline, blast furnace slag leachate is somewhat alkaline, and the virgin aggregate (i.e. limestone and natural gravel) leachates are near a neutral pH. The pH levels for all four coarse aggregate types evaluated in this experiment are below the maximum threshold of 12.5, as currently defined for hazardous corrosive waste by the Environmental Protection Agency (EPA) Hazard Code D002 (EPA 2010). Based on the work of this study, it can be concluded that use lower gradation (coarse) RCA as OGDC satisfies the existing environment requirements as related to pH value.

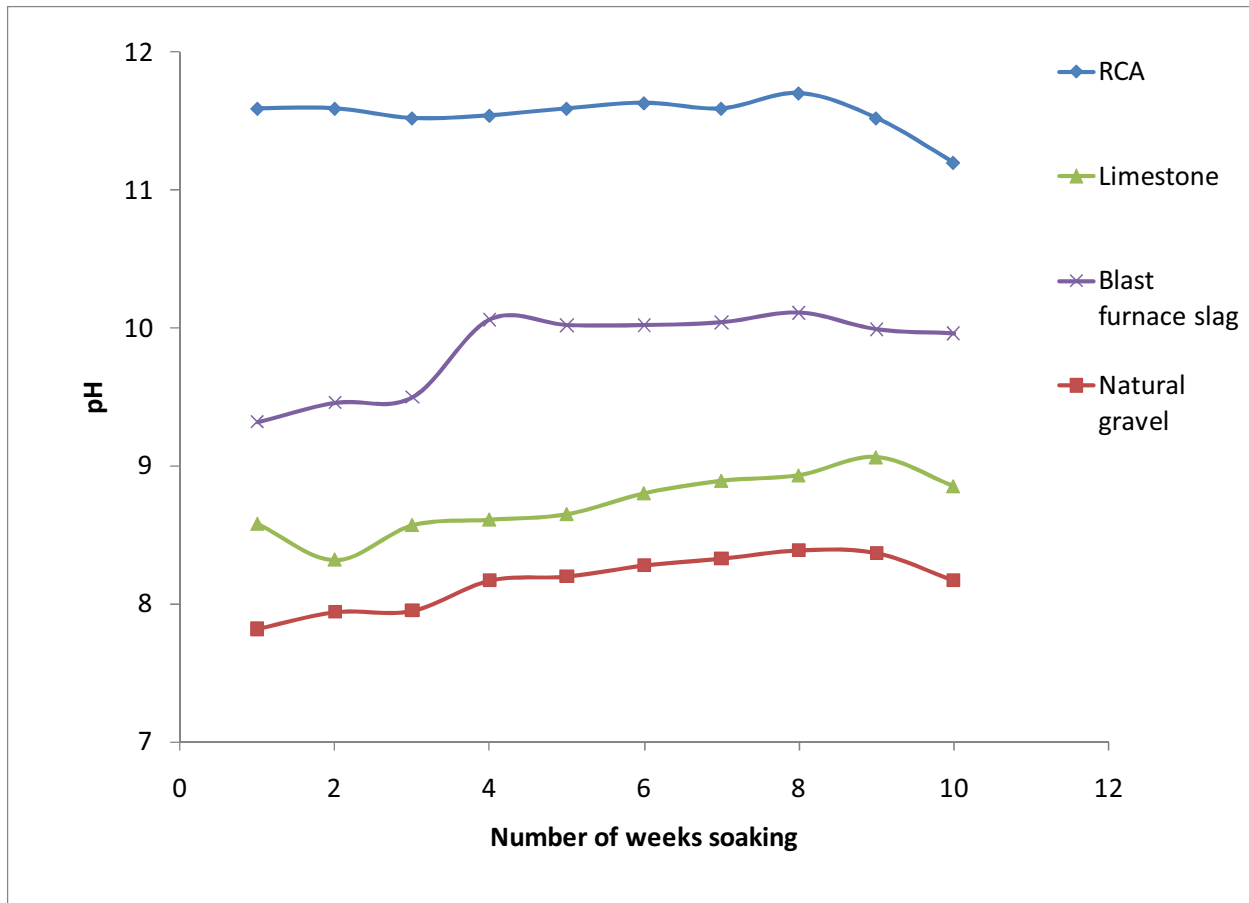


Figure 5-10. pH vs. number of weeks soaking (4G lower (coarse) gradation—deionized water).

5.5. Discussion

The use of blast furnace slag in pavement support layers poses issues when placed in OGDC situations with high moisture movement. Although the leachate from blast furnace slag contains primarily gypsum, which is not defined as a hazardous material, larger amounts of this material will be continually leached. Issues with the clogging of drain outlets could be a distinct concern.

RCA base coarse material can potentially be used as an OGDC in pavement since the alkalinity of the coarse and middle graded RCA leachate is lower than maximum threshold, 12.5, as defined for hazardous waste by the EPA Hazard Code D002 for corrosivity. While the volume of leachate from the lower (coarse) and middle graded RCA material is significant, it is quite small compared to that of blast furnace slag. Based on this study, use of upper (fine)

gradation RCA in base structures should be used with caution due additional expected leachate volume.

As mentioned before, the analysis from both SEM and XRD shows that the leached chemical composition is calcium sulfate hydrate product. However, as mentioned above, the leachate of fine graded RCA is of high alkalinity, distinguishing from the other leachate effluents. This difference fails to be detected by both SEM and x-ray diffraction methods due to the evaporation and subsequent partial re-hydration of the leached material.

5.6. Summary and Conclusions

Based on this research, the following recommendations can be drawn:

1. It is recommended that for OGDC, the prohibition of RCA materials should be reconsidered. This recommendation is based on 1) the composition of the leachate precipitate being calcium sulfate, not defined as hazard by the EPA Hazard Code D002; 2) the leachability of RCA is lower than blast furnace slag; and 3) the pH of RCA leachate is consistently lower than 12.5.
2. The use of fine graded RCA as an OGDC material is not recommended due to relatively higher leachability of this material.
3. When blast furnace slag or RCA are used in an OGDC layer, leachate may accumulate on the rodent screens to completely plug the drain outlets in the first few years. Therefore, it is essential that regular maintenance checks and cleaning of the outlets be scheduled during the first two years, at a minimum.
4. The standard plan details for the edge drain outlet rodent screen (909.11) should be modified from the current wire mesh screen (0.30 inch opening with 0.057 inch gauge) to a “finger” type screen in order to facilitate the flow of leachate and thus reduce the incidence of plugged screens. However, the opening size of the fingers must be sufficient to prevent small animal entrance to the outlets, which will inhibit free drainage to the edge drain system.

CHAPTER 6. ASR EXPANSION ASSESSMENT USING ASTM C1260 MORTAR BAR TESTING

6.1. Background and Experimental Procedures

To assess the potential for alkali-silica reaction (ASR) in various coarse aggregate and fine aggregate combinations, testing was conducted using a mortar bar expansion experiment based on the procedures outlined in ASTM C1260, Standard Test Method for Potential Alkali Reactivity of Aggregates (Mortar-Bar Method) (2008).

6.1.1 Aggregate Preparation

For this experiment, the fine aggregate source was kept constant. The fine aggregate originated from Quaternary deposits derived from glacial till associated with the Laurentide glaciation and was produced at a commercial sand and gravel pit near Hancock, Michigan. The fine aggregate is primarily siliceous and is representative of rock types typical of the Canadian Shield (Laurentian Plateau). Five different coarse aggregate sources were tested in combination with the fine aggregate as follows:

- Natural gravel from the same source as the fine aggregate
- Devonian limestone, (Traverse group) quarried near Alpena, Michigan
- Recycled concrete aggregate (RCA) produced from a pavement that utilized blast furnace slag as a coarse aggregate described in Chapter 3
- Fresh blast furnace slag
- Same source of blast furnace slag after an artificial weathering regimen

All of the coarse aggregate sources were crushed and sieved to obtain material passing the no. 4 sieve and retained on the no. 16 sieve. The crushed and sieved materials produced from the natural gravel, the limestone, and the RCA were washed with water and oven dried.

In an effort to alleviate the potential that washing may have on the properties of fresh blast furnace slag, the fresh blast furnace slag material was cleaned by agitating the particles over a no. 16 sieve while sweeping a shop vacuum with brush attachment against the opposite side of the sieve to draw away loose fine material. After cleaning, the fresh blast furnace slag material was oven dried. Additional blast furnace slag material was subjected to artificial weathering by washing with dilute hydrochloric acid followed by washing with water. After cleaning, the

artificially weathered blast furnace slag material was oven dried. The diluted hydrochloric acid wash was used to evolve the calcium sulfide fraction exposed at the surface of the blast furnace slag particles as hydrogen sulfide gas according to the equation below:



6.1.2 Mortar Bar Preparation

In an effort to establish a control case for the first phase of this experiment, the gradation listed in ASTM C1260 was followed and provided the basis for differentiation between the coarse and fine aggregates. Materials passing the no. 4 sieve and retained on the no. 16 sieve consisted of the crushed coarse aggregate sources, and materials passing the no. 16 sieve consisted of the fine aggregate source.

Three prism specimens were cast for each aggregate type in accordance with ASTM C1260. The dry materials were proportioned using 1 part cement to 2.25 parts of graded aggregate by mass. Water was added to the mix to achieve a w/c ratio of 0.47 for the mortar.

Prism specimens were cast in molds within 2 minutes and 15 seconds of completion of the mixing process. The specimens were cast in two lifts and tamped to assure proper distribution and avoid segregation. Specimens were then trowelled to strike off any excess mortar above the rim of the rectangular prism mold.

6.1.3 Mortar Bar Testing Procedure

To facilitate initial storage, the molds were placed in a moist cure room for 24 hours before demolding. After demolding, each specimen was marked and an initial length reading was taken. After this demolding, the specimens were placed in water and heated to 176°F (80°C) for another 24 hours. After this second 24 hour curing, each specimen was removed and a length measurement was taken within 15 seconds of removal from the heated water bath.

The prism specimens were then placed into a container with sufficient 1M sodium hydroxide (NaOH) solution at 176°F (80°C) for the remainder of the testing regime. Length measurements were taken every 2-3 days for 14 consecutive days.

6.2. ASR Expansion Results

As shown in Figure 6-1, only the blends containing the natural gravel coarse aggregate and the RCA coarse aggregate exceeded the expansion threshold of 0.10% at 14-days as specified in ASTM C1260. The mixtures shown in Figure 6-1 also serve as the control samples for the remainder of the ASR experiments.

For the next phase of the experiment, a fraction of the fine aggregate material passing the no. 16 sieve and retained on the no. 30 sieve was replaced with a crushed, washed, and oven-dried chert of the same gradation in an effort to accelerate ASR expansion. The source of the chert was nodules picked from a limestone quarry (Devonian, Grand Rapids group) near Bayport, Michigan. An x-ray diffraction analysis of the chert source identified quartz and calcium carbonate as the primary constituents. Two different replacement levels of chert for the fine aggregate fraction were made based on weight replacement of 1.0% and 2.5%. Mortar bars were subsequently prepared and tested according to ASTM C1260 as described above for each level of chert replacement.

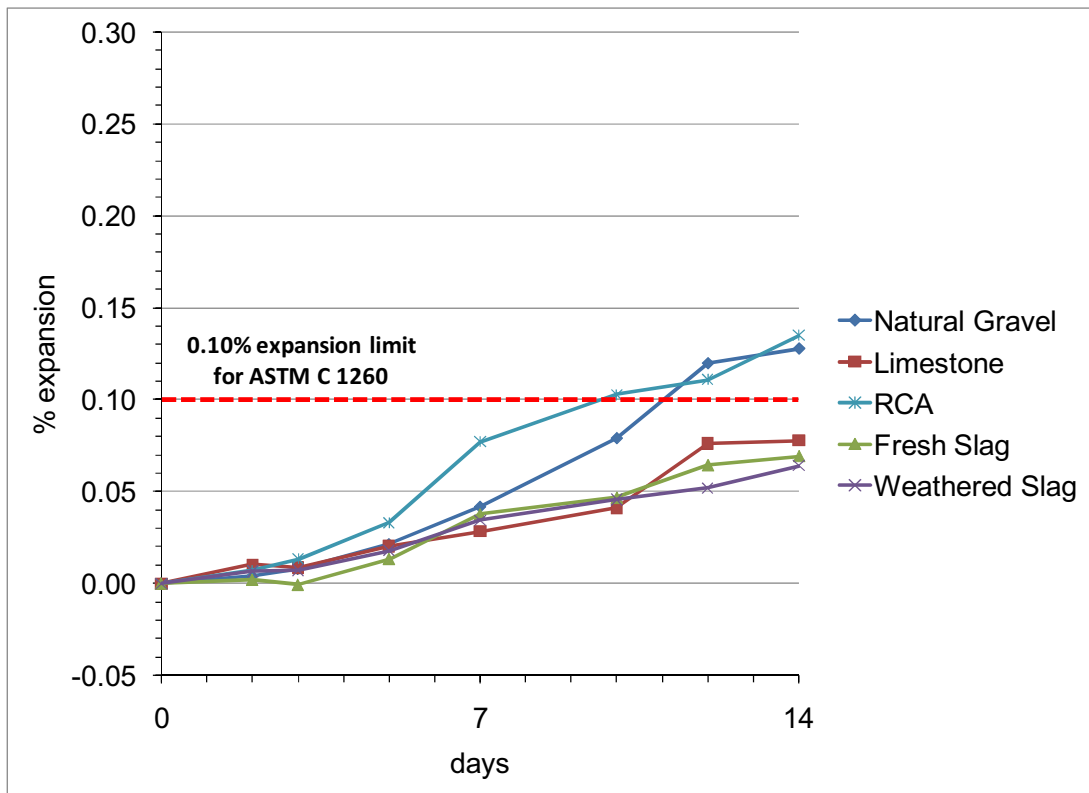


Figure 6-1. Results of ASTM C1260 expansion tests for control experiment (no chert addition).

Figure 6-2 and Figure 6-3 show the expansion plots for the 1.0% and 2.5% chert replacement experiments, respectively. Figure 6-4 through Figure 6-8 compare expansion plots for the coarse/fine blends individually. Expansion plots representing 0%, 1.0%, and 2.5% chert replacement are presented in these figures for each respective coarse aggregate type.

At the 1.0% chert replacement level, the expansions were similar to the control experiment with the exception of the fresh blast furnace slag blend, which exceeded the 14 day 0.10% expansion criteria in a manner similar to the 2.5% chert replacement level experiment. At the 2.5% chert replacement level, all five of the coarse/fine aggregate blends achieved expansions more than twice the 14 day 0.10% expansion criteria.

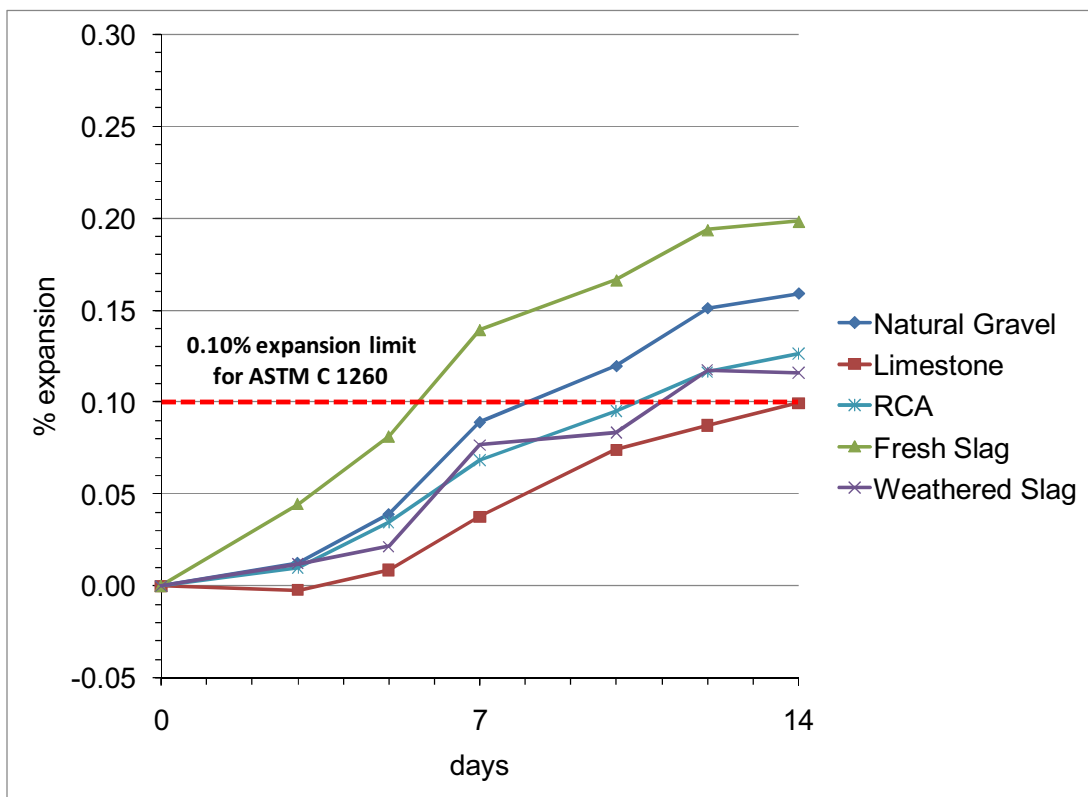


Figure 6-2. Expansion plot of 1.0% chert replacement experiment.

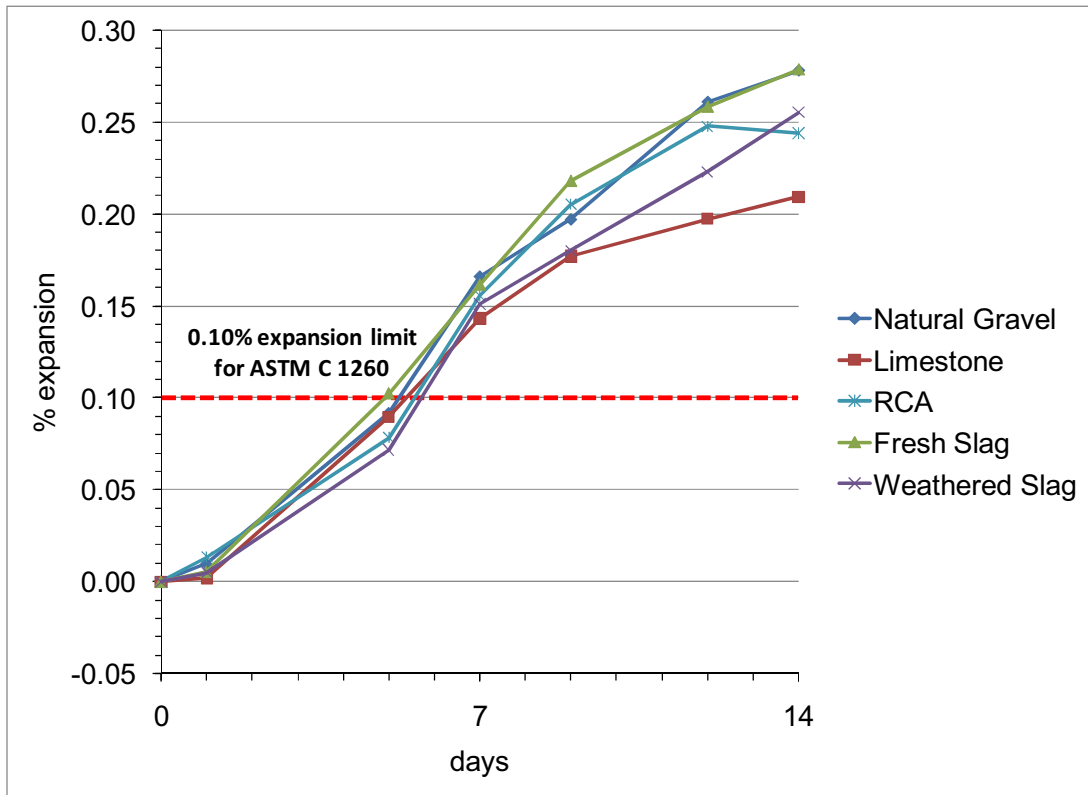


Figure 6-3. Expansion plot of 2.5% chert replacement experiment.

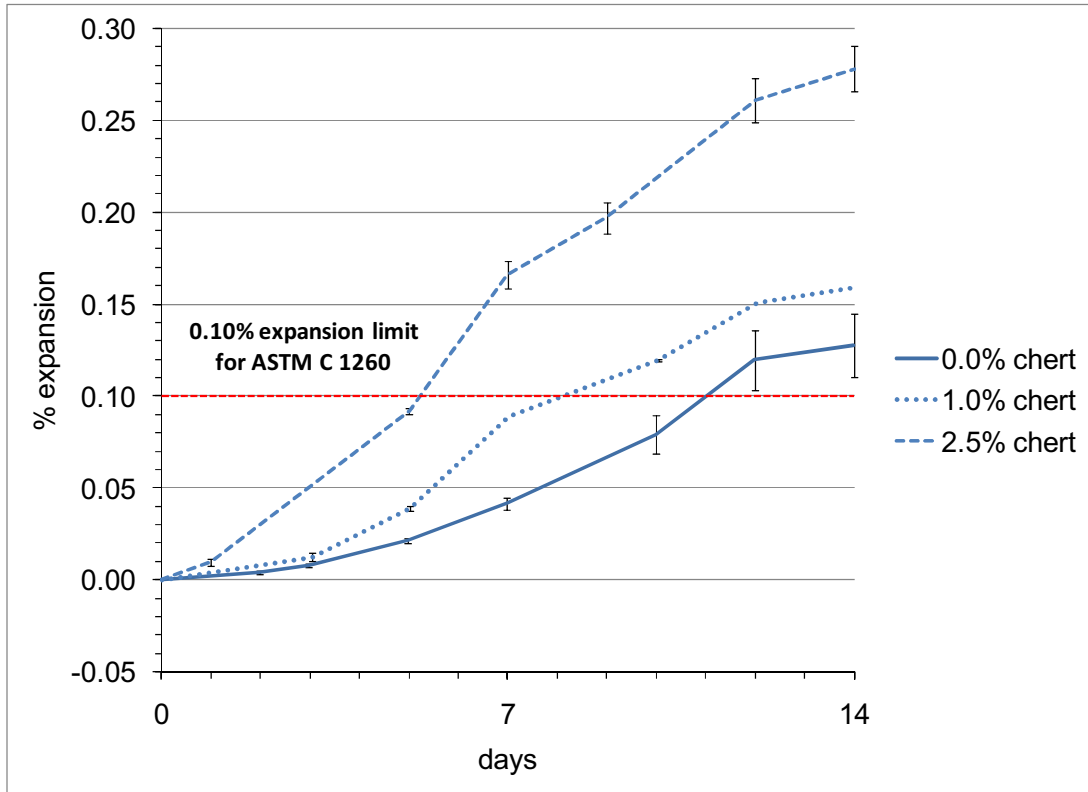


Figure 6-4. Expansion plots for natural gravel blends with error bars at one std deviation.

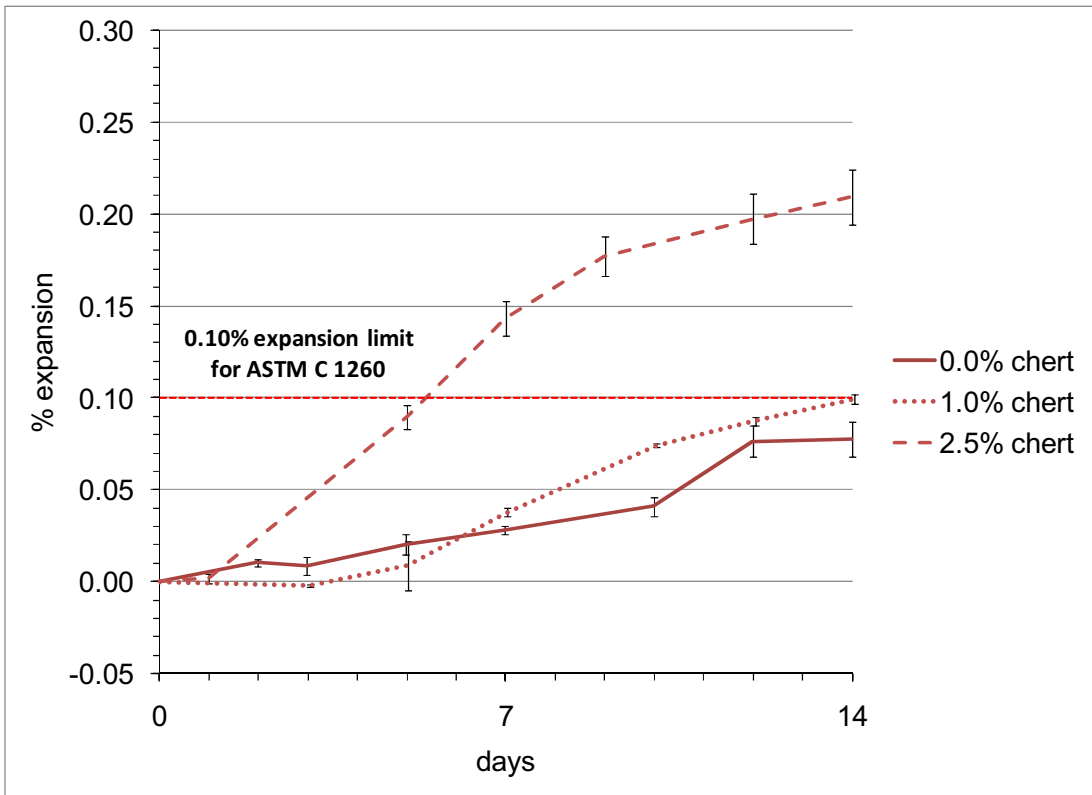


Figure 6-5. Expansion plots for limestone blends with error bars at one standard deviation.

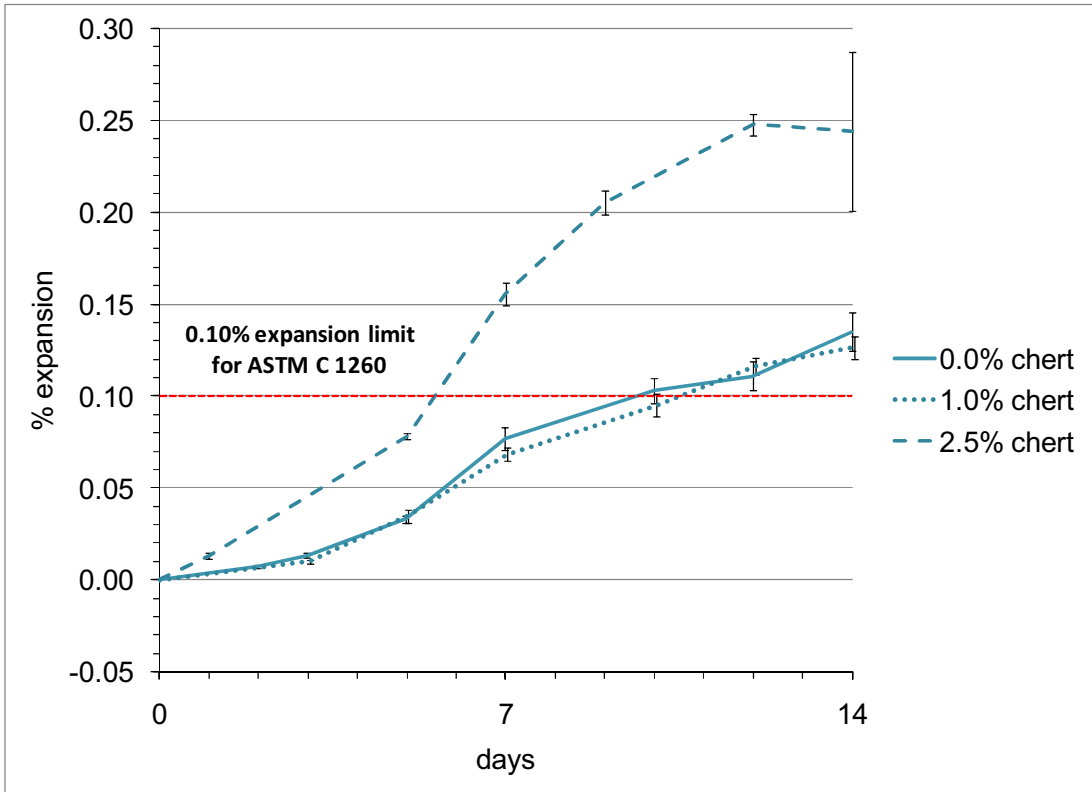


Figure 6-6. Expansion plots for RCA blends with error bars at one standard deviation.

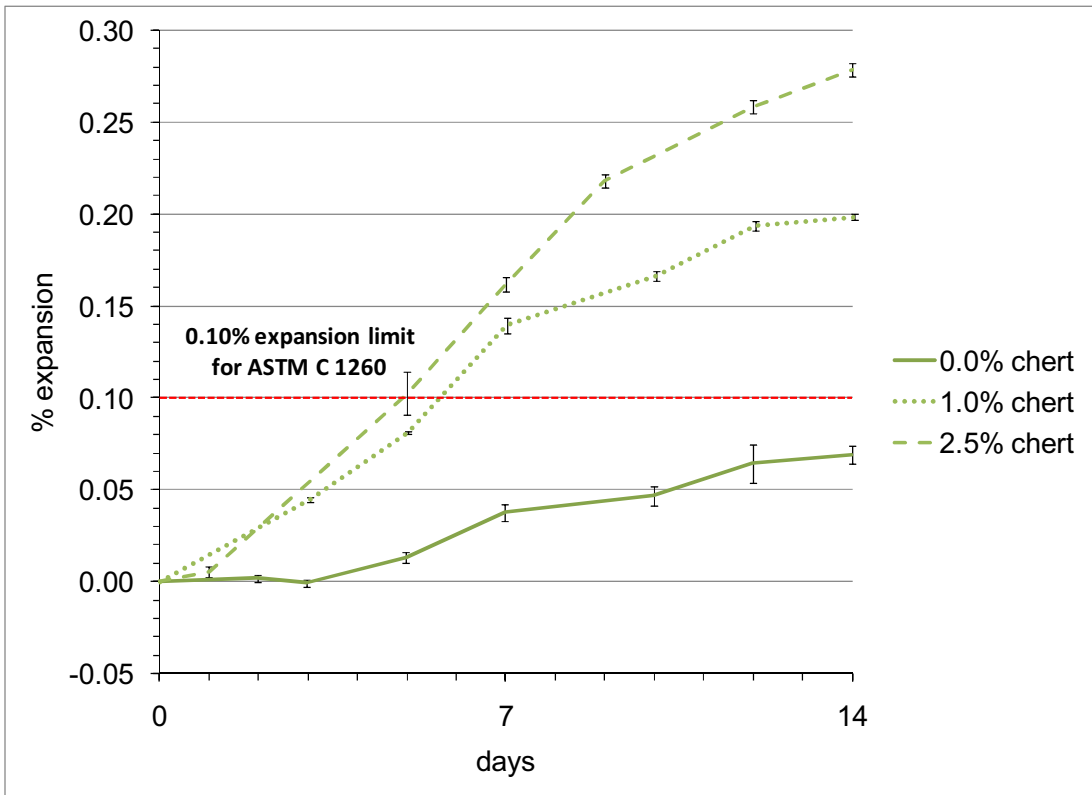


Figure 6-7. Expansion plots for fresh slag blends with error bars at one standard deviation.

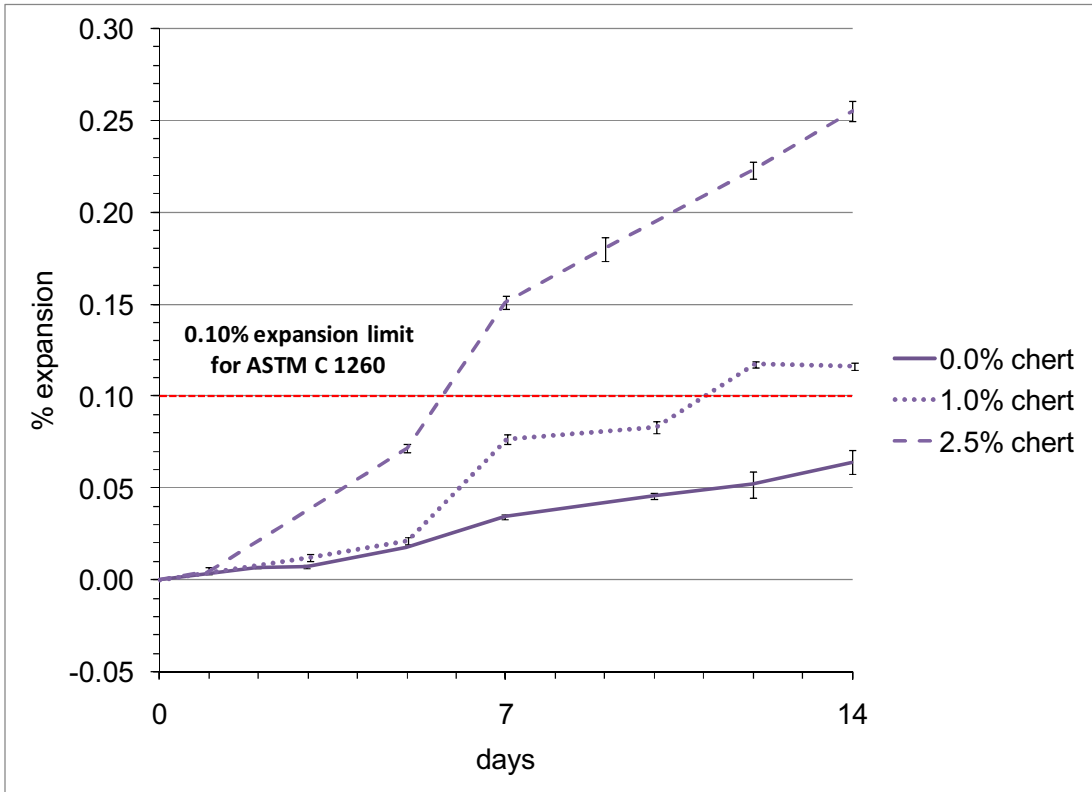


Figure 6-8. Expansion plots for weathered slag blends with error bars at one std deviation.

6.3. ASTM C1260 Discussion

In the ASTM C1260 mortar bar test, the mortar beams are immersed in a solution of sodium hydroxide at an elevated temperature for 14 days. In this environment, hydroxyl anions (OH⁻) attack the silicon-oxygen bonds present in the chert particles, resulting in the formation of complex polymers that incorporate additional OH⁻ anions, alkali cations, (Na⁺ and K⁺) and water molecules. The volume increase associated with the formation of the ASR gel is related to the expansion of the mortar beams.

According to an expansion mechanism put forth by Ichikawa and Miura (2007), ASR gel formed at the surface of a reactive particle is alkali-rich and fluid in nature. Over time, the ASR gel incorporates calcium cations (Ca²⁺) and forms a rigid reaction perimeter around the reactive particle. This rigid membrane tends to trap ASR gel but remains permeable enough to allow additional OH⁻, K⁺, and Na⁺ ions to pass into the reactive particle to form additional ASR gel. This newly formed ASR gel is of higher viscosity than prior to entering the reactive particle and cannot escape the semi-permeable rigid membrane at the perimeter. Due to this, pressure builds within the particle until it cracks, along with the surrounding mortar matrix.

It is hypothesized that the unusual behavior of the fresh blast furnace slag blend at the 1.0% chert replacement level may be related to the presence of calcium sulfide. The dissolution of calcium sulfide may contribute additional Ca²⁺ ions to the pore solution and increase the rate of hardening of ASR gel formed at the exteriors of the chert particles, allowing pressures to build within, leading to cracking and expansion. Why this should occur so dramatically for the fresh blast furnace slag blend at the 1.0% chert replacement level by weight, while at the 2.5% chert replacement level all of the coarse/fine aggregate blends expanded uniformly is unknown at this time. Further repetitions of the experiment, as well as variations on the experiment, (e.g., alternative chert replacement levels, alternative chert gradations, etc.) coupled with scanning electron microscope examinations of tested mortar beams to measure ASR gel compositions may assist in the interpretation of the results reported here.

6.4. Recommendations

It is important to note that ASTM C1260 specifically states that the test “does not evaluate combinations of aggregate” and is designed to test single aggregate sources. In this respect the experiment described here departs drastically from the standard testing regime. In this

study, ASTM C1260 was used to assess a general concept of ASR potential by aggregate source. Generally, when assessing the ASR potential for combinations of coarse and fine aggregate, ASTM C1293, Standard Test Method for Determination of Length Change of Concrete Due to Alkali-Silica Reaction, is employed using concrete prisms instead of mortar bars (ASTM-C1293 2008). However, the duration of this test (a minimum of 12 months) exceeded the timeframe allotted for this portion of the project. Touma et al. (2001) suggest that an accelerated version of the ASTM C1293 test (3 months) could be utilized to address ASR expansion in concrete prisms as an alternative. As such, before drawing any conclusions regarding the performance of the coarse and fine aggregate combinations tested in this experiment, it is recommended that experiment be repeated using ASTM C1293.

CHAPTER 7. SUMMARY AND CONCLUSIONS

This report summarizes the state-of-the-practice for the use of RCA in transportation infrastructure applications. The provided literature review includes information regarding material characterization of RCA as well as a review of the use of RCA in new PCC, new HMAC, and as a supporting layer for pavement structures.

Positive aspects (e.g. higher creep for stress relaxation in pavement structures), negative aspects (e.g. higher drying shrinkage, lower elastic modulus, lower fracture resistance, etc.), as well as undetermined trends (e.g. coefficient of thermal expansion, compressive strength) were investigated relative to the use of RCA in new PCC. Pavement performance using RCA in new PCC has been varied, but several sites have shown good long-term performance that can be built upon to improve future performance.

The use of RCA was found to have characteristics suitable for use in HMAC pavement structures at virgin aggregate replacement levels up to 75%.

The use of RCA as base aggregate was also investigated. While RCA has some positive characteristics relative to long-term base support (e.g. angularity for stability, the ability to create specific gradations required for application, the ability for re-cementing to increase the resilient modulus of the base material), concerns related to leachate ingress into the sub-surface drainage system have limited RCA use in this important application. This study investigated the leachate produced when aggregate materials commonly used in OGDC applications (i.e. blast furnace slag, natural gravel, limestone, and recycled concrete) are exposed to either simulated acid rain or de-ionized water. All of the aggregate materials tested leached a material that appeared to be gypsum anhydrate and showed pH levels of the leachate solution less than the threshold level of 12.5 to be considered a corrosive waste by the EPA. However, with proper engineering of the base structure, concerns relative to the leachate inhibiting the performance of the pavement underdrain system can be managed through proper aggregate gradation and proactive cleaning of the engineered drain system. Addressing these issues will ultimately help promote the use of old concrete in transportation applications.

Based on the review of state, national, and international RCA practices, the focus of the laboratory study was established. One major issue with RCA application is the material's

inherent high porosity due to the adhered mortar system. Standard methods for determining the porosity of aggregates, and the related water absorption, tend to be subjective and may pose problems when used on highly porous materials. The subjectivity traces back to the determination of the threshold for saturated-surface dry conditions, which requires the technician to use judgment to assess for aggregates with high surface porosity. Automated tests such as helium pycnometer and EDA may provide consistent laboratory results for specific gravity and porosity measurements with lower standard deviation in comparison with the conventional test methods. However, these techniques are not proven to be accurate for field application. Although these automated methods can provide more consistent results for determining the specific gravity and porosity of RCA, the resulting water absorption results obtained from gas pycnometry are systematically higher in comparison to the standard ASTM C127 characterization and can potentially result in production of concrete mixtures with excess mixture water. Careful determination of the actual amount of water absorbed during and shortly after the mixing process is essential to guarantee the intended quality of the new concrete mortar and its effect on the resulting concrete. This factor deserves further investigation to determine a proper and consistent technique for specific gravity and absorption capacity characterization of porous materials like RCA.

Four different types of RCA were examined for their suitability in concrete. Mixtures were produced using RCA with the following as the original aggregate type:

- blast furnace slag
- limestone
- crushed gravel
- crushed gravel RCA as the original aggregate, or third generation aggregate (3rdGen RCA)

Concrete mixtures using these RCA sources were compared in standard index tests to concrete mixtures made from high-quality virgin crushed gravel aggregate. RCA concrete mixtures were produced with initially workable fresh properties, with the exception of the 3rdGen RCA concrete. However, the window for good workability using RCA in concrete was consistently less than with using virgin aggregates. The high porosity of RCA tended to absorb mix water after the mixing process was completed, thereby increasing the difficulty at placement. This may be controlled by saturating RCA before mixing, but tests should be

conducted to assure good workability, strength requirements, and a lack of bleed water near the aggregates in the new concrete.

The total air content in hardened RCA concrete mixtures was found to be consistently higher than mixtures prepared using virgin aggregate if no differentiation between voids in the new and old mortar is accounted for in the analysis. This trend is primarily due to the existing air void system in the adhered mortar of the RCA, which is dependent on the air void system of the original concrete. While opportunities for reduced entrained air may help solve this problem, the connectivity of the old mortar's air void system to the new concrete should be further investigated to assure durability of the RCA concrete mixtures. If the coarse aggregates in the original concrete were susceptible to D-cracking, extensive characterization of these materials as aggregates as well as in a new concrete mixture must be done to assure these issues will not manifest themselves again in the RCA concrete.

In comparison with concrete mixtures prepared with virgin aggregates, RCA concrete mixtures performed poorly in resistance to chloride penetrability, compressive strength, and elastic modulus testing. Partial replacement of virgin aggregate by RCA may help diminish this situation as other researchers have shown promising results.

A major focus of this research was to further understand the volumetric stability of RCA concrete mixtures. This issue was identified as a major concern based upon the literature review and reported experiences using RCA. While the drying shrinkage of RCA concrete mixtures was found to be consistently higher than measured in virgin aggregate concrete mixtures, the higher creep potential of RCA concrete helped to alleviate some stresses induced in a restrained shrinkage test. In a pavement system, the restraint from dowels, tie bars, or even reinforcing steel will induce significant stresses on an RCA concrete. The increased capacity for creep, or time-dependent response of the concrete, may help dissipate stress due to curling, warping, and built-in restraint. In general, the quality and amount of mortar present in the RCA makes a difference in the fresh and hardened properties of RCA concretes. Mixture design methods such as the two-stage mixing process (TMSA) and equivalent mortar volume (EMV) methods may be important to investigate for use in reducing some of the detrimental effects that RCA can induce in concrete.

While a preliminary examination of the ASR potential of concrete with different aggregates sources using ASTM C1260 was conducted, results showed that the increase in chert

replacement affected concrete regardless of aggregate type. ASTM C1260 mortar bar expansions were quite similar for all chert replacement levels for both fresh and weathered slag aggregates, with the exception of the mid-level chert replacement (1.0%) that showed higher expansion for fresh slag. In general, this study was inconclusive as the ASTM C1260 specification is not recommended for use across aggregate types. It is recommended that further investigation of ASR potential of these recycled materials be assessed using ASTM C1293 or an accelerated version of this test in addition to SEM examinations.

While the use of RCA in transportation applications provides challenges, with better characterization and understanding of how materials and structures work together, this material can be successfully implemented in Michigan's transportation infrastructure.

REFERENCES

- AASHTO-PP-34. (2005). "Estimating the Cracking Tendency of Concrete." American Association of State Highway and Transportation Officials.
- Abrams, D. A. (1922). "Proportioning Concrete Mixtures." *Eighteenth Annual Convention*, Cleveland, Ohio, 174-181.
- ACPA. (2009). *Recycled Concrete Pavement*, American Concrete Pavement Association, Skokie, IL.
- Ajdukiewicz, A., and Kliszczewicz, A. (2002). "Influence of Recycled Aggregates on Mechanical Properties of HS/HPC." *Cement and Concrete Composites*, 24, 269-279.
- Al-Negheimish, A. I., and Alhozaimy, A. M. (2008). "Impact of Extremely Hot Weather and Mixing Method on Changes in Properties of Ready Mixed Concrete during Delivery." *ACI Materials Journal*, 105(5).
- ARA. (2007). "Interim Mechanistic-Empirical Pavement Design Guide Manual of Practice. Final Draft. ." National Cooperative Highway Research Program Project 1-37A.
- ASTM-C39. (2008). "Standard Test Method for Compressive Strength of Cylindrical Concrete Specimens." Annual Book of ASTM Standards, American Society for Testing and Materials.
- ASTM-C88. (2008). "Standard Test Method for Soundness of Aggregates by Use of Sodium Sulfate or Magnesium Sulfate." Annual Book of ASTM Standards, American Society for Testing and Materials.
- ASTM-C127. (2008). "Standard Test Method for Density, Relative Density (Specific Gravity), and Absorption of Coarse Aggregate, Annual Book of ASTM Standards." American Society for Testing and Materials.
- ASTM-C128. (2008). "Standard Test Method for Density, Relative Density (Specific Gravity), and Absorption of Fine Aggregate." Annual Book of ASTM Standards, American Society for Testing and Materials.
- ASTM-C150. (2008). "Standard Specification for Portland Cement." Annual Book of ASTM Standards, American Society for Testing and Materials.
- ASTM-C157. (2008). "Standard Test Method for Length Change of Hardened Hydraulic-Cement Mortar and Concrete." Annual Book of ASTM Standards, American Society for Testing and Materials.
- ASTM-C173. (2008). "Standard Test Method for Air Content of Freshly Mixed Concrete by the Volumetric Method." Annual Book of ASTM Standards, American Society for Testing and Materials.
- ASTM-C204. (2008). "Standard Test Methods for Fineness of Hydraulic Cement by Air-Permeability Apparatus." Annual Book of ASTM Standards, American Society for Testing and Materials.
- ASTM-C231. (2008). "Standard Test Method for Air Content of Freshly Mixed Concrete by the Pressure Method, Annual Book of ASTM Standards." American Society for Testing and Materials.
- ASTM-C260. (2008). "Standard Specification for Air-Entraining Admixtures for Concrete, Annual Book of ASTM Standards." Annual Book of ASTM Standards, American Society for Testing and Materials.

- ASTM-C457. (2008). "Standard Test Method for Microscopical Determination of Parameters of the Air-Void System in Hardened Concrete." American Society for Testing and Materials.
- ASTM-C469. (2008). "Standard Test Method for Static Modulus of Elasticity and Poisson's Ratio of Concrete in Compression." Annual Book of ASTM Standards, American Society for Testing and Materials.
- ASTM-C666. (2008). "Standard Test Method for Resistance of Concrete to Rapid Freezing and Thawing." Annual Book of ASTM Standards, American Society for Testing and Materials.
- ASTM-C856. (2008). "Standard Practice for Petrographic Examination of Hardened Concrete." Annual Book of ASTM Standards, American Society for Testing and Materials.
- ASTM-C1202. (2008). "Standard Test Method for Electrical Indication of Concrete's Ability to Resist Chloride Ion Penetration." Annual Book of ASTM Standards, American Society for Testing and Materials.
- ASTM-C1260. (2008). "Standard Test Method for Potential Alkali Reactivity of Aggregates (Mortar-Bar Method)." Annual Book of ASTM Standards, American Society for Testing and Materials.
- ASTM-C1293. (2008). "Standard Test Method for Determination of Length Change of Concrete Due to Alkali-Silica Reaction." Annual Book of ASTM Standards, American Society for Testing and Materials.
- Attarian, J. L. (2007). "CDOT'S Sustainable Development Initiative." *Transportation Research Board 86th Annual Meeting*, Washington D.C.
- Ayano, T., Fujii, A., and Sakata, K. (2009). "Drying Shrinkage of Recycled Concrete." *Proceedings of Creep, Shrinkage and Durability Mechanics of Concrete and Concrete Structures*, Japan, 805-810.
- Ayano, T., and Wittmann, F. H. (2002). "Drying, Moisture Distribution, and Shrinkage of Cement-based Materials." *Materials and Structures*, 35, 134-140.
- bama.ua.edu. (2006). "SEM Sample Preparation."
- Berndt, M. L. (2009). "Properties of Sustainable Concrete containing Fly Ash, Slag and Recycled Concrete Aggregate." *Construction and Building Materials*, 23(7), 2606-2613.
- Black, R. W. (1986). "The Determination of Specific Gravity Using the Siphon Can Method." *Cement, Concrete and Aggregates; American Society for Testing and Materials*, 46.
- Blankenagel, B. J., and Guthrie, W. S. (2006). "Laboratory characterization of recycled concrete for use as pavement base material." *Transportation Research Record*(1952), 21-27.
- Bordelon, A. M., Cervantes, V., and Roesler, J. R. (2009). "Fracture properties of concrete containing recycled concrete aggregates." *Magazine of Concrete Research*, 61(9), 665-670.
- Bruinsma, J. E. (1995). "Formation and Mitigation of Calcium Carbonate Precipitate and Insoluble Residue from Recycled Concrete Aggregate Bases.," University of Minnesota, Minneapolis, MN.
- Buch, N., Frabizzio, M., and Hiller, J. (2000). "Impact of coarse aggregates on transverse crack performance in jointed concrete pavements." *ACI Materials Journal*, 3(97), 325-332.
- Casuccio, M., Torrijos, M. C., Giaccio, G., and Zerbino, R. (2008). "Failure mechanism of recycled aggregate concrete." *Construction and Building Materials*, 22(7), 1500-1506.

- Chatterji, S., and Gudmundsson, H. (1977). "Characterization of entrained air bubble systems in concretes by means of an image analysing microscope." *Cement and Concrete Research*, 7(4), 423-428.
- Chini, S. A., Serghian, T. J., and Armaghani, J. M. (1996). "Use of Recycled Aggregates for Pavement." *Materials for the New Millennium Proceedings of the Materials Engineering Conference*, Washington, D.C., 154-162.
- Cross, S. A., Abou-Zeid, M. N., Wojakowski, J. B., and Fager, G. A. (1996). "Long-term Performance of Recycled Portland Cement Concrete Pavement." *Transportation Research Record 1525, TRB*, Washington, D.C., 115-123.
- Cusson, D., and Hoogeveen, T. (2008). "Internal Curing of High-Performance Concrete with Pre-Soaked Fine Lightweight Aggregate for Prevention of Autogenous Shrinkage Cracking." *Cement and Concrete Research*, 38, 757-768.
- Cuttell, G. D., Snyder, M. B., Vandenbossche, J. M., and Wade, M. J. (1996). "Performance of Rigid Pavements Containing Recycled Concrete Aggregates." *Transportation Research Record 1574, TRB*, Washington, D.C., , 89-98.
- Deretzky, Z. (2009). "How Solid is Concrete's Carbon Footprint?" http://www.nsf.gov/news/news_images.jsp?cntn_id=109892&org=NSF
- Deshpande, Y. S. (2006). "Evaluation of Commercial Rapid-Setting Materials and Rapid-Setting Self-Consolidating Concrete for Dowel Bar Retrofit Applications," Purdue University, West Lafayette, Indiana.
- Domingo-Cabo, A., Lázaro, C., López-Gayarre, F., Serrano-López, M. A., Serna, P., and Castaño-Tabares, J. O. (2009). "Creep and shrinkage of recycled aggregate concrete." *Construction and Building Materials*, 23(7), 2545-2553.
- Dykens, S. E., and Epps, J. A. (1987). "Portland Cement Concrete Pavement Pulverizing Equipment." *Transportation Research Record 1126, TRB*, Washington, D.C., 136-144.
- EPA. (2010). "Hazardous Waste Generator Regulations." E. P. Agency, ed., Washington, D.C., 430.
- Fathifazl, G. (2008). "Structural Performance of Steel Reinforced Recycled Concrete Members," Carleton University, Ottawa, Ontario, Canada.
- FHWA. (1992). *Report on the 1992 U.S. Tour of European Concrete Highways*, Federal Highway Administration., Washington, D.C.
- FHWA. (2004). "Transportation Applications of Recycled Concrete Aggregate: FHWA State of the Practice National Review." U.S. Department of Transportation, Washington, D.C.
- FHWA. (2005). "Summary of Minnesota Recycled Concrete Aggregate Review." <http://www.fhwa.dot.gov/pavement/recycling/rcamn.cfm>
- FHWA. (2008a). "Recycled Concrete Aggregate Federal Highway Administration National Review." <http://www.fhwa.dot.gov/pavement/recycling/rca.cfm>
- FHWA. (2008b). "Summary of Michigan Recycled Concrete Aggregate Review." <http://www.fhwa.dot.gov/pavement/recycling/rcami.cfm>
- Fick, G. (2008). "National Open House Two-Lift Concrete Paving: Project Test Results." <http://www.cptechcenter.org/projects/two-lift-paving/index.cfm>
- Frabizzio, M. A., Hiller, J. E., and Buch, N. (2000). "Factors Affecting Shear Capacity of Transverse Cracks in Jointed Concrete Pavements." MDOT.
- Gebhardt, R. F. (1995). "Survey of North American Portland Cements: 1994." *Cement, Concrete, and Aggregates*, 17(2), 145-189.

- Goldstein, J. I., Newbury, D. E., Echlin, P., Joy, D. C., Jr, A. D. R., Lyman, C. E., Fiori, C., and Lifshin, E. (1992). *Scanning Electron Microscopy and X-Ray Microanalysis: A Text for Biologists, Materials Scientists, and Geologists*, Springer-Verlag, New York.
- Gómez-Soberón, J. M. V. (2003). "Relationship Between Gas Adsorption and the Shrinkage and Creep of Recycled Aggregate Concrete." *Cement, Concrete, and Aggregates*, 25(2), 1-7.
- Gress, D. L., and Kozikowski, R. L. (2000). "Accelerated Alkali-Silica Reactivity Testing of Recycled Concrete Pavement." *Transportation Research Record 1698*, TRB, Washington, D.C., 1-8.
- Gudmundsson, H., Chatterji, S., Jensen, A. D., Thaulow, N., and Christensen, P. (1979). "The measurement of paste content in hardened concrete using automatic image analyzing technique." *Cement and Concrete Research*, 9(5), 607-612.
- Guthrie, W. S., Sebesta, S., and Scullion, T. (2002). "Selecting Optimum Cement Contents for Stabilized Aggregate Base Materials." Texas Transportation Institute, College Station, TX.
- Halverson, A. D. (1982). "Recycling Portland Cement Concrete Pavement." *Transportation Research Record 853*, TRB, Washington, D.C., 14-17.
- Hansen, W. (1995). "Uses of recycled concrete in Michigan." Department of civil and environmental engineering, University of Michigan, Ann Arbor.
- Hearn, N., Hooton, D. R., and Mills, R. H. (1994). "Pore Structure and Permeability " Significance of Tests and Properties of Concrete and Concrete making Materials STP 169C, P. Klieger and J. Lamond, eds., ASTM 240-262.
- Heath, A. C., Roesler, J. R., and Harvey, J. T. (2003). "Modeling Longitudinal, Corner and Transverse Cracking in Jointed Concrete Pavements." *International Journal of Pavement Engineering*, 4(1), 51 - 58.
- Higginson, E. G. (1970). "The Effects of Cement Fineness on Concrete." *ASTM Special Technical Publication*, 71-81.
- Hiller, J. E., Buch, N., and Van Dam, T. J. (1999). "A Study of Materials-Related Distress (MRD) in Michigan's PCC Pavements - Phase I." MDOT.
- Hiller, J. E., and Roesler, J. R. (2006). "Alternative Failure Modes for Long-Life Jointed Plain Concrete Pavements." *Proceedings of the International Conference on Long-Life Concrete Pavements*, Chicago, IL, 265-284.
- Hiller, J. E., and Roesler, J. R. (2008). "Location and Timing of Fatigue Cracks on Jointed Plain Concrete Pavements." *Proceedings of the ASCE 2008 Airfield & Highway Pavements Conference*, Bellevue, Washington, USA, 509-520.
- ICDD. (2009). "The International Centre for Diffraction Data." <http://www.icdd.com/>
- Ichikawa, T., and Miura, M. (2007). "Modified Model of Alkali-Silica Reaction." *Cement and Concrete Research*, 37, 1291-1297.
- Jianzhuang, X., Bin, L., and Zhang, C. (2010). "Effects of recycled coarse aggregates on the carbonation evolution of concrete." *Key Engineering Materials*, 697-700.
- Jung, Y. s., Zollinger, D. G., Won, M., and Wimsatt, A. J. (2009). "Subbase and Subgrade Performance Investigation for Concrete Pavement." Texas Transportation Institute, College Station, TX.
- Kakizaki, M., Harada, M., Soshiroda, T., Kubota, S., and Ikeda, Y. (1988). "Strength and elastic modulus of recycled concrete aggregate." *Demolition and Reuse of Concrete and Masonry*, London, UK, 565-574.

- Kuennen, T. (2007). "FHWA throws weight, funding toward two-lift concrete paving." http://concreteproducts.com/mag/concrete_fhwa_throws_weight/
- Li, X. P. (2007). "Study on mechanical properties of recycled aggregate concrete (II)." *Jianzhu Cailiao Xuebao/Journal of Building Materials*, 10(6), 699-704.
- Lim, S., Kestner, D., Zollinger, D. G., and Fowler, D. W. (2003). "Characterization of Crushed Concrete Materials for Paving and Non-paving Applications." Texas Transportation Institute, College Station, TX.
- Limbachiya, M., Leelawat, T., and Dhir, R. (2000). "Use of recycled concrete aggregate in high-strength concrete." *Materials and Structures*, 33(9), 574-580.
- Limbachiya, M. C., Marrocchino, E., and Koulouris, A. (2007). "Chemical-mineralogical characterisation of coarse recycled concrete aggregate." *Waste Management*, 27(2), 201-208.
- Love, R. M. (1987). "State DOT Experiments with Concrete Pavement Recycling." *Public Works*, 118(6), 83-85.
- Mahmoud, A. F. F., and Bahia, H. (2004). "Using the gyratory compactor to measure the mechanical stability of asphalt mixtures." Wisconsin Highway Research Program, Madison, WI.
- MDOT. (2003). "Michigan Department of Transportation, Standard Specification for Construction." <http://mdotwas1.mdot.state.mi.us/public/specbook/>.
- MDOT. (2007). "Manual for the Michigan Test Methods." Michigan Department of Transportation, Construction and Technology Division.
- Mills-Beale, J., and You, Z. (2010). "The mechanical properties of asphalt mixtures with Recycled Concrete Aggregates." *Construction and Building Materials*, 24(3), 230-235.
- Mindess, S., Young, J. F., and Darwin, D. (2002). *Concrete* Prentice Hall.
- NCHRP. (2008). "Performance-related tests of recycled aggregates for use in unbound pavement layer." Transportation research board, Vicksburg, MS.
- Neville, A. M. (1996). *Properties of Concrete*, John Wiley & Sons, Inc., New York, NY.
- NHI. (1998). *Techniques for Pavement Rehabilitation-Participant's Manual.*, National Highway Institute, USDOT Washington, D.C.
- Nishibata, S., Watanabe, T., Hashimoro, C., and Kohno, K. (2006). "Evaluation of fracture in concrete with recycled aggregate by acoustic emission." *International Journal of Modern Physics B*, 20(25-27), 3652-3657.
- Paranavithana, S., and Mohajerani, A. (2006). "Effects of recycled concrete aggregates on properties of asphalt concrete." *Resources, Conservation and Recycling*, 48(1), 1-12.
- Park, K., Paulino, G. H., and Roesler, J. R. (2008). "Determination of the kink point in the bilinear softening model for concrete." *Engineering Fracture Mechanics*, 75(13), 3806-3818.
- Poon, C.-S., Kou, S.-c., Wan, H.-w., and Etxeberria, M. (2009). "Properties of concrete blocks prepared with low grade recycled aggregates." *Waste Management*, 29(8), 2369-2377.
- Poon, C. S., Shui, Z. H., and Lam, L. (2004a). "Effect of Microstructure of ITZ on Compressive Strength of Concrete Prepared with Recycled Aggregates." *Construction and Building Materials*, 18(6), 461-468.
- Poon, C. S., Shui, Z. H., Lam, L., Fok, H., and Kou, S. C. (2004b). "Influence of Moisture States of Natural and Recycled Aggregates on the Slump and Compressive Strength of Concrete." *Cement and Concrete Research*, 34(1), 31-36.

- Price, W. H. (1974). "Practical Qualities of Cement." *Journal of the American Concrete Institute*, 71(9), 436-444.
- Raja, Z. I., and Snyder, M. B. (1991). "Factors Affecting Deterioration of Transverse Cracks in Jointed Reinforced Concrete Pavements." *Transportation Research Record 1307, TRB*, Washington, D.C., 162-168.
- Rao, S., and Roesler, J. J. (2005a). "Characterization of Effective Built-in Curling and Concrete Pavement Cracking on the Palmdale Test Sections--Draft report prepared for the California Department of Transportation. Pavement Research Center." Pavement Research Center, Institute of Transportation Studies, University of California Berkeley & University of California Davis.
- Rao, S., and Roesler, J. R. (2005b). "Nondestructive Testing of Concrete Pavements for Characterization of Effective Built-In Curling." *ASTM Journal of Testing and Evaluation*, 33(5), 356-363.
- Ravindrarajah, R. S., Loo, Y. H., and Tam, C. T. (1987). "Recycled Concrete as Fine and Coarse Aggregates in Concrete." *Magazine of Concrete Research*, 39(141), 214-220.
- Reiner, M. (2008). "Evaluation of Potential pH Environmental Hazards and Mitigation Measures when Utilizing Recycled Concrete Aggregate in the Field." Symbiotic Engineering, Boulder, CO.
- Roberts, L. R., and Scali, M. J. (1984). "Factors Affecting Image Analysis for Measurement of Air Content in Hardened Concrete." *Proceedings of the International Conference on Cement Microscopy*, 402-419.
- Robinson Jr, G. R., Menzie, W. D., and Hyun, H. (2004). "Recycling of construction debris as aggregate in the Mid-Atlantic Region, USA." *Resources, Conservation and Recycling*, 42(3), 275-294.
- Roesler, J., Lange, D. A., and Salas, A. (2009). "Properties of recycled aggregate concrete." University of Illinois, Urbana.
- Salem, R. M., and Burdette, E. G. (1998). "Role of Chemical and Mineral Admixtures on Physical Properties and Frost-resistance of Recycled Aggregate Concrete." *ACI Materials Journal*, 95(5), 558-563.
- Saxer, E. L. (1956). "A Direct Method of Determining Absorption and Specific Gravity of Aggregates,." *Rock Products*, 56.
- Smiley, D. L., and Parker, D. (1993). "Ten-year performance review of michigan concrete recycled pavement." Michigan Department of Transportation, Lansing, MI.
- Smith, J. T., and Tighe, S. L. (2009). "Recycled concrete aggregate coefficient of thermal expansion: Characterization, variability, and impacts on pavement performance." *Transportation Research Record*, 53-61.
- Snyder, M., and Bruinsma, J. (1996). "Review of Studies Concerning Effects of Unbound Crushed Concrete Bases on PCC Pavement Drainage." *Transportation Research Record: Journal of the Transportation Research Board*, 1519, 51-58.
- Snyder, M. B., and Raja, Z. I. (1991). "Factors Affecting Deterioration of Transverse Cracks in Jointed Reinforced Concrete Pavements." Ann Arbor, MI.
- Snyder, M. B., Vandenbossche, J. M., Smith, K. D., and Wade, M. (1994). "Physical and mechanical properties of recycled PCC aggregate concrete." University of Minnesota & University of Illinois, Champaign, Illinois.

- Sommer, H. (1994). "Recycling of Concrete for the Reconstruction of the Concrete Pavement of the Motorway Vienna-Salzburg." 7th International Symposium on Concrete Roads, Vienna, Austria.
- Steffes, R. (1999). "Laboratory study of the leachate from crushed portland cement concrete base material." Iowa Department of Transportation, Ames, Iowa.
- Sturtevant, Y. R. (2007). "Performance of rigid pavement containing recycled concrete aggregate," University of New Hampshire, Durham, NH.
- Tam, V., and Tam, C. (2008). "Diversifying two-stage mixing approach (TSMA) for recycled aggregate concrete." *Construction and Building Materials*, 22, 2068-2077.
- Tam, V. W. Y., Gao, X. F., Tam, C. M., and Chan, C. H. (2008). "New approach in measuring water absorption of recycled aggregates." *Construction and Building Materials*, 22(3), 364-369.
- Tam, V. W. Y., Gao, X. F., Tam, C. M., and Ng, K. M. (2009). "Physio-chemical reactions in recycle aggregate concrete." *Journal of Hazardous Materials*, 163(2-3), 823-828.
- Tavakoli, M., and Soroushian, P. (1996a). "Drying Shrinkage Behavior of Recycled Aggregate Concrete." *Concrete International*, 18(11), 58-61.
- Tavakoli, M., and Soroushian, P. (1996b). "Strengths of Recycled Aggregate Concrete Made using Field-demolished Concrete as Aggregate." *ACI Materials Journal*, 93(2), 182-190.
- Tennis, P. D., and Bhatti, J. I. (2006). "Characteristics of Portland and Blended Cements: Results of a Survey of Manufacturers." Cement Industry Technical Conference, IEEE, 83-101.
- Tia, M., Hossiney, N., and Bekoe, P. (2009a). "Modulus of elasticity, Creep and shrinkage of concrete, Phase II, Part 2--low modulus concrete." Department of Civil and Coastal engineering, University of Florida, Gainesville, Florida.
- Tia, M., Liu, Y., Haranki, B., and Su, Y.-M. (2009b). "Modulus of elasticity, creep and shrinkage of concrete--Phase II, Part 1--creep study." Frost resistance of recycled aggregate concrete, University of Florida, Gainesville, FL.
- Tompkins, D., Khazanovich, L., Darter, M. I., and Fleischer, W. (2009). "Design and construction of sustainable pavements: Austrian and German two-layer concrete pavements." *Transportation Research Record*, 75-85.
- Touma, W. E., Fowler, D. W., Carrasquillo, R. L., Folliard, K. J., and Nelson, N. R. (2001). "Characterizing Alkali-Silica Reactivity of Aggregates Using ASTM C1293." *Transportation Research Record*, 1757, 157-165.
- USDOT. (2004). "Transportation application of recycled concrete aggregate." Washington, DC.
- Van Dam, T. J., Sutter, L. L., Peterson, K. R., and Buch, N. (2002). "A Study of Materials-Related Distress (MRD) in Michigan's PCC Pavements - Phase II." MDOT.
- Vancura, M., Khazanovich, L., and MacDonald, K. (2010). "Relationship of Pervious Concrete Pavement Distress and Success to Design, Construction, Maintenance, and Environment." *TRB 89th annual meeting*, Washington D.C.
- Vitton, S., Lehman, M., and Van Dam, T. (1998). "Automated soil particle specific gravity analysis using bulk flow and helium pycnometry, Nondestructive and Automated Testing for Soil and Rock Properties."
- Wade, M. J., Cuttell, G. D., Vandenbossche, J. M., Yu, H. T., Smith, K. D., and Snyder, M. B. (1997). "Performance of Concrete Pavements Containing Recycled Concrete Aggregate." FHWA, U.S. Department of Transportation.
- Wai K., C., Kim, C., and Warren, D. J. (2006). "Examine the Opportunitites of a Recycling Program of C&D Waste for Highway Construction Projects in Kansas City (KC)

- Metropolitan Area. Transportation Research Board." *Transportation Research Board*, Washington D.C.
- Walton, W. H. (1948). "Feret's statistical diameter as a measure of particle size [2]." *Nature*, 162(4113), 329-330.
- Winslow, D. (1994). "The Pore System of Coarse Aggregates " Significance of Tests and Properties of Concrete and Concrete- Making Materials STP 169C, P. Klieger and J. Lamond, eds., ASTM 429-437.
- Wong, Y. D., Sun, D. D., and Lai, D. (2007). "Value-added utilisation of recycled concrete in hot-mix asphalt." *Waste Management*, 27(2), 294-301.
- Zaharieva, R., Buyle-Bodin, F., and Wirquin, E. (2004). "Frost resistance of recycled aggregate concrete." *Cement and Concrete Research*, 34(10), 1927-1932.

APPENDIX A

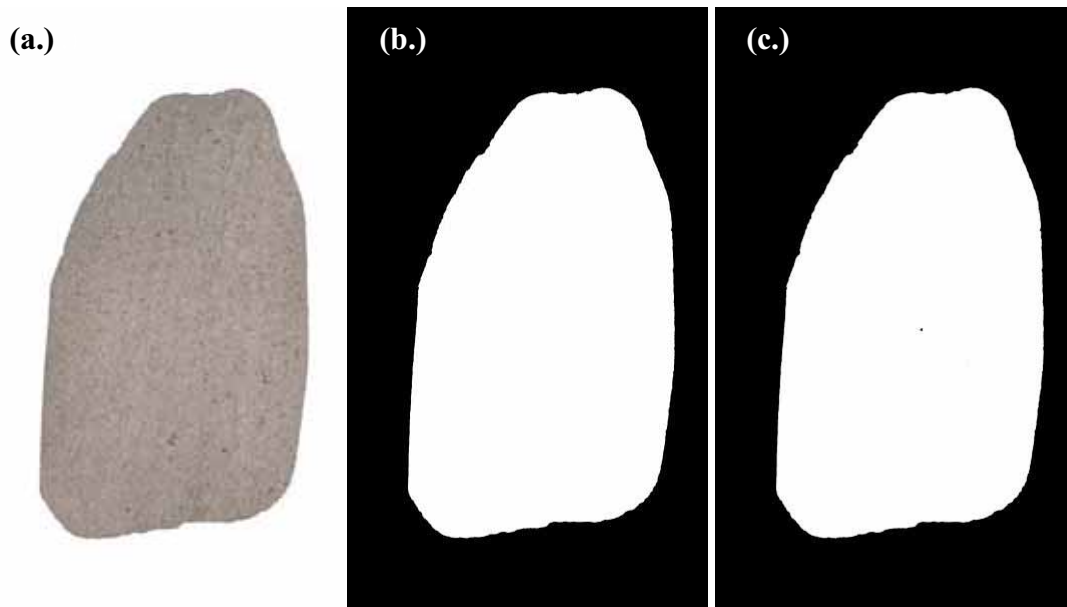


Figure A-1. Image Analysis for Crushed Gravel Sample #1 for (a.) Original Image, (b.) Image Processed for Blue Resin (Surface Porosity), and (c.) Image Processed for Yellow Resin (Internal Porosity).

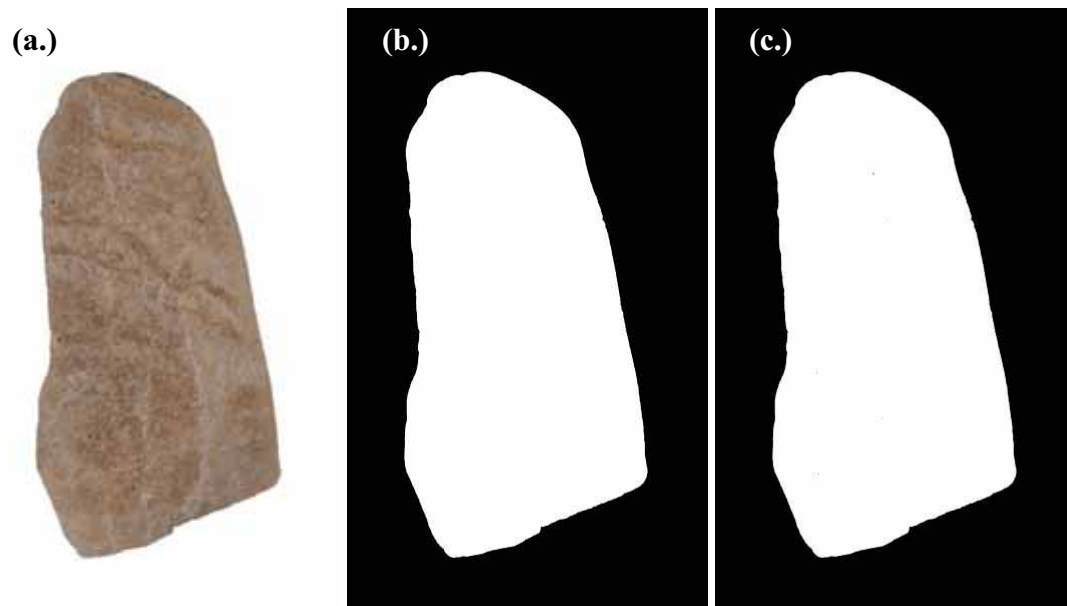


Figure A-2. Image Analysis for Crushed Gravel Sample #2 for (a.) Original Image, (b.) Image Processed for Blue Resin (Surface Porosity), and (c.) Image Processed for Yellow Resin (Internal Porosity).

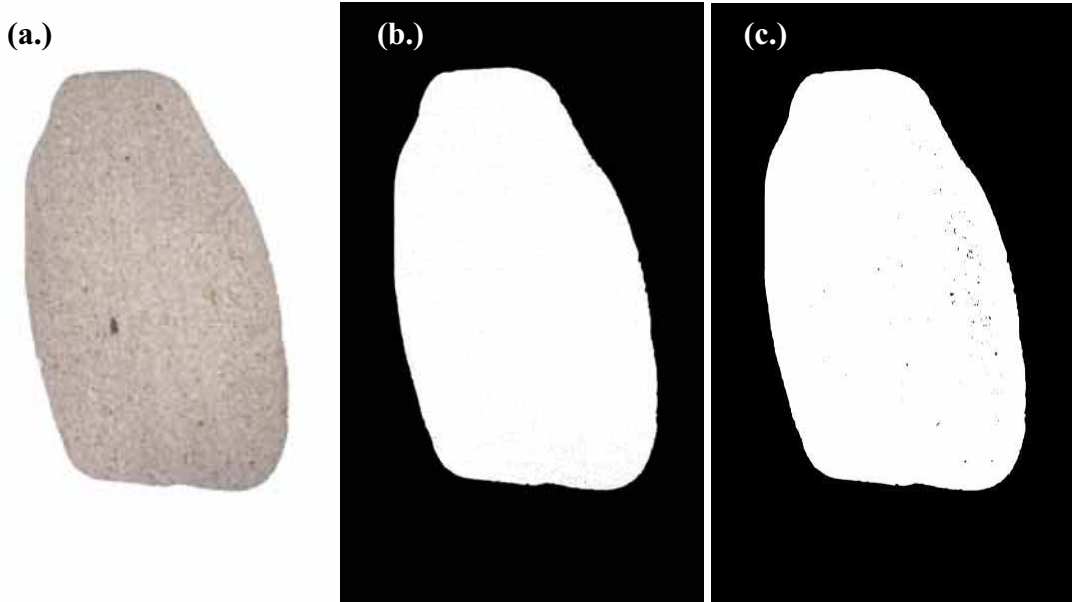


Figure A-3. Image Analysis for Crushed Gravel Sample #3 for (a.) Original Image, (b.) Image Processed for Blue Resin (Surface Porosity), and (c.) Image Processed for Yellow Resin (Internal Porosity).

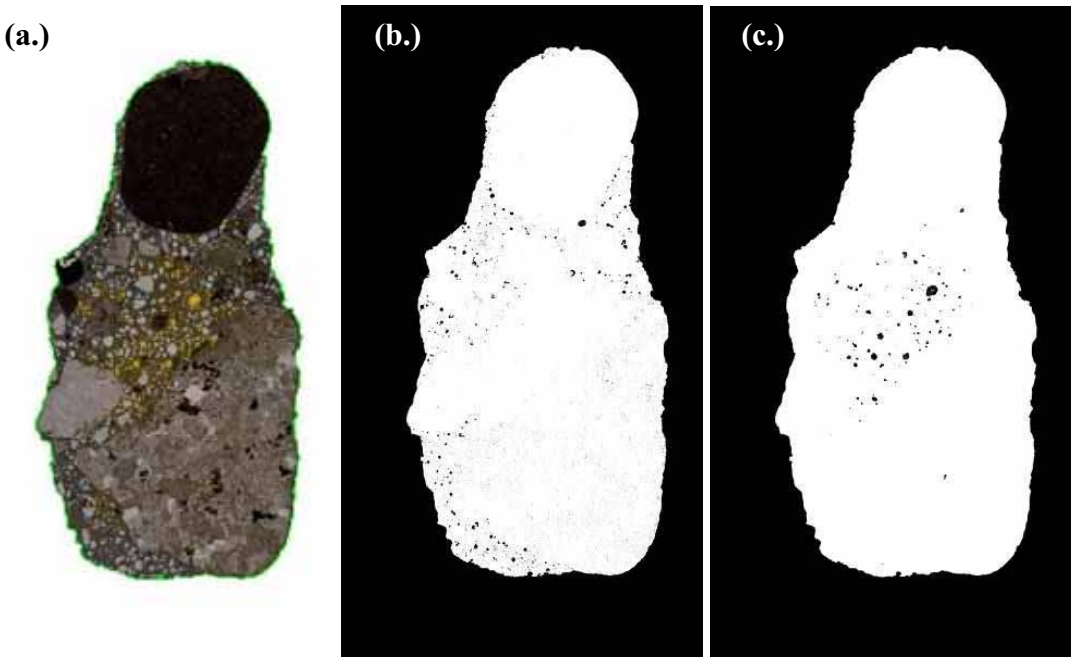


Figure A-4. Image Analysis for Crushed Gravel RCA Sample #1 for (a.) Original Image, (b.) Image Processed for Blue Resin (Surface Porosity), and (c.) Image Processed for Yellow Resin (Internal Porosity).

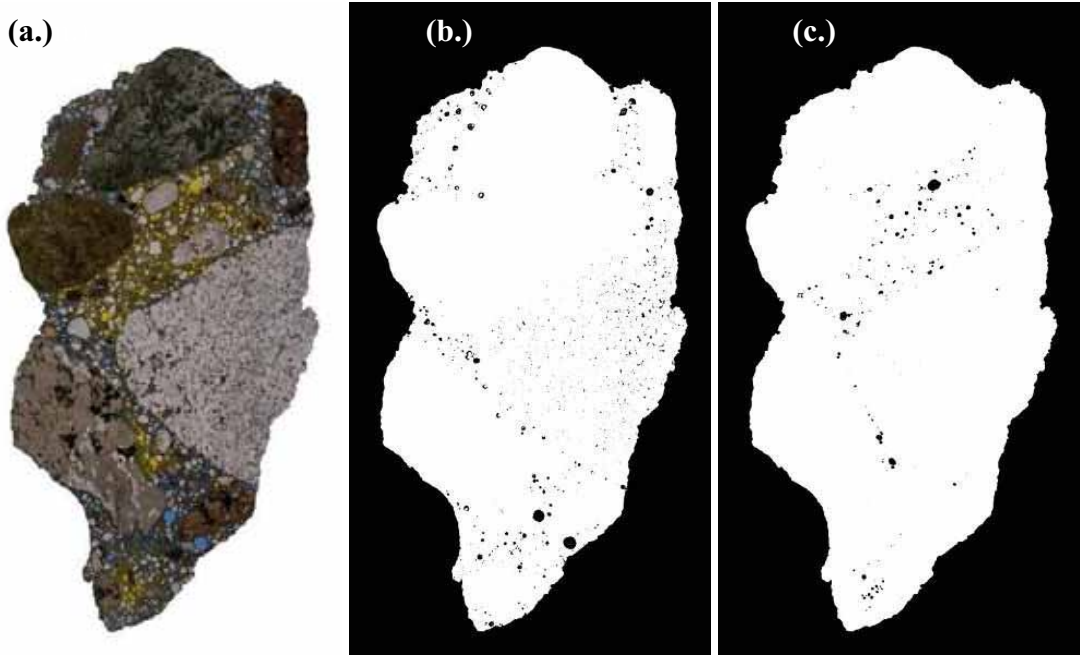


Figure A-5. Image Analysis for Crushed Gravel RCA Sample #2 for (a.) Original Image, (b.) Image Processed for Blue Resin (Surface Porosity), and (c.) Image Processed for Yellow Resin (Internal Porosity).

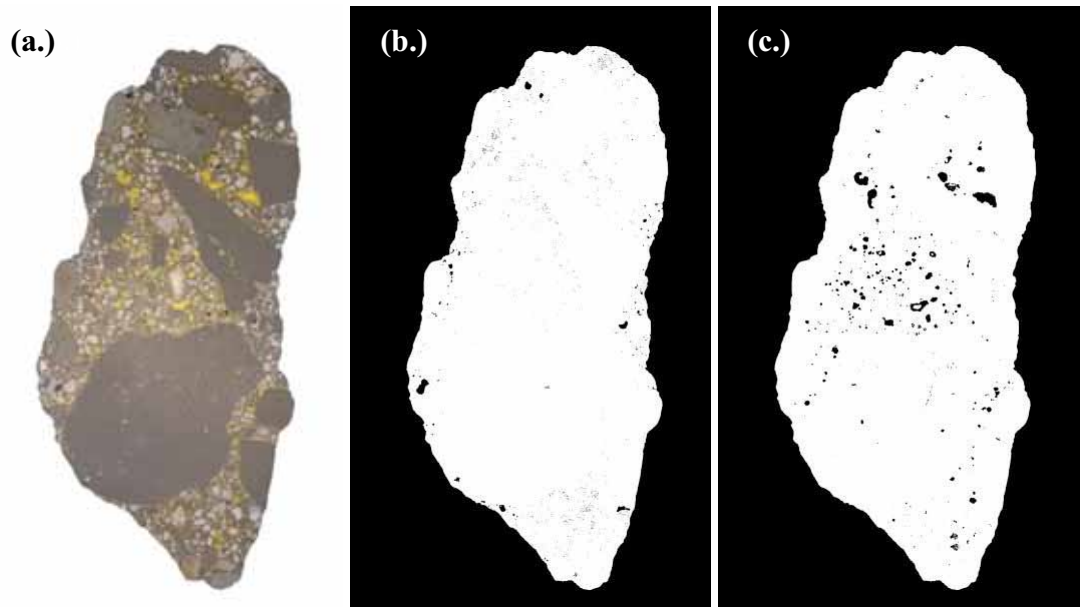


Figure A-6. Image Analysis for Crushed Gravel RCA Sample #3 for (a.) Original Image, (b.) Image Processed for Blue Resin (Surface Porosity), and (c.) Image Processed for Yellow Resin (Internal Porosity).

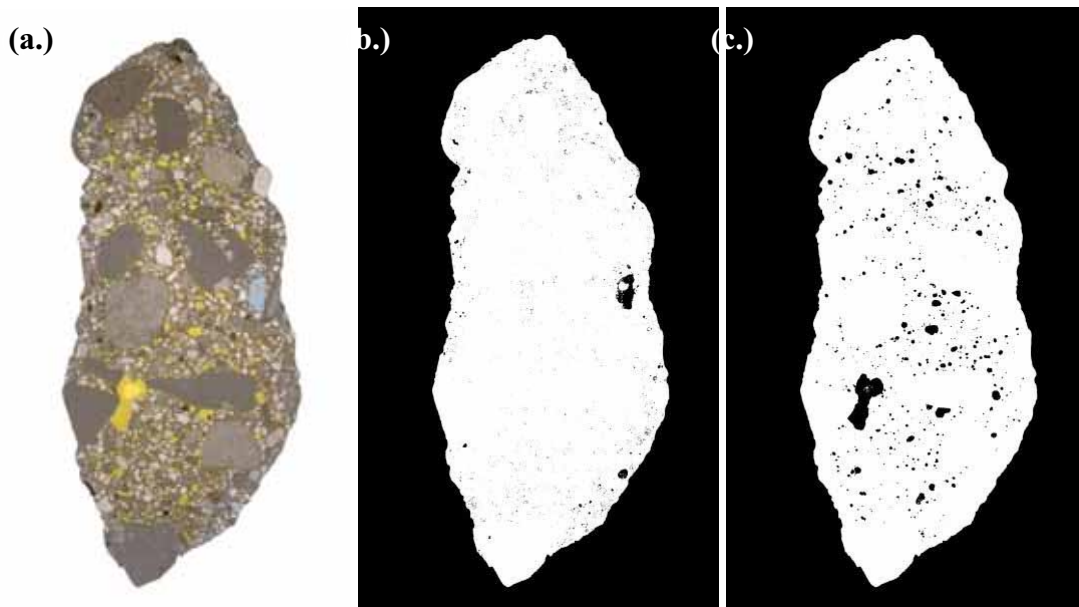


Figure A-7. Image Analysis for Limestone RCA Sample #1 for (a.) Original Image, (b.) Image Processed for Blue Resin (Surface Porosity), and (c.) Image Processed for Yellow Resin (Internal Porosity).

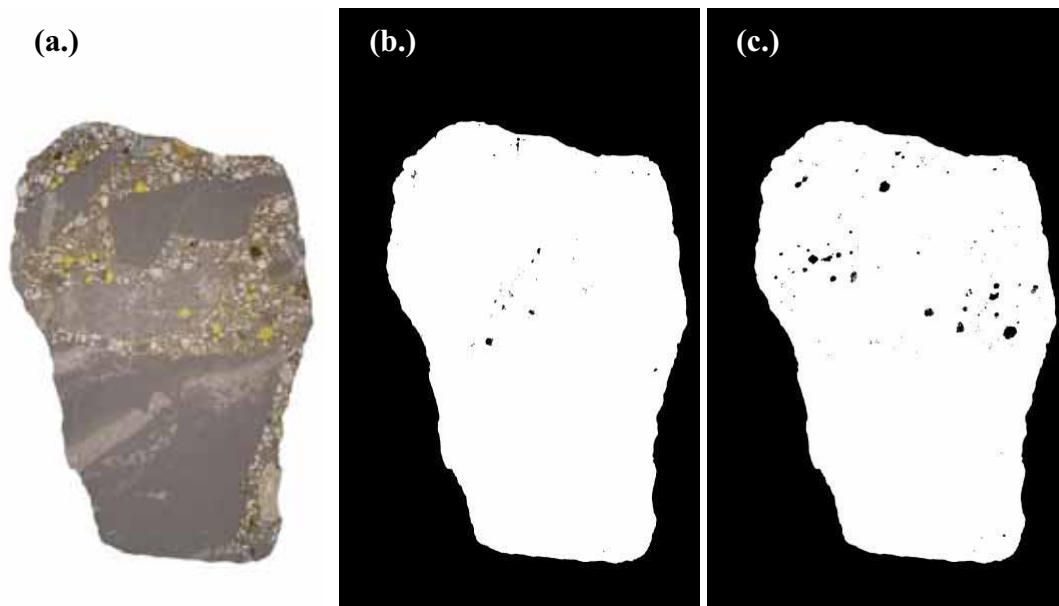


Figure A-8. Image Analysis for Limestone RCA Sample #2 for (a.) Original Image, (b.) Image Processed for Blue Resin (Surface Porosity), and (c.) Image Processed for Yellow Resin (Internal Porosity).

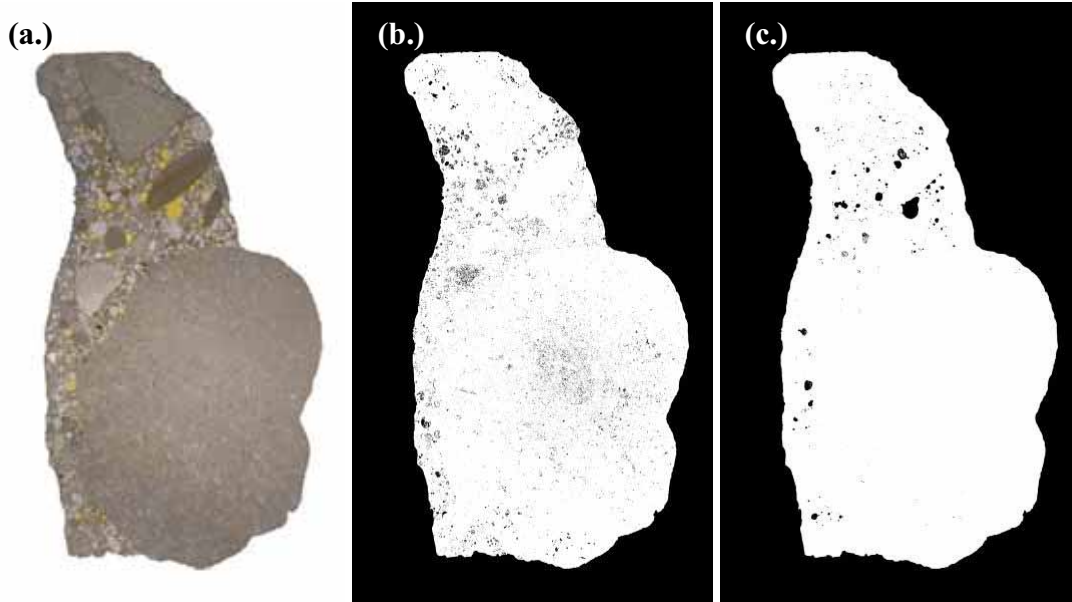


Figure A-9. Image Analysis for Limestone RCA Sample #3 for (a.) Original Image, (b.) Image Processed for Blue Resin (Surface Porosity), and (c.) Image Processed for Yellow Resin (Internal Porosity).

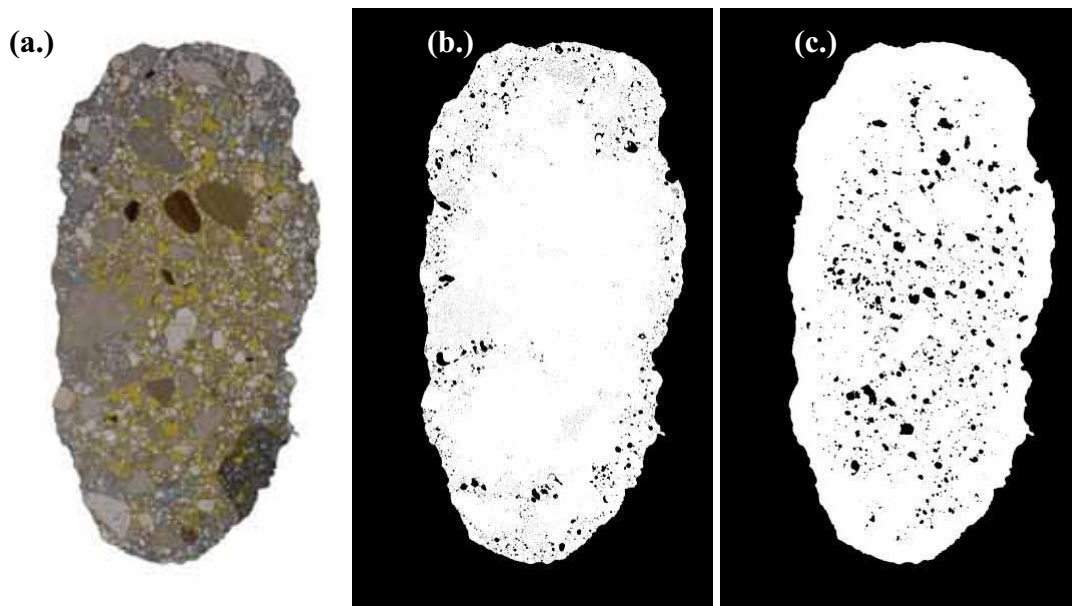


Figure A-10. Image Analysis for Blast Furnace Slag RCA Sample #1 for (a.) Original Image, (b.) Image Processed for Blue Resin (Surface Porosity), and (c.) Image Processed for Yellow Resin (Internal Porosity).

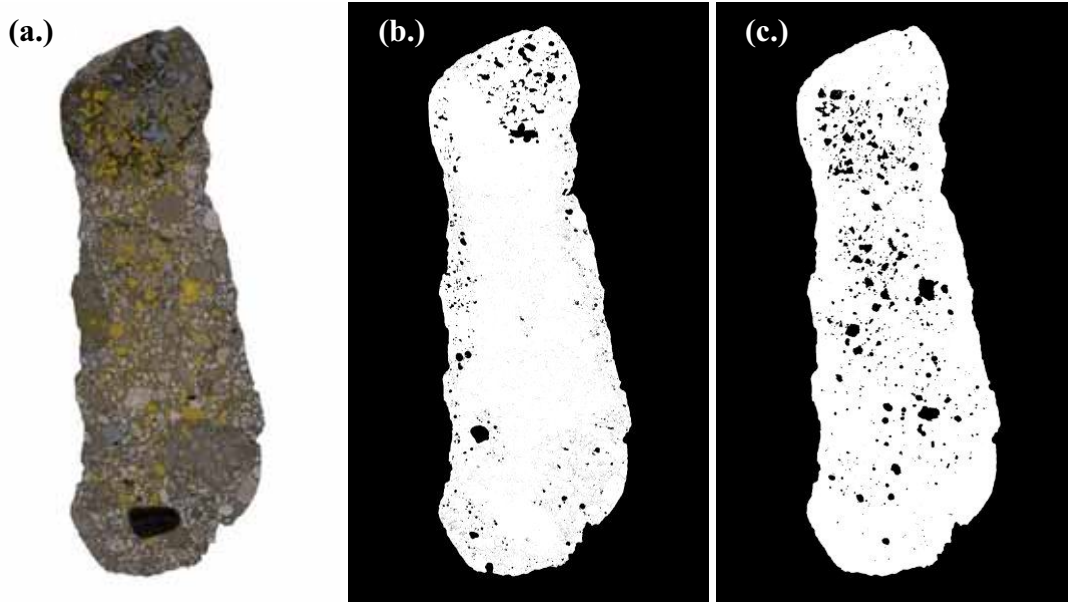


Figure A-11. Image Analysis for Blast Furnace Slag RCA Sample #2 for (a.) Original Image, (b.) Image Processed for Blue Resin (Surface Porosity), and (c.) Image Processed for Yellow Resin (Internal Porosity).

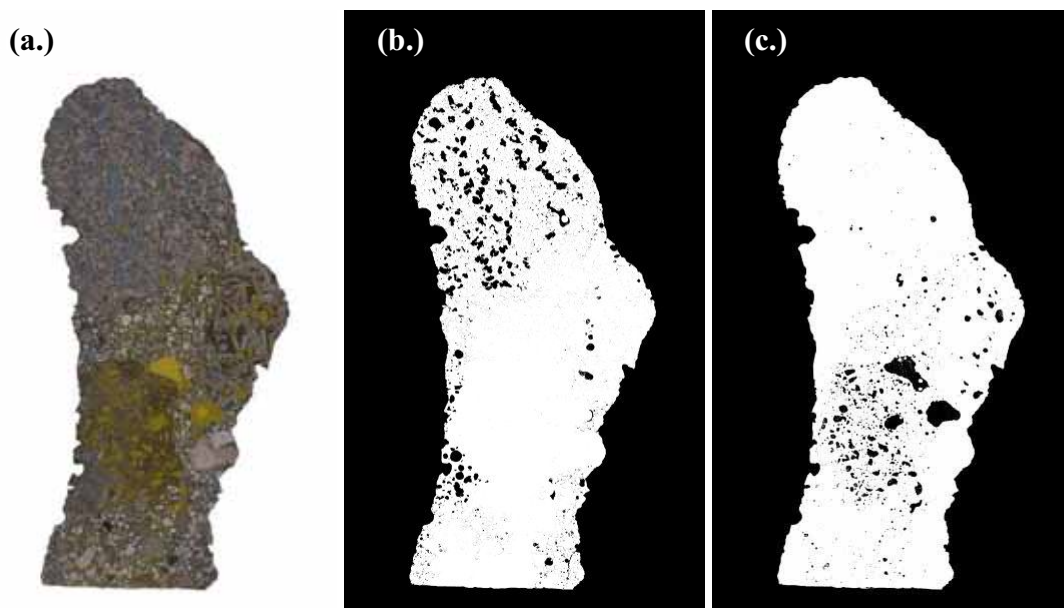


Figure A-12. Image Analysis for Blast Furnace Slag RCA Sample #3 for (a.) Original Image, (b.) Image Processed for Blue Resin (Surface Porosity), and (c.) Image Processed for Yellow Resin (Internal Porosity).

APPENDIX B

Table B-1. Helium Pyc and Geo Pyc results for Crushed Gravel for each sieve size.

Aggregate Size	Specific Gravity		Std Deviation	Porosity (%)	Std Deviation	Absorption Capacity (%)	Std Deviation
1"	G _s	2.8364	0.068382	0.758897	1.177397	0.639755	0.446391
	G _b	2.799995	0.122707				
	G _{b (SSD)}	4.009543	0.338281				
3/4"	G _s	2.736789	0.092883	2.29191	2.884529	0.302935	0.226936
	G _b	2.668667	0.20442				
	G _{b (SSD)}	3.83356	3.271867				
1/2"	G _s	2.775293	0.101966	1.377089	1.559343	0.209889	0.016124
	G _b	2.878297	0.143774				
	G _{b (SSD)}	1.539367	1.036696				
3/8"	G _s	2.885548	0.11821	1.158877	0.439422	1.18136	0.050356
	G _b	2.759323	0.069235				
	G _{b (SSD)}	0.742094	0.797093				

Table B-2. Helium Pyc and Geo Pyc results for Crushed Gravel for combined grading.

Test #	G _s	G _s ASTM	G _b	G _b ASTM	G _{b (SSD)}	G _{b (SSD)} ASTM	Abs cap. (%)	Abs cap. ASTM (%)
1	2.79555	2.78	2.685619	2.71	2.5789	2.73	0.848159	0.92
2	2.779237	2.81	2.84405	2.69	2.54265	2.73	0.943831	0.98
3	2.830702	2.75	2.809536	2.34	2.54865	2.42	0.64792	0.94
4	2.845663		2.827024		2.53896		0.83975	
5	2.881725		2.740047		2.56478		0.79547	
Avg	2.826575	2.78	2.781255	2.58	2.554788	2.626667	0.815026	0.946667

Table B-3. Helium Pyc and Geo Pyc results for Crushed Gravel Aggregate RCA for combined grading.

Test #	G _s	G _s ASTM	G _b	G _b ASTM	G _{b (SSD)}	G _{b (SSD)} ASTM	Abs cap. (%)	Abs cap. ASTM (%)
1	2.7353	2.61	2.473285	2.45	2.569535	2.53	3.934408	3.07
2	2.65095	2.65	2.366208	2.45	2.473631	2.51	4.541488	2.44
3	2.7062	2.63	2.327844	2.45	2.467733	2.52	6.021586	2.75
4	2.69535		2.324422		2.460498		5.839631	
5	2.7933		2.531278		2.625819		3.81163	
Avg	2.69535	2.63	2.404607	2.45	2.519443	2.52	4.829748	2.753333

Table B-4. Helium Pyc and Geo Pyc results for Limestone RCA for each sieve size.

Aggregate Size	Specific Gravity		Std Deviation	Porosity (%)	Std Deviation	Absorption Capacity (%)	Std Deviation
	G _s	G _b	G _{b (SSD)}				
1"	G _s	2.5814	0.043875	10.02877	3.651461	3.081578	0.302924
	G _b	2.32376	0.132161				
	G _{b (SSD)}	2.424047	0.09578				
3/4"	G _s	2.57248	0.036691	10.66216	2.039843	4.387265	0.304824
	G _b	2.298422	0.071046				
	G _{b (SSD)}	2.405044	0.053334				
1/2"	G _s	2.6174	0.037575	7.081939	2.840027	3.865391	0.348489
	G _b	2.432721	0.104683				
	G _{b (SSD)}	2.50354	0.077039				
3/8"	G _s	2.63018	0.015254	11.43089	0.788958	4.913128	0.476111
	G _b	2.329568	0.029179				
	G _{b (SSD)}	2.443877	0.022267				

Table B-5. Helium Pyc and Geo Pyc results for Limestone RCA for combined grading.

Test #	G _s	G _s ASTM	G _b	G _b ASTM	G _{b (SSD)}	G _{b (SSD)} ASTM	Abs cap. (%)	Abs cap. ASTM (%)
1	2.625025	2.6	2.378841	2.34	2.472583	2.44	3.947618	4.25
2	2.587725	2.51	2.289214	2.33	2.40485	2.4	5.101922	3.84
3	2.59145	2.56	2.356086	2.34	2.446856	2.42	3.864307	3.65
4	2.6029		2.357573		2.357573		3.864307	
5	2.594725		2.348875		2.444004		4.120029	
Avg	2.600365	2.56	2.346118	2.34	2.425173	2.42	4.179636	3.913333

Table B-6. Helium Pyc and Geo Pyc results for Slag RCA for each sieve size.

Aggregate Size	Specific Gravity		Std Deviation	Porosity (%)	Std Deviation	Absorption Capacity (%)	Std Deviation
	G_s						
1"	G_s	2.59378	0.033185	15.35324	2.60047169	7.077312	0.754825
	G_b	2.195217	0.058734				
	G_b (SSD)	2.348749	0.036758				
3/4"	G_s	2.68698	0.127911	17.45802	5.31841799	9.835884	0.196991
	G_b	2.217081	0.164497				
	G_b (SSD)	2.391661	0.126608				
1/2"	G_s	2.66414	0.070437	18.10533	3.17925025	7.512502	0.283715
	G_b	2.181943	0.10623				
	G_b (SSD)	2.362996	0.081594				
3/8"	G_s	2.72924	0.066494	17.40831	3.26448093	7.798466	0.854701
	G_b	2.252791	0.059076				
	G_b (SSD)	2.426874	0.038124				

Table B-7. Helium Pyc and Geo Pyc results for Slag RCA for combined grading.

Test #	G_s	G_s ASTM	G_b	G_b ASTM	G_b (SSD)	G_b (SSD) ASTM	Abs cap. (%)	Abs cap. ASTM (%)
1	2.652825	2.5	2.309564	2.23	2.439447	2.34	5.68472	4.76
2	2.612475	2.42	2.142345	2.22	2.321826	2.3	8.490692	3.84
3	2.717325	2.46	2.189361	2.22	2.382853	2.32	8.829337	4.3
4	2.671075		2.169462		2.255981		8.829337	
5	2.688975		2.248058		2.411896		7.287032	
Avg	2.668535	2.46	2.211758	2.223333	2.362401	2.32	7.82442	4.3

APPENDIX C

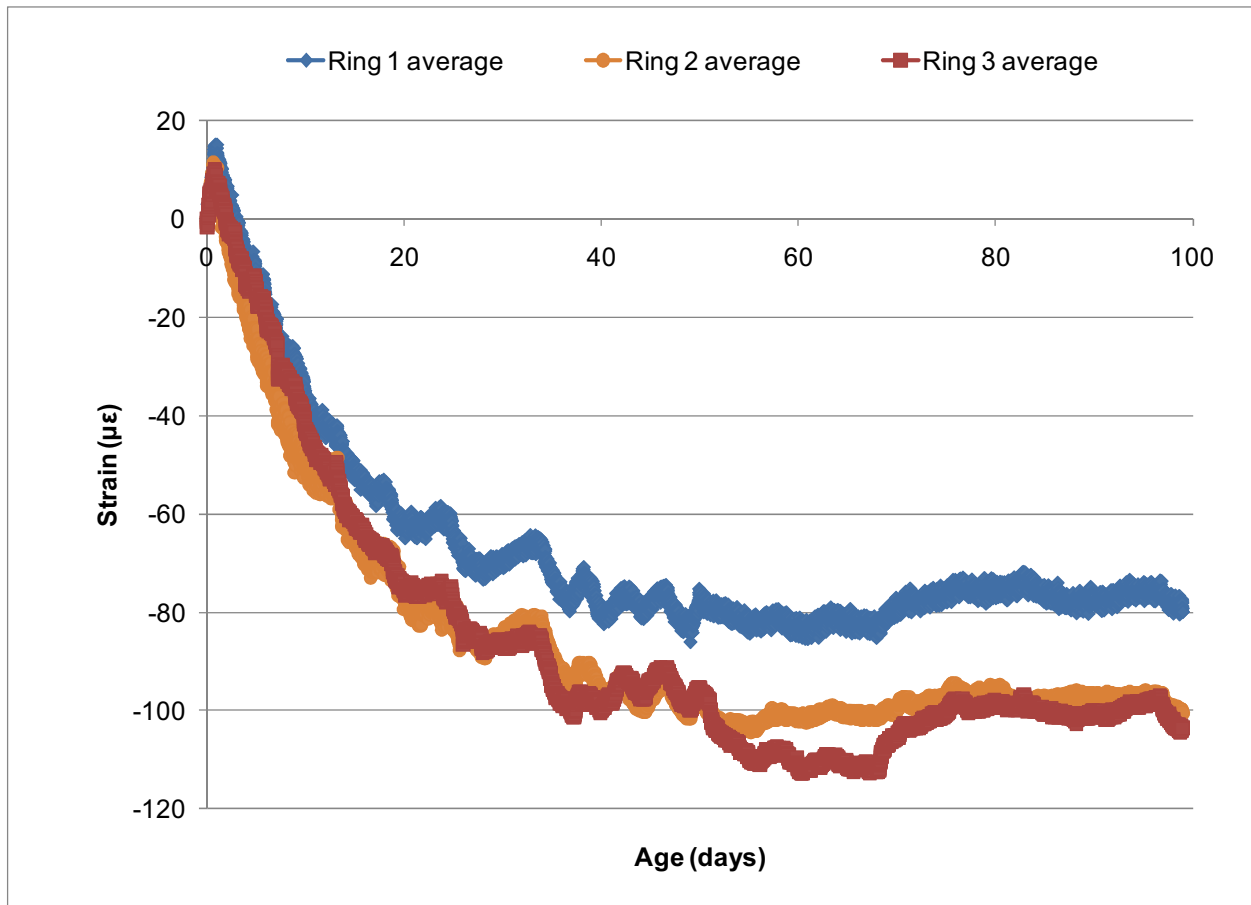


Figure C-1. Restrained Ring Shrinkage Strain for Crushed Gravel (ASTM) MDOT P1 Concrete.

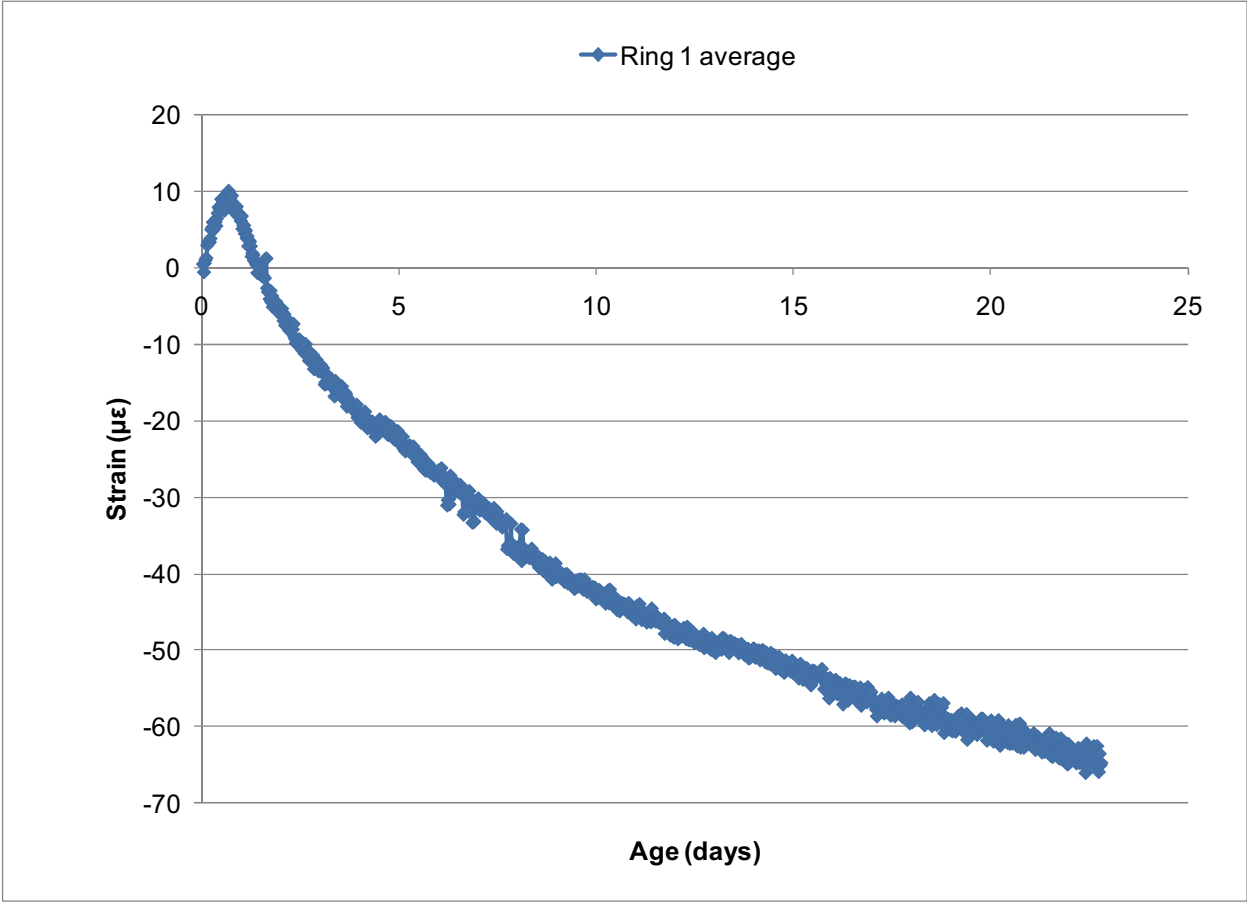


Figure C-2. Restrained Ring Shrinkage Strain for Crushed Gravel (He Pyc) MDOT P1 Concrete.

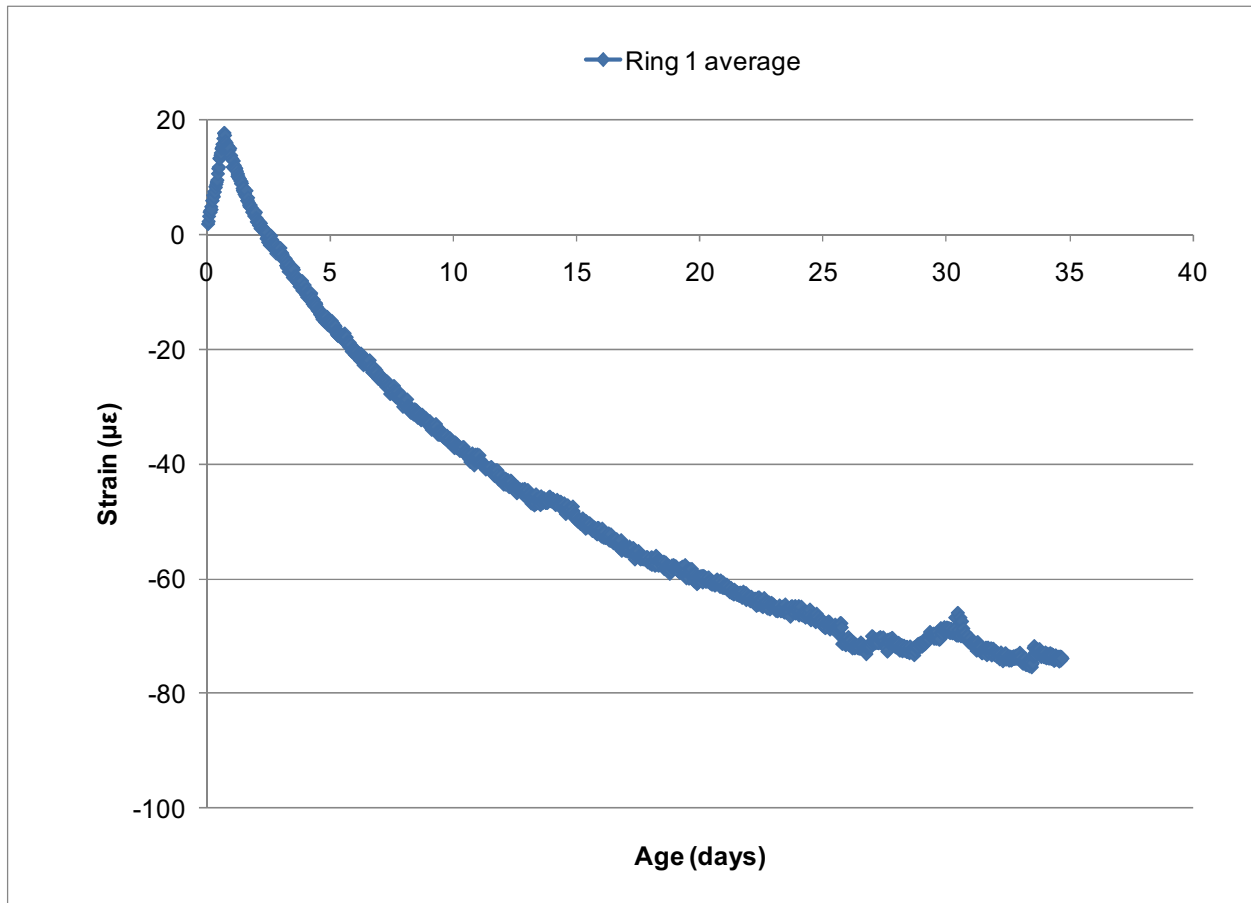


Figure C-3. Restrained Ring Shrinkage Strain for Crushed Gravel RCA (ASTM) MDOT P1 Concrete.

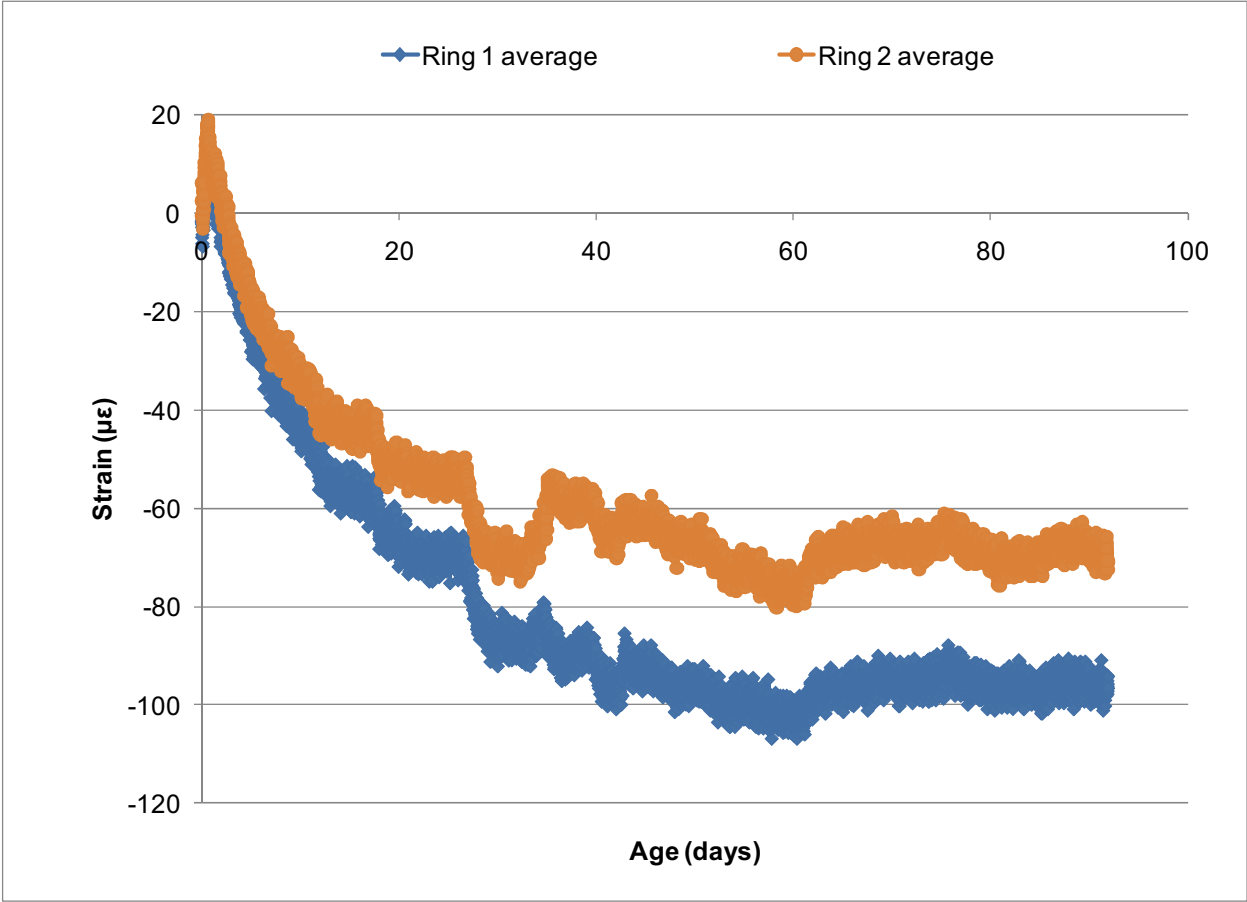


Figure C-4. Restrained Ring Shrinkage Strain for Crushed Gravel RCA (He Pyc) MDOT P1 Concrete.

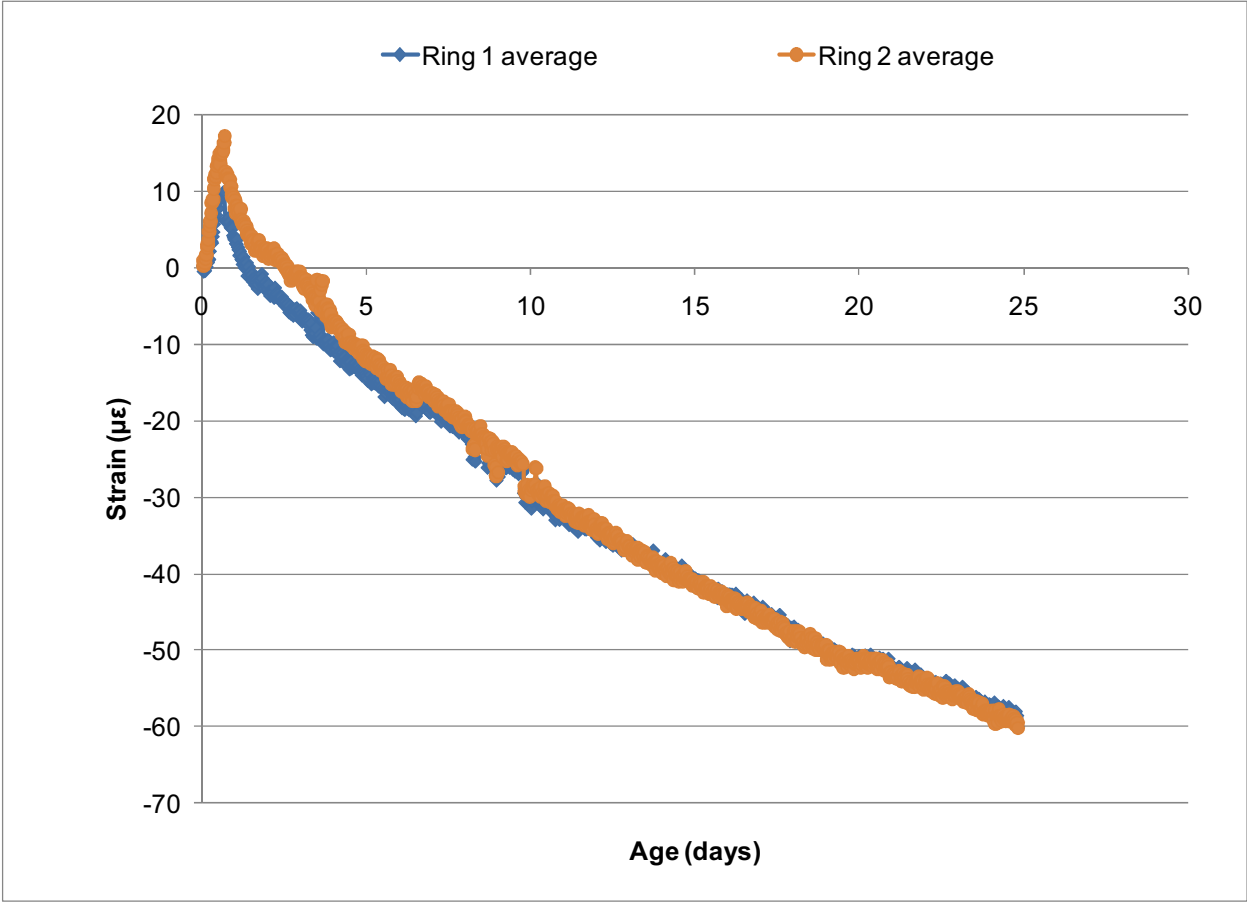


Figure C-5. Restrained Ring Shrinkage Strain for 3rdGen RCA MDOT P1 Concrete.

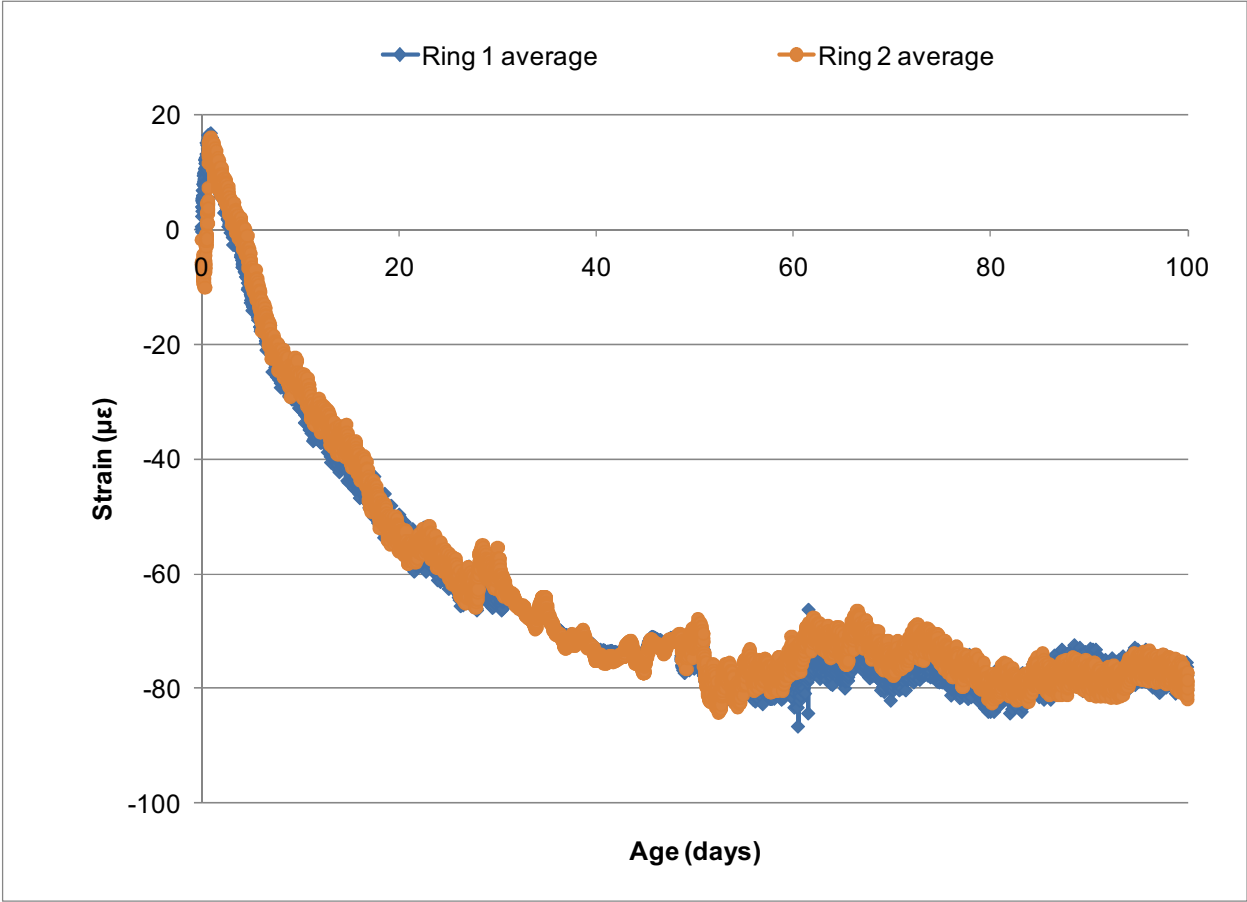


Figure C-6. Restrained Ring Shrinkage Strain for Limestone RCA MDOT P1 Concrete.

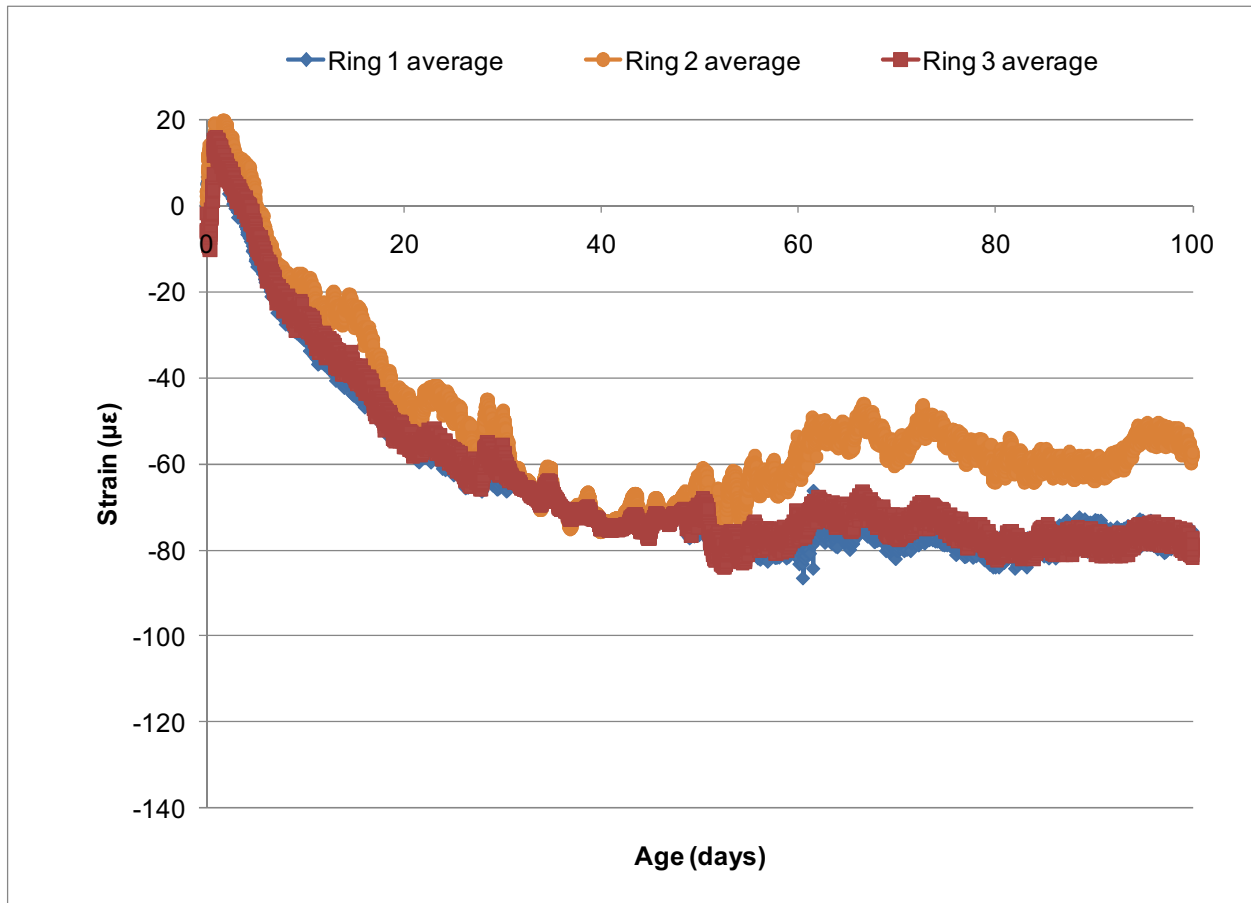


Figure C-7. Restrained Ring Shrinkage Strain for Blast Furnace Slag RCA MDOT P1 Concrete.

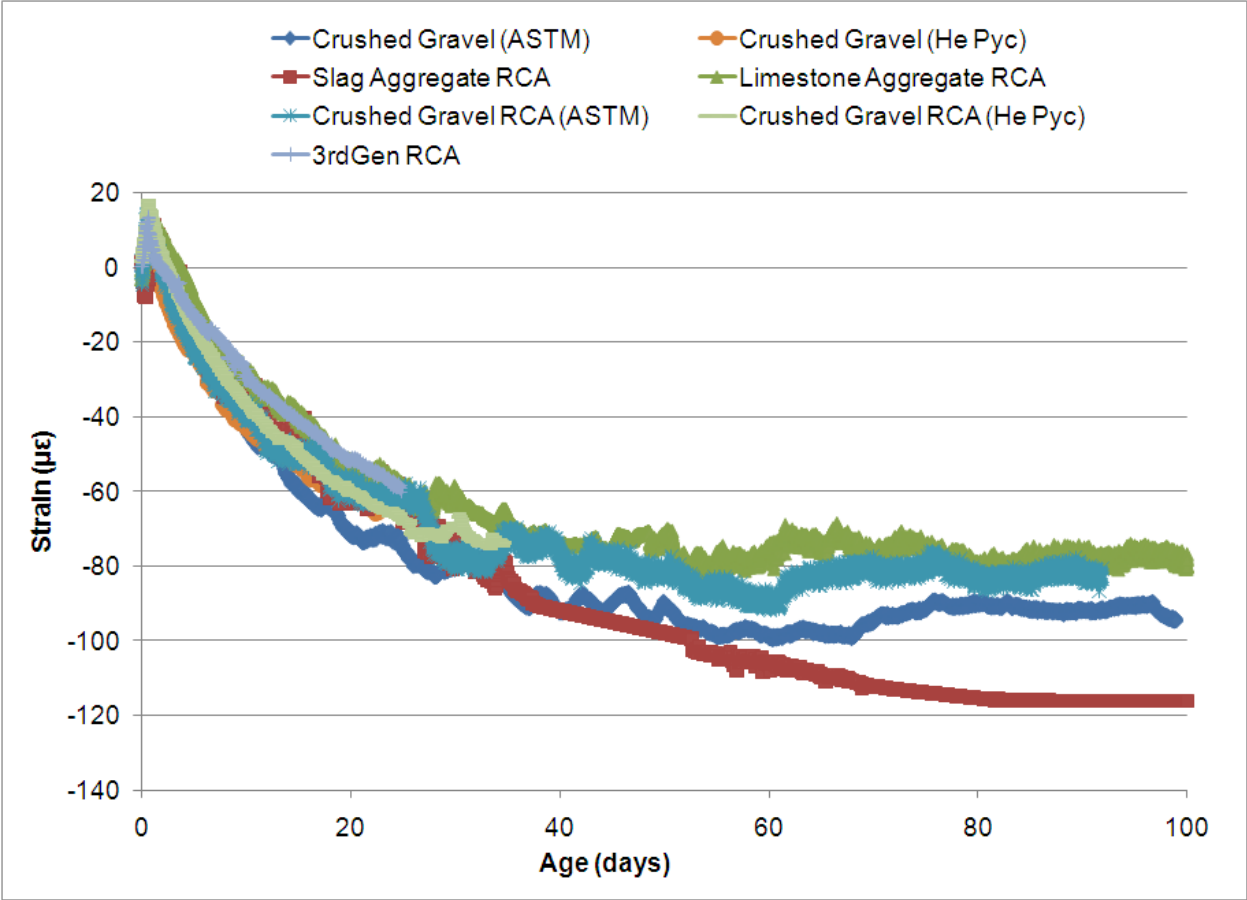


Figure C-8. Restrained Ring Shrinkage Strain for All Virgin and RCA MDOT P1 Concretes.